Adv Polym Sci (2006) 201: 45–155
DOI 10.1007/12_079
© Springer-Verlag Berlin Heidelberg 2006
Published online: 23 February 2006

Liquid Crystalline Dendrimers and Polypedes

Bertrand Donnio · Daniel Guillon (✉)

Groupe des Matériaux Organiques—GMO,
Institut de Physique et Chimie des Matériaux de Strasbourg—IPCMS,
UMR 7504—CNRS/Université Louis Pasteur, 23, rue du Loess, BP 43,
67034 Strasbourg Cedex 2, France
daniel.guillon@ipcms.u-strasbg.fr

Abstract The purpose of this review article is to give an account of the various types of dendritic systems that form liquid-crystalline mesophases and to describe the way they are organized within supramolecular organizations. It is shown that tuning of the mesophase structure can be achieved by an appropriate molecular design depending upon the chemical nature of the terminal mesogenic groups, dendritic core and dendrimer generation. The division of the subject in this review is made by the nature of the dendritic scaffold. After a general introduction on dendrimers, supramolecular liquid-crystalline dendrimers are first discussed. Then, a large part of the review is devoted to side-chain liquid-crystalline dendrimers with different chemical skeletons. The section concerning main-chain liquid-crystalline dendrimers is divided into two parts, the willow-like and the octopus dendrimers. Liquid crystals based on other types of dendritic matrices are finally discussed, including shape-persistent dendrimers, metallodendrimers, fullerodendrimers, polypedes and rod-coil block co-dendrimers.

Keywords Dendrimer · Dendritic · Liquid crystal · Mesogen · Mesophase · Polypede

Abbreviations

2D	two-dimensional
3D	three-dimensional
AFM	atomic force microscopy
Cr	crystalline phase
Col_h, Col_{ho}	hexagonal columnar phase (*p6mm* symmetry)
Col_r	rectangular columnar phase (*p2gg* or *c2mm* symmetry)
Col_{squ}	square columnar phase (*p4mm* or *p4mg* symmetry)
Col_{tet}	tetragonal columnar phase
Col_x	unidentified columnar phase
Cub	Cubic phases ($Pm\bar{3}n$ and $Im\bar{3}m$ lattice symmetries)
DMF	*N*,*N*′-dimethylformamide
DOBOB	3,4,5-tris[(4-dodecyloxy)benzyloxy]benzene unit
DP	degree of polymerization
DSC	differential scanning calorimetry
Fc	ferrocene
G	glassy or amorphous solid phase
I	isotropic liquid
LC	liquid crystalline
LCD	liquid crystalline dendrimer
MC-LCD	main-chain liquid crystalline dendrimer
M, M1, M2	unidentified mesophases
Tet, M_{tet}	3D body-centered tetragonal phase
MD	molecular dynamics
N	nematic phase
N*	chiral nematic or cholesteric phase
OPV	oligo(phenylenevinylene)
PAMAM	polyamidoamine
Pc	phthalocyanine
PE	pentaerythritol
PEO	polyethylene oxide
PPI	polypropyleneimine
Ps	spontaneous polarization
SC-LCD	side-chain liquid crystalline dendrimer

SmA	smectic A phase
SmB	smectic B phase
SmC	smectic C phase
SmC*	chiral smectic C phase
$SmCP_R$, $SmCP_F$	polar smectic phases
SmX	unidentified smectic phase
THF	tetrahydrofuran
UV	ultraviolet
XRD	X-ray diffraction

1 Introduction

Since their discovery in the late 1970s [1], dendrimers have led to the most impressive developments and rapidly expanding areas of current science [2–11]. This extraordinary enthusiasm is caused by the intrinsic and unique molecular features of the dendrimers [2–11] and the possibility of generating numerous and original chemical architectures, offering new synthetic concepts and challenges for chemists [12, 13] as well as raising several interesting theoretical questions [14, 15]. The word dendrimer comes from the Greek *dendros* meaning tree and *meros* meaning part. This is a class of aesthetic, compartmentalized, practically monodisperse supermolecules possessing a regular and controlled three-dimensional branched topology [2–11], with a geometrical rate of growth as the generation number increases. Consequently, these molecules can possibly carry a large number of functional groups per volume unit [16]. These features are the result of sophisticated genealogically directed syntheses consisting of controlled iterative methods involving successive and specific elementary steps (convergent or divergent directed sequential construction). Furthermore, such "supermolecules" are unique in that they lack entanglements, leading to a good solubility in almost all organic solvents and in principle to a lower intrinsic viscosity.

The combination of a precise functionality at the termini or in the cavities with large and defined macromolecular structures also offers many opportunities in materials science and medicine, as well as many fundamental aspects. Research in this area has been further boosted by the appreciation of their uses as potentially interesting candidates in widespread applications [17, 18]. They may be used, when suitably functionalized, in biology as drug or gene delivery devices (encapsulation of guests in the cavities of dendritic hosts) [19], because of their rough resemblance to some living components (bio-mimetism) [20–24], or in chemistry (multiredox, chiroptical, catalytic properties). Alternatively, as ideal functionalized oligomeric substances (incorporating active or reactive functions), they may be designed as materials with precise functionalities in which molecular level information is transferred from the initiator core to the periphery (or vice versa) with

the expectation of complementary and synergic phenomena (i.e. induction of new properties), and/or cooperative effects (i.e. amplification of the existing properties) [25–31]. Several excellent comprehensive review articles have emphasized many of these interesting assets of dendrimers [2–11, 14–16, 32–45].

Molecular engineering of liquid crystals is also an important issue for controlling the self-assembling ability [46, 47] and the self-organizing process of single moieties into controlled meso- and nanostructures [48–52]. It was therefore logical to functionalize such supermolecules in order to obtain well-defined giant-like liquid crystalline materials [53–58] with the possibility of discovering new types of mesophases and original morphologies [59–66]. The first liquid crystalline dendrimers (LCDs) to be reported were obtained by simply incorporating mesogenic groups within a hyperbranched dendritic scaffold either by random self-polymerization of an appropriate difunctionalized mesogenic monomer [67–73] or by the grafting of monofunctionalized mesogenic units at the terminal branches of a pre-formed tree-like polymer [71]: such hyperbranched polymers [74], a denomination presently preferred to dendrimers, are characterized by randomly branched structures with a high degree of branching and broad molecular weight distributions [75–77]. Despite their great interest, these systems will not be further discussed here as they are out of the scope of this review.

So far, most studies have focused on side-chain liquid crystalline dendrimers (SC-LCDs; Fig. 13). Induction of liquid crystalline properties may simply be achieved by grafting mesogenic promoters on the periphery of a dendrimer, though a few LCDs with non-mesogenic end-groups have also been reported [53–57]. Mesomorphism results essentially from both the enthalpic gain provided by anisotropic interactions, and the strong tendency for microphase separation due to the chemical incompatibility between the flexible dendritic core and the terminal groups as in AB-block copolymers [78]. The structure of the mesogen as well as the topology of attachment to the core (end-on and side-on; Fig. 13) determine the mesomorphism of the entire compound. The control of the ultimate molecular architecture (size and shape) can be modulated by the generation growth, the multiplicity of the branches and the connectivity of the focal core. Other sub-classes of LCDs that will also be considered in this review include supramolecular dendromesogens, shape-persistent, main-chain, polypedic, metal- and fullerene-containing LCDs.

2
Supramolecular Liquid-Crystalline Dendrimers

Such mesogenic systems represent a class by themselves often referred to as dendromesogens. The dendritic concept results from the self-organization of these dendromesogens into various liquid crystalline morphologies. Cylindrical supramolecular dendrimers are generally obtained by the self-assembly

of first generation monodendrons [79–85] (and of their corresponding side-group polymers [86–95]) that exhibit a tapered fan shape. The wide end of these molecules is usually made up of three flexible aliphatic chains such as in the DOBOB (3,4,5-tris[(4-dodecyloxy)benzyloxy]benzene unit; Fig. 1A) and 3,4,5-trialkoxybenzene derivatives (Fig. 1B), whereas the summit is made hydrophilic by using acid, ester or alcohol functions, or by grafting crown ethers or ethylene oxide chains. Malthête already successfully demonstrated the great aptitude of systems containing the DOBOB unit (Fig. 1A, $m = 12$) to self-organize into columnar mesophases. Indeed, unconventional mesogens such as the conical-like, pyramidal-like and the so-called diabolo-like mesogenic molecules [96–98] were produced by the connection of the DOBOB units to various multivalent molecular sub-units.

Self-assembly of such tapered dendritic molecules into infinite columns can be seen as an arrangement of "parts of a cake" to form a flattened circular slice followed by the stacking of these slices on top of another (Fig. 2), the central core of the columns being filled by the polar parts (crown ether, ethylene oxide segments) or the polymer backbone. This process is driven by micro-segregation of the different parts constituting the molecules, steric constraints as well as in some cases H-bonding interactions. The self-assembly ability of these systems into columnar organizations is strongly enhanced

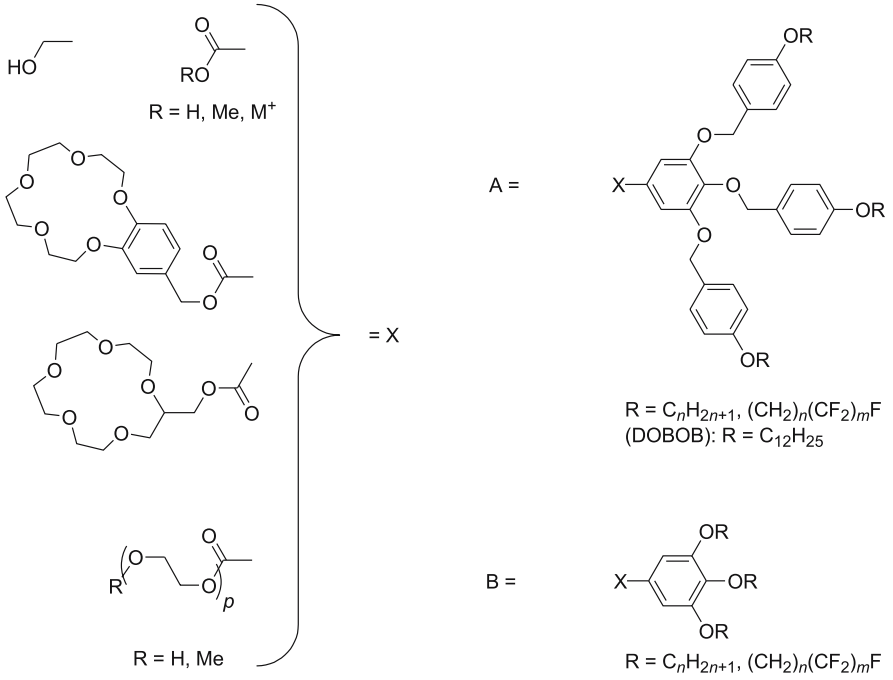

Fig. 1 Various types of flat tapered molecules self-assembling into cylindrical columns

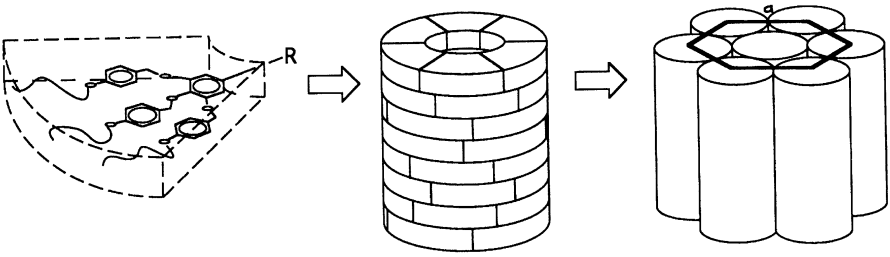

Fig. 2 Schematic representation of the self-assembling of flat tapered monodendrons into cylindrical columns and their self-organization into the Col_h phase

by fluorination of the dodecyl side chains (Fig. 1, R = $C_nH_{2n}C_mF_{2m+1}$ with $n + m = 12$ and $n, m = 4, 6, 8$) [99–101]. A rich mesomorphism was also promoted in alkali metal salts of 3,4,5-trialkoxybenzoic acids (G1-CO_2M, $n = 12$, 14, 16, 18) that were found to self-organize at low temperatures into Col_r ($M^+ = Na^+$, $m = 12$) or Col_h ($M = Li^+$, Na^+, K^+, Rb^+, Cs^+, $m = 12$, 14, 16, 18) phases and at high temperature into both $Pm\bar{3}n$ and $Im\bar{3}m$ cubic phases or only the cubic $Im\bar{3}m$ phase ($M = Li^+$, $m = 12$; $M = Li^+$, Na^+, K^+, $m = 14$; $M = Li^+$, Na^+, K^+, Rb^+, $m = 16$; $M = Li^+$, Na^+, K^+, Rb^+, Cs^+, $m = 18$), depending on chain-length and alkali metal [102].

Thus, essentially all the flat tapered molecules are found to lead to columnar structures, but when laterally attached to a flexible polymer backbone, the nature and symmetry of the phase was found to be determined by the degree of polymerization. And indeed, for some polystyrene, poly(methacrylate) [90] and poly(ethyleneimine) [92] polymers containing 3,4,5-tri(dodecyloxy)benzoyl minidendritic side-groups, those with a DP > 15–20 led to hexagonal columnar organizations, whereas those with lower DP self-organize into "inverse micellar-like" thermotropic cubic mesophases with $Pm\bar{3}n$ and $Im\bar{3}m$ space groups, respectively [90, 92]. About two macromolecules pair up to form inverse micellar-like objects with globular cores containing polymer backbones and aromatic groups, the alkyl chains radiating out to ensure a continuous matrix.

It was anticipated that a change in dendritic shape to a nearly spherical one should occur upon increasing the generation number [103]. And indeed, cone-shaped, hemisphere-like and even spherical monodendrons were obtained by increasing the generation number, producing spherical supramolecular dendrimers that in turn self-assemble into micellar cubic phases (Fig. 3). In addition, the rate of this dendritic deformation can be modulated by the degree of branching (branching multiplicity) and the "surface"-chain topology (position and number of terminal aliphatic chains).

This is first illustrated by the four generations of monodendrons based on the AB_3 building block unit shown in Fig. 4 [104, 105]. The substitution of the terminal benzyl ethers by three alkoxy groups (in their 3,4,5 positions)

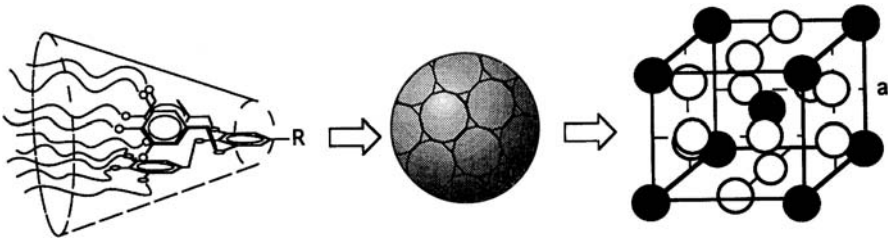

Fig. 3 Schematic representation of the self-assembling of conical-like monodendrons into spherical supramolecular dendrimers and their self-organization into cubic phases (here $Pm\bar{3}n$ symmetry)

allows only a restricted-cooperative rotation that requires the external benzyl ethers to be approximately orthogonal to the internal one, thus favoring the conical shape of the monodendron (Fig. 3). Starting from the second generation, all the dendrons (benzoates, corresponding benzyl alcohols and benzoic acids) exhibit in addition to the crystalline phase an isomorphous cubic liquid-crystalline phase with the $Pm\bar{3}n$ space group (Table 1).

Studies of electron density profiles and histograms computed from the X-ray diffraction data demonstrate that the cubic phase results from the self-assembly of these supramolecular dendrimers; the aromatic regions are centered around the corners, the center of the cubic lattice, and in the 1/4 and 3/4 positions along one of the bisectors of each face [106]. This model was finally confirmed by the analysis of the electron density profiles of the phase exhibited by a G2-CO_2H derivative with perfluorinated side-chains (Fig. 4, G2-CO_2H, R = $C_4H_8C_8F_{17}$) and doped with small amounts of the equivalent rubidium salt to modify the contrast [107]. This model is quite similar to that generally found in micellar lyotropic systems with the same symmetry [108–111]. The aggregation of the monodendrons into a supramolecular dendrimer is also favored by the H-bonding network generated by the apical acid or alcohol functions of the monodendrons, the former leading to the most stable cubic mesophase (Table 1). A convenient way to describe the cubic phase formed by these supramolecular dendrimers is to consider micelles with "polyhedral" shapes (vide infra). The fluorination of the terminal chains of the G2-CO_2Me monodendron (Fig. 4, R = $C_{12}H_{25}$ to R = $C_4H_8C_8F_{17}$) led to the transformation of the "spherical" supramolecular dendrimer into a pyramidal columnar supramolecular dendrimer. As a consequence, not only the phase symmetry was changed (cubic-$Pm\bar{3}n$ vs. Col_h-*p6mm*), but the stability considerably enhanced (Cr 22 Col_h 92 I) [112]. This unique result shows an interesting alternative for the control of the molecular conformation and its mechanism of self-assembly into pre-designed morphologies.

Continuing their investigations, Percec and coworkers also considered several generations of benzyl ether monodendrons containing only one aliphatic terminal chain on the outside benzyl groups (Fig. 5) [113]. Optical polarizing

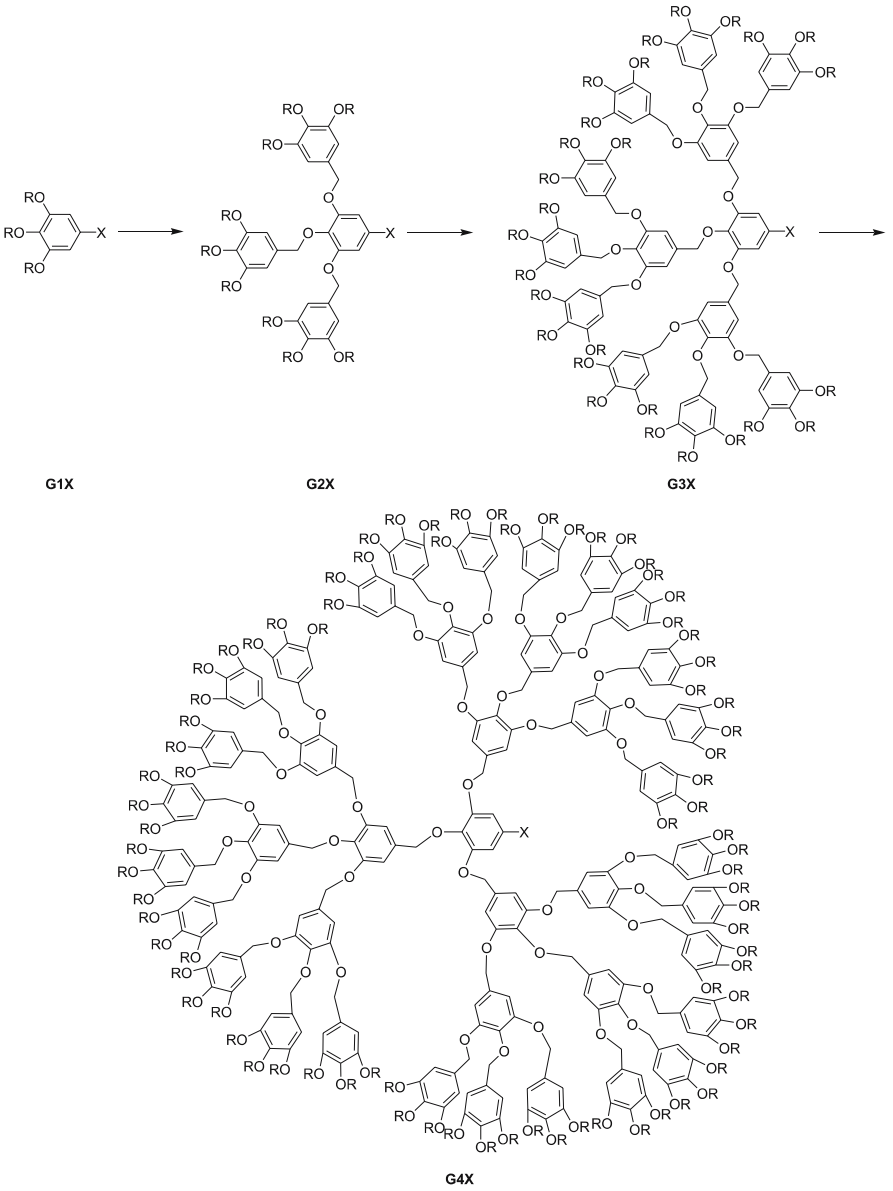

Fig. 4 Monodendrons based on the AB_3 building block unit (X = CO_2Me, CO_2H, CH_2OH; R = $OC_{12}H_{25}$)

microscopy studies and X-ray diffraction data show unambiguously the existence of a columnar mesophase (*p6mm* lattice) for the low generation dendrons and of a cubic mesophase ($Pm\bar{3}n$ lattice) for the third generation dendron (Table 2). Thus, the first two generations of monodendrons (G1-CO_2H

Table 1 Mesomorphic behavior of the monodendrons based on the AB_3 building block methyl 3,4,5-trishydroxybenzoate (X = CO_2Me, CO_2H, CH_2OH; R = $OC_{12}H_{25}$) [a,b]

G*n*X	X = CO_2CH_3	CH_2OH	CO_2H
G1	Cr 23 I	Cr 47 I	Cr 59 I
G2	Cr 58.5 (Cub 56) I	Cr 58 Cub 88 I	Cr 83 Cub 117 I
G3	Cr –11 Cub 94 I	Cr –12 Cub 106 I	Cr –12 Cub 139 I
G4	Cr –11 G 42 Cub 77 I		Cr –12 Cub 85 I

[a] Cubic phase with the $Pm\bar{3}n$ symmetry
[b] Phase in brackets: monotropic phase

and G2-CO_2Me) self-assemble into cylindrical supramolecular dendrimers. For an idealized model, it is convenient to view the columns as resulting from the stacking of cylindrical strata (taken at about ca. 4.5–4.7 Å thick), each containing a precise number of dendrons. In this idealized view, the former system is made up of four monodendrons, each having a shape equivalent to a quarter of a disk, whereas the latter is formed by two monodendrons with a half disk shape. The third generation monodendrons self-assemble into a spherical supramolecular dendrimer containing six monodendrons; those monodendrons undergo the most dramatic change in shape and become cone-like. So, a continuous change in the shape of the monodendron is induced by the generation number.

Therefore, for identical arborescence (here AB_3-type for both families of dendrons; Figs. 4 and 5), the number of terminal alkoxy chains can be greatly modified, simply by changing the nature of the terminal group. This straightforward modification affects significantly the mesophase behavior, as well as the self-assembling process. Indeed, the apparition of the cubic phase is delayed, and the increase in the number of alkyl tails (from 27 to 81) increases the size of the monodendrons from a sixth of a sphere (Fig. 5, G3-CO_2Me) to a hemisphere (Fig. 4, G4X).

In order to assess the criteria that govern the control of the shape and size of their supramolecular assemblies, Percec also investigated libraries of monodendrons that differ in their architecture on the periphery (number of peripheral aliphatic chains), in the internal repeat unit architecture (type of arborescence, i.e. branching multiplicity), in the generation number or core functionality and connectivity. For example, they studied the evolution of the mesomorphism in a series of dendrimers related to that shown in Fig. 5, but instead of grafting three 4-dodecyloxybenzyloxy groups at the periphery of the monomeric AB_3 building units, only two of them were attached to the AB_2 unit (the terminal chain number was changed from 3, 9, 27 in the former to 2, 6 to 18 for the latter from G1 to G3, respectively) [114]. The cubic phase appears from the second generation onwards ($Pm\bar{3}n$ lattice), whereas the first

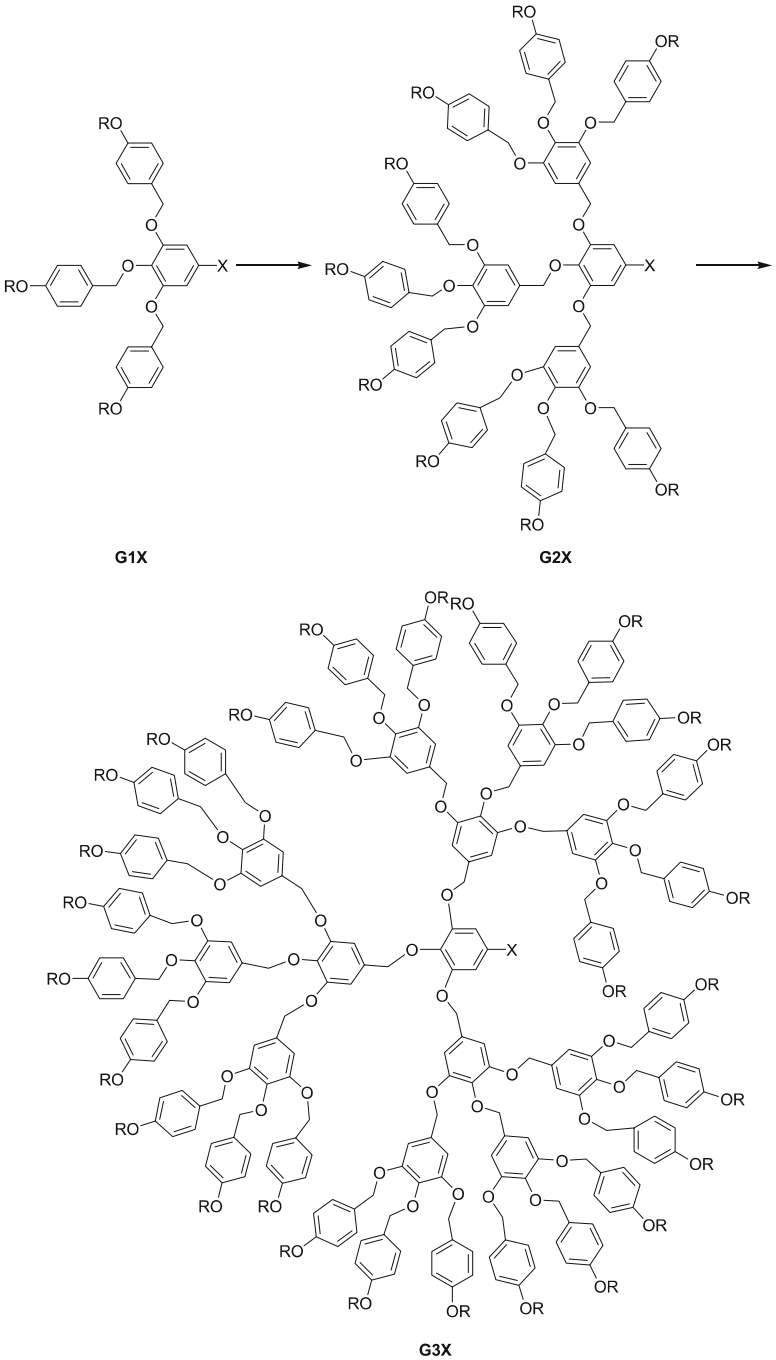

Fig. 5 Monodendrons based on the 3,4,5-AB_3 arborescence and with DOBOB as terminal group (X = CO_2Me, CO_2H; R = $OC_{12}H_{25}$)

Table 2 Mesomorphic behavior of the monodendrons based on the 3,4,5-AB_3 arborescence and with DOBOB as terminal group (X = CO_2Me, CO_2H; R = $OC_{12}H_{25}$) [a]

G*n*X	X = CO_2CH_3	CO_2H
G1	Cr 66 I	Cr 43 Col_h 145 I
G2	Cr –18 Col_{h1} 98 Col_{h2} 117 I	Cr 182 Cub 195 I
G3	Cr –17 G 47 Cub1 179 Cub2 197 I	

[a] Cubic phase with the $Pm\bar{3}n$ symmetry

generation forms a Col_h phase. Comparing these two series showed that the use of the AB_2 unit versus the AB_3 unit at the periphery led to an increase of the diameter of the supramolecular dendrimer, consequent to a decrease of the solid angle of the dendron. Upon increasing the generation number, all the dendrimers increase their solid angle until they become a single sphere. This trend was generally confirmed for this class of materials.

In another example, they considered the attachment of the first generation 3,4-bis(*n*-dodecan-1-yloxy)benzoyl ether monodendron to the periphery of Fréchet-type dendritic units (3,5-disubstituted benzyl ethers) leading to another class of mixed monodendrons (Fig. 6) [115]. Interestingly the second, third and fourth generation monodendrons (4, 8 and 16 terminal chains) self-assemble into supramolecular cylinders which in turn self-organize into a hexagonal columnar *p6mm* liquid-crystalline lattice. The fourth generation dendron is shown to be the first monodendron with a disk-like shape. The fifth generation dendron (32 chains) self-assemble into a cubic phase of $Pm\bar{3}n$ symmetry, where each monodendron is equivalent to a fifth of the supramolecular pseudo-spherical micelle.

Monodendrons based on the AB_3 arborescence (as those shown in Figs. 4 and 5) but with two terminal chains per peripheral phenyl group (as those shown in Fig. 6) were also synthesized up to the fifth generation (6, 18, 54, 162 dodecyloxy chains for G2 to G5, respectively) [116]. A cubic phase only with the same $Pm\bar{3}n$ 3D lattice was detected right from the second generation. All the above examples of cubic phases were found to result from the self-organization of dendrons which are conical or hemispherical in shape. However, the fifth generation monodendron is the first quasi-spherical functional monodendron that self-organizes into a cubic lattice ($Pm\bar{3}n$) to be reported (Fig. 12). The oblate spherical shape was confirmed by scanning force microscopy (the average diameter and average height of the molecule were found to be 6 and 5 nm, respectively, in a disordered monolayer of dendrons on a mica surface).

Two other isomeric libraries of self-assembling AB_2 monodendrons based on 3,4- and 3,5-disubstituted benzyl ether internal repeat units containing four first generation monodendrons, i.e., 3,4,5-tris(*n*-dodecan-1-

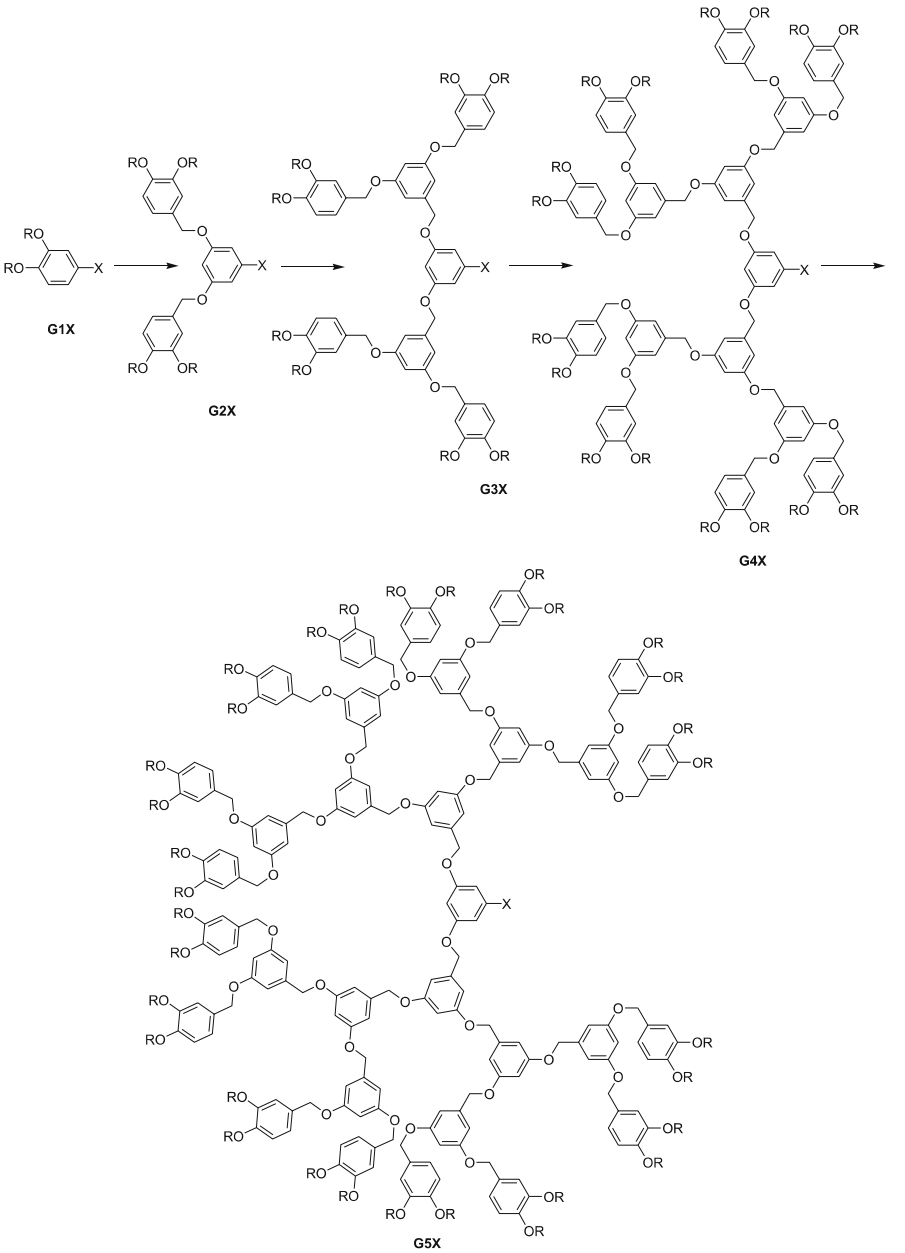

Fig. 6 Monodendrons based on the 3,5-AB_2 arborescence with 3,4-bis(*n*-dodecan-1-yloxy)benzoyl ether terminal groups (X = CO_2Me, CO_2H, CH_2OH; R = $OC_{12}H_{25}$)

yloxy)benzoyl ether, 3,4-bis(*n*-dodecan-1-yloxy)benzoyl ether, 3,4,5-tris(*n*-dodecan-1-yloxy)benzyloxy ether, 3,4-bis(*n*-dodecan-1-yloxy)benzyloxy ether, on their periphery were also considered (Fig. 7) [117]. It was shown that the supramolecular dendrimers derived from 3,4-dibenzyl ether monodendrons are spherical while the supramolecular dendrimers derived from 3,5-dibenzyl ether monodendrons are cylindrical. As a consequence, the monodendritic building blocks of the 3,4-disubstituted series have a cone-like shape while those of the 3,5-disubstituted series have a shape which corresponds to fragment of a disk or a disk-like shape (Fig. 12). In all the previous

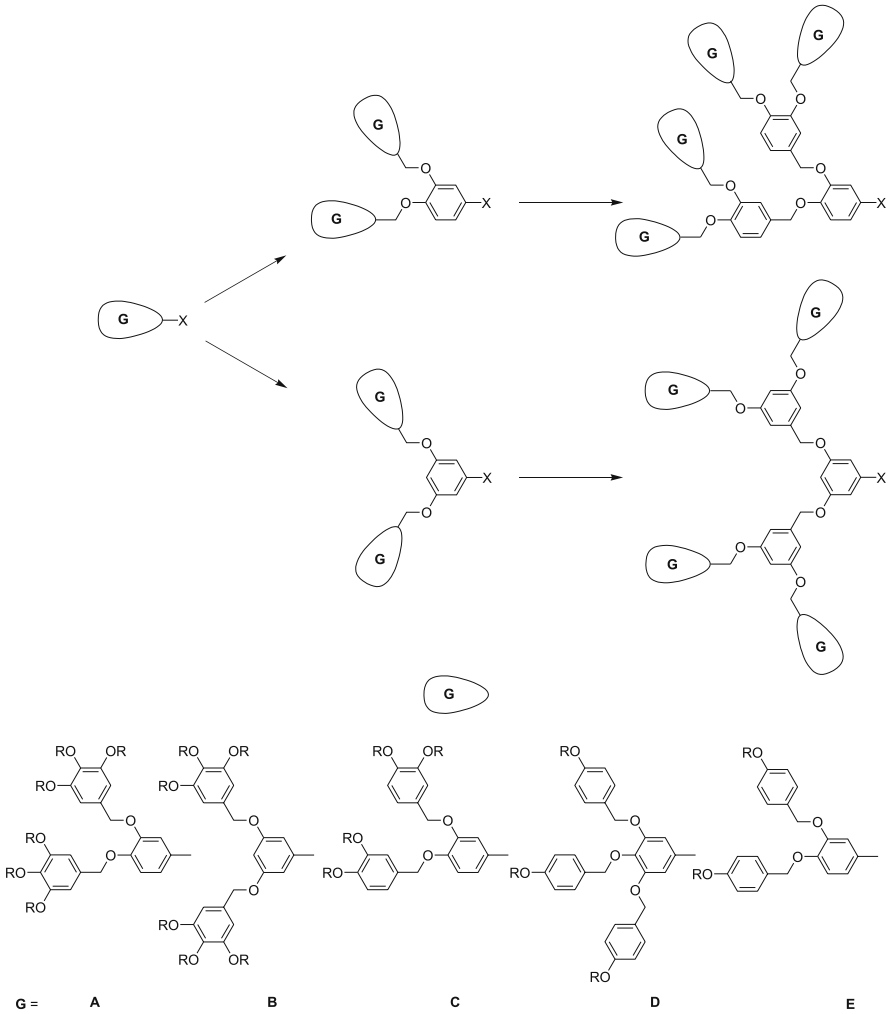

Fig. 7 Library of dendromesogens built up from a 3,4-AB_2, 3,5-AB_2, and mixed 3,4-3,5-type of arborescence (R = $OC_{12}H_{25}$, X = CO_2Me, CH_2OH, CO_2H)

libraries, the structure of the internal repeat unit determines the shape of the monodendron and of the supramolecular dendrimer. However, for the same internal repeat unit, the size of the monodendron and of the supramolecular dendrimer is determined by the structure of the unit on its periphery. On increasing the generation number, the shape of the monodendron changes from a fragment of a disk to a disk, to a cone, to half a sphere, and ultimately to a sphere. Please note that within all these libraries the library based on 3,5-disubstituted benzyl ethers provides the first example of supramolecular dendrimers able to change their shape in a reversible way as a function of temperature and also the first example of a spherical supramolecular dendrimer that self-organizes into a cubic phase of $Im\bar{3}m$ symmetry (Fig. 12).

Further studies by electron microscopy on some of the samples exhibiting the $Pm\bar{3}n$ cubic phase show the existence of grain boundaries and stacking faults [118]. These are all consistent with the presence of quasi-spherical assemblies or more precisely to polyhedral-like micelles, and moreover suggest that the supramolecular spheres are deformable, interacting with one another through a relatively soft pair potential [119]. The majority of such quasi-spherical assemblies are thus distorted into an oblate shape.

Wedge-shaped dendrons such as those described above form mainly columnar and cubic phases. However, a liquid-crystalline phase with a tetragonal three-dimensional unit cell (Tet phase) containing 30 globular supramolecular dendrimers has been reported recently. Each of these supramolecular dendrimers is the result of the self-assembly of 12 dendrons, as is shown in Fig. 8 [120, 121]. Interestingly, the complex tetragonal phase of symme-

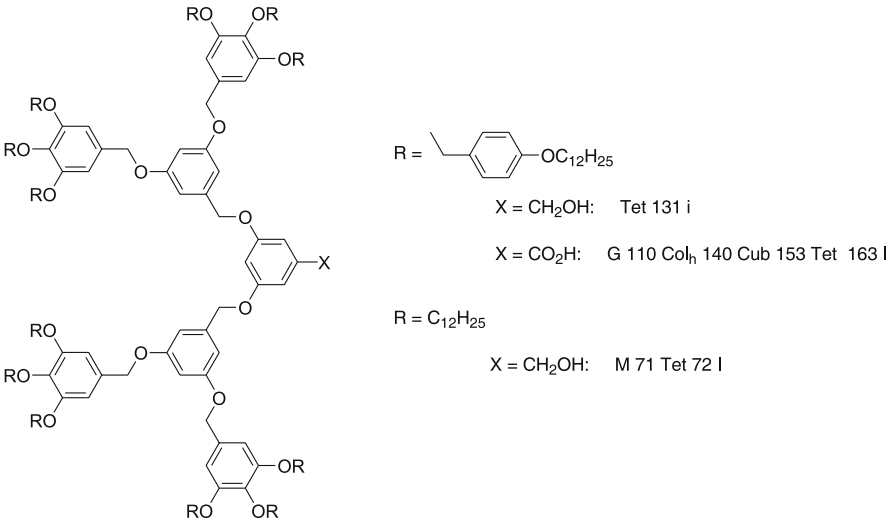

Fig. 8 Structure of the monodendrons with a 3,5-AB_2 arborescence showing the tetragonal phase

try $P4_2/mmm$ is shown to be the equivalent of tetrahedral closely packed Frank–Kasper structures [122] found in metals and metal alloys. The authors suggest that the analogy between dendrimers and metals lies in the role played by the "soft" *d* orbitals in the metals and the soft globular supramolecular dendrimers. In addition, with dendrons of the same family, quasiperiodic structures analogous to those found with some metal alloys, have been found. Whereas the characteristic length of the self-assembled quasicrystal is of a few Å in metal alloys, it is nearly 10 nm in the case of self-assembled dendrons.

Note that this geometrical model—that can be compared to the spherical micelle model used for cubic phases—which visualizes these 3D structures as an arrangement of space-filling polyhedra [123], as in the case of foams [124], appears more convenient for the description of the cubic structures than the 3D packing of spheres. In this view, the mean distances between the micellar nuclei can be represented by polyhedral hollow solids, the nature and type of which obviously are related to the symmetry of the cubic phase. Thus, for the $Im\bar{3}m$ phase, the symmetry is generated by the use of a single semi-regular Archimedean polyhedron, namely the truncated octahedron (a regular tetrakaidecahedron with 8 hexagonal and 6 square faces of identical edge) and located at the nodes of the cubic lattice ($N = 8 \times 1/8 + 1 \times 1 = 2$). Concerning the $Pm\bar{3}n$ space group, two polyhedra must be considered, namely the regular Platonic dodecahedron (12 pentagonal faces of same edge) located at the center and corners of the cubic cell ($8 \times 1/8 + 1 \times 1 = 2$) and a semi-regular 14-faced polyhedron (tetrakaidecahedron with two hexagonal faces and 12 pentagonal faces of same edge), occupying two of the four tetrahedral sites of each face of the cubic lattice ($6 \times 2 \times 1/2 = 6$).

In view of obtaining functional dendrons, crown ethers have been incorporated at the focal point of some of these dendromesogens (as in Fig. 1). The dendritic building blocks thus prepared self-assemble either spontaneously or after complexation with NaOTf in two-dimensional smectic B, smectic A, and *p6mm* hexagonal columnar and three-dimensional $Pm\bar{3}n$ cubic lattices with increasing generation [125]. A very delicate dependence is described between the shape of the dendritic crown ether and the stability of its supramolecular lattice obtained by complexation with NaOTf. Nevertheless, these supramolecular dendrimers represent interesting materials for selective ion transport.

In all the examples reported above concerning the self-assembly of dendrons based on AB_3, AB_2, and combinations of AB_3 and AB_2 building blocks, the shape and the diameter of the resulting supramolecular dendrimers were limited to less than 8 nm, mainly because of the solid angle of the dendron. In fact, because of the shape change of the self-assembling dendron as a function of generation, the increase in generation is generally not accompanied by an exaggerated increase of the supramolecular dimensions, despite the fact that the molecular weight increases exponentially. In order to produce supramo-

lecular dendrimers of larger dimensions, new libraries of compounds based on various combinations of AB, AB_2 and AB_3 building blocks have been designed and synthesized. This led to a very broad and original study (34 new compounds were reported) where the length of the branches, the number of terminal chains, the degree of branching and the multiplicity were systematically varied. Thus, two new families of dendritic mesogens such as the $(AB)_y$-AB_3 and $(AB)_y$-AB_2 series (Fig. 9; *y*: number of AB blocks; for the $(AB)_y$-AB_3 system, $y = 3n + 3 + m = 3 - 11$, and for the $(AB)_y$-AB_2 system $y = 2n + 3 + m = 2 - 7$) were first prepared [126].

Most of the first generation supramolecular dendrimers thus synthesized from the AB_3 building block (Fig. 9) self-organize into lamellar ($n = 1, 2$; $m = 0$), columnar hexagonal and rectangular ($n = 0, 1, 2$; $m = 0, 1$) and $Pm\bar{3}n$ cubic phases ($n = 0$; $m = 1, 2, 3$), whereas those derived from the AB_2 unit (Fig. 9) form lamellar ($n = 1, 2$; $m = 0, 3$) and columnar ($n = 0, 1, 2$; $m = 1, 2, 3$) phases only. The dimensions of the mesostructures are much larger (up to three times) than those of the phases of same symmetry exhibited by the highest generations of the supramolecular dendrimers obtained through the self-assembling of dendrons based on AB_3, AB_2, and combinations of AB_3 and AB_2 building blocks.

The corresponding families of the second generation of the AB_3 hybrid dendrons of the type $(AB)_y$-$(AB_3)^2$ (Fig. 10, $y = 0, 9, 18, 27$) and $(AB)_y$-$(AB_2)(AB_3)$ (Fig. 10, $y = 0, 6, 12$) were also prepared by varying the total number of benzyl AB groups *n* and *m*. A hexagonal columnar phase was obtained for the first series $(AB)_y$-$(AB_3)^2$ (Fig. 10, $n = 1, 2$), except for $n = 0$ which shows a $Pm\bar{3}n$ cubic phase and $n = 3$, which is crystalline. As for the mixed hybrid series $(AB)_y$-$(AB_2)(AB_3)$, a $Pm\bar{3}n$ cubic phase was obtained for all *n* (Fig. 10, $n = 0, 1, 2$), with an additional Col_h phase for $n = 2$. Unlike the previous series of the first generation, no smectic phases were detected.

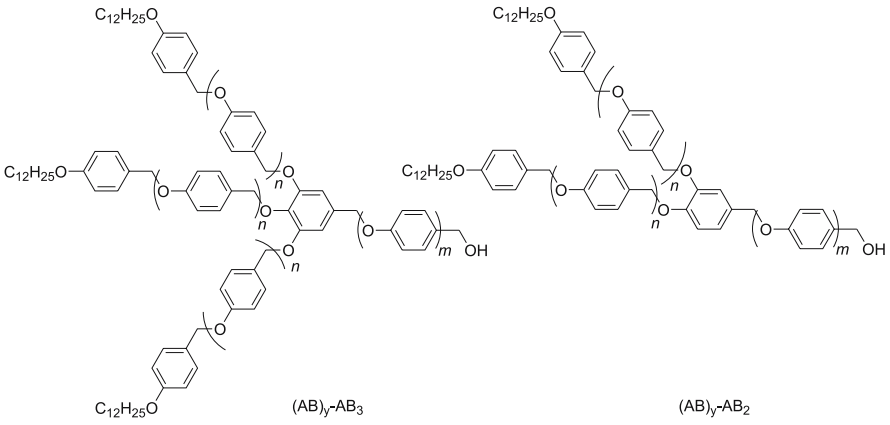

Fig. 9 Structure of the $(AB)_y$-AB_3 and $(AB)_y$-AB_2 dendrons of the first generation (*y*: number of AB blocks, see text)

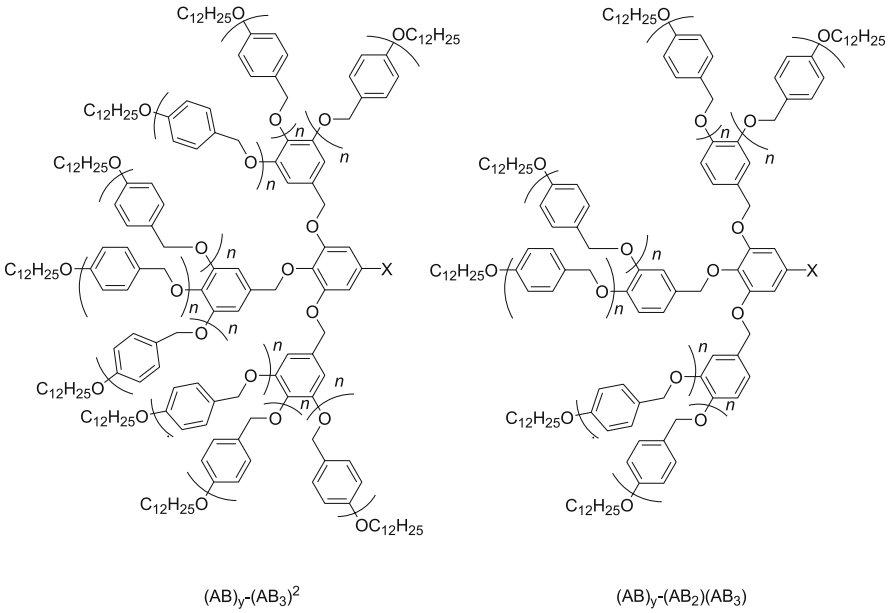

Fig. 10 Structure of the $(AB)_y$-$(AB_3)^2$ and $(AB)_y$-$(AB_2)(AB_3)$ hybrid dendrons of the second generation (y: number of AB blocks, see text)

Continuing in this direction, because of the large structural possibilities offered by this synthetic approach, other compounds with mixed hybrid structures could be prepared. A few isomeric dendrimers based on the (AB_2) unit with the 3,4 and 3,5 arborescence were also synthesized. The AB_2 hybrid dendrons $(AB)_y$-(3,4-AB_2)-$AB)_z$-(3,4-AB_2) (Fig. 11, $y + z = 4, 6, 12$, $z = 0, 2, 4$) yielded 3D cubic structures with an additional Col_h phase for the compound with $m = 1$ and $n = 0$. In contrast, the isomeric series $(AB)_y$-(3,4-AB_2)-$(AB)_z$-(3,5-AB_2) yielded mainly 2D columnar phases, namely a Col_h, then both Col_r and Col_h, and finally a single Col_r phase for the three compounds with $m = n = 0$, $m = 1$ and $n = 0$, and $m = 2$ and $n = 1$, respectively.

All the above examples show that supramolecular dendromesogens of various shape and dimensions (in the nanometer scale) can be obtained through a large variety of AB building blocks connected together according to various topologies, and through an efficient three-dimensional self-assembling process (Fig. 12). There is no doubt that such supramolecular nanostructures are of particular interest in complex soft matter in general, but represent also promising materials for optoelectronics, electronics and surface nanopatterning. Surface alignment and control of self-assembled columnar dendritic liquid crystals in thin films [127–129] as well as formation of Langmuir monolayers were also reported [130, 131].

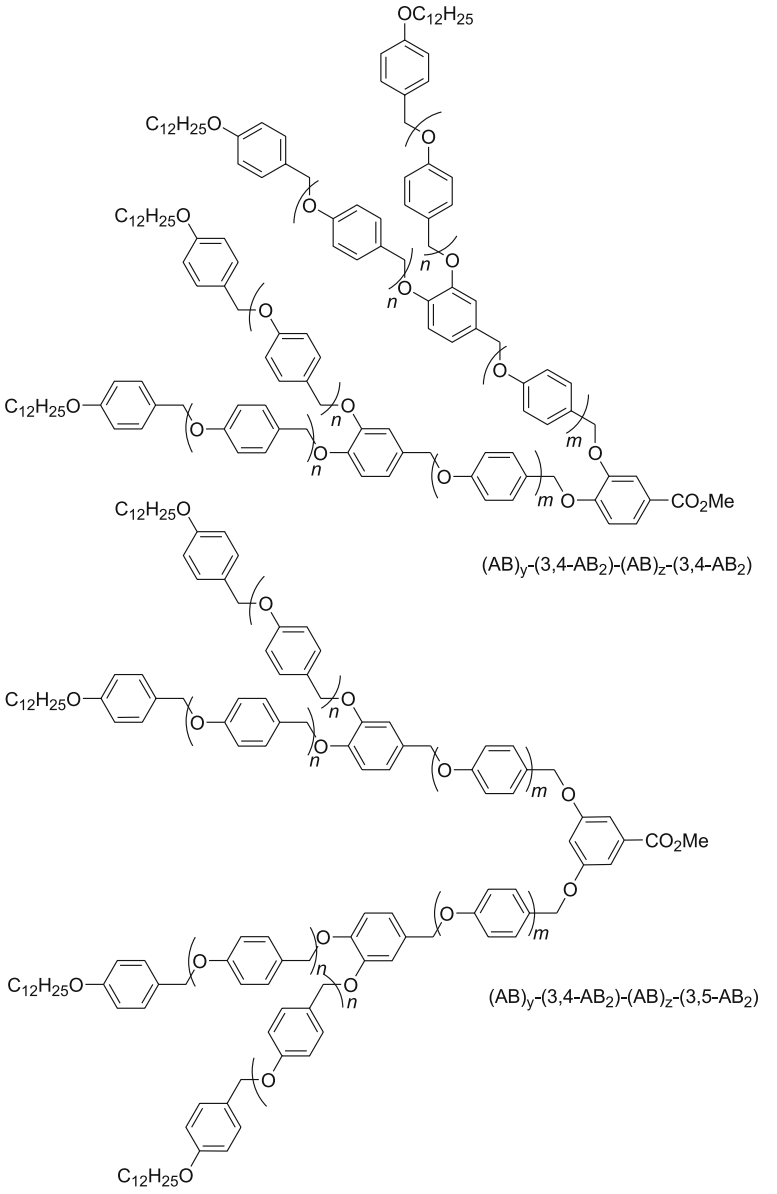

Fig. 11 Structure of the isomeric $(AB)_y$-(3,4-AB_2)-$(AB)_z$-(3,4-AB_2) and $(AB)_y$-(3,4-AB_2)-$(AB)_z$-(3,5-AB_2) hybrid dendrons of the second generation (*y* and *z*: number of AB blocks, see text)

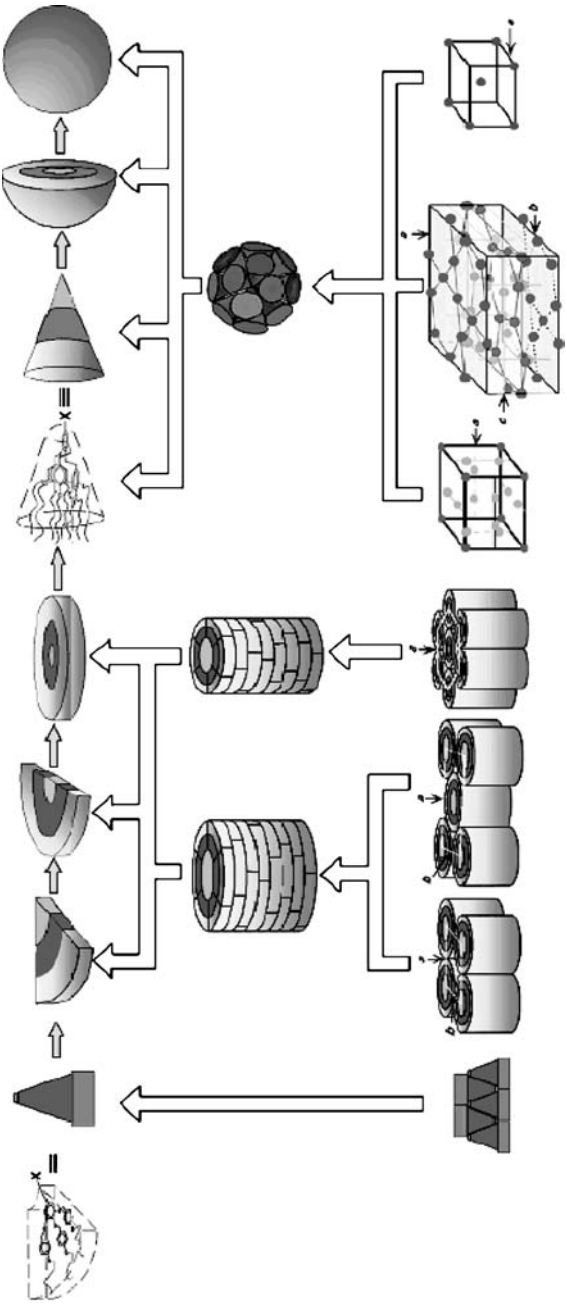

Fig. 12 Schematic representation of the self-assembly of dendromesogens into various type of mesophases (smectic, hexagonal and rectangular columnar, micellar cubic, and tetragonal phases) by the control of the molecular shape conformation (from flat tapered to cylindrical to conical and to spherical shape). From [126]

3
Side-Chain Liquid-Crystalline Dendrimers

The overall structure of such side-group LCDs (this terminology is used by analogy to side-chain liquid crystal polymers) consists of a flexible branched network with a branching multiplicity N_B, emanating from a single multivalent initiator core with a connectivity N_C, and mesogenic or pro-mesogenic units attached laterally (end-on) or terminally (side-on) at the termini of the branches (Fig. 13). The number of peripheral groups, Z, depends on these two structural parameters (N_C and N_B) as well as the generation number, G, according to the geometrical law: $Z = N_C N_B^G$. The control of the molecular conformation in such side-chain LC dendrimers will be considered thoroughly hereafter.

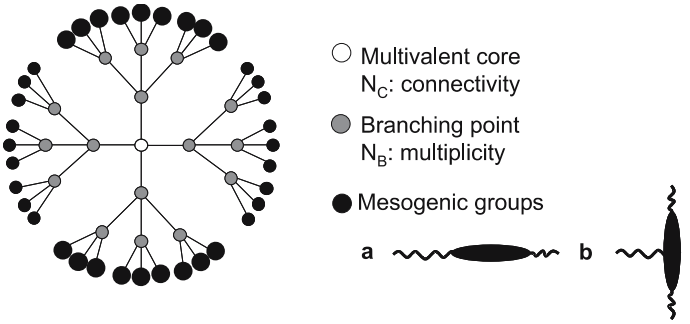

Fig. 13 Schematic 2D representation of an end-group dendrimer of second generation with a 4-fold core connectivity ($N_C = 4$), and a ternary branch multiplicity ($N_B = 3$). The mesogen can be attached terminally or laterally to yield **a** end-on or **b** side-on LCDs

3.1
Silicon-Containing Dendrimers

Silicon-containing dendrimers were the first heteroatom-based dendrimers synthesized, and three types of linkage were used at the branching points: carbosilane (Si – C), siloxane (Si – O) and carbosilazane (Si – N) bonds [41–45]. The carbosilane type represents the most important class of silicon-containing dendrimers mainly because of their excellent chemical and thermal stability, and the versatility of Si – C chemistry allowing access to macromolecules of high generation (up to the seventh) [43, 44]. Liquid crystalline dendrimers based on polycarbosilane and polysiloxane branched backbones have been reported by several groups.

3.1.1
Carbosilane Dendrimers

Frey and coworkers have prepared dendrimers-based on the carbosilane backbone with 4 (G0), 12 (G1), 36 (G2), and 108 (G3) cholesteryl end-groups via esterification of dendritic carbosilane polyols with cholesteryl chloroformate (Fig. 14) [132–134]. The fast increase in the number of terminal groups

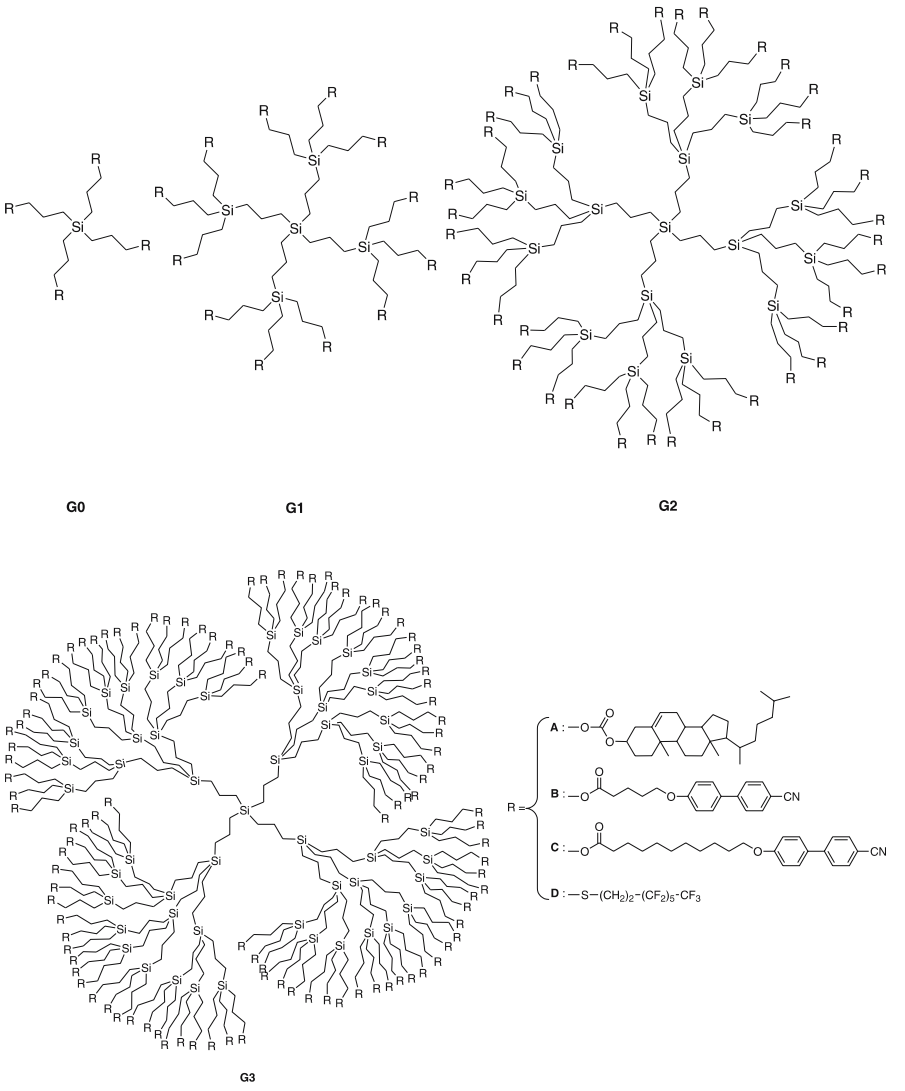

Fig. 14 Carbosilane dendrimers ($N_C = 4$, $N_B = 3$) from the zeroth to the second generation and the various groups attached at the periphery (R = A, B, C, D)

was because of the combination of a high core connectivity ($N_C = 4$) and the ternary degree of branching ($N_B = 3$), and despite the synthetic challenge, the polydispersity indices were in all cases close to unity. The mesomorphism of these dendrimers is nevertheless not totally clear. Indeed, the authors first reported that the G1 and G2 dendrimers (Fig. 14, R = A) were crystalline powders at ambient temperature and formed smectic mesophases between 80–90 °C and 130 °C, whereas that of the third generation was not mesomorphic. However, in a subsequent paper, and on the basis of X-ray diffraction experiments, they reported a lamellar structure for G1, but a 3D Col_h phase for G3, whereas it was not definite that G2 was mesomorphic [135]. These dendrimers were also found to be capable of self-assembly into ultrathin monolayers and multi-layer films.

In further studies, the same group investigated the effect of the nature of the mesogenic end groups and of the spacer length between the dendritic scaffold and the mesogen on the liquid crystalline properties. Thus, dendrimers of the first and second generation were prepared by esterification of the hydroxyl groups of the carbosilane arborols by derivatized cyanobiphenyl units (Fig. 14, R = B and C) [136, 137]. The four dendrimers possess a smectic mesomorphism identified by X-ray diffraction as SmA (R = B, G1: G 17 SmA 98 I and G2: G 17 SmA 130 I) and SmE and SmA phases (R = C, G1: G 14 SmE 67 SmA 106 I, G2: G 7 SmE 61 SmA 130 I). The clearing temperature was independent of the spacer length, but increased from G1 to G2.

Interestingly, besides the use of such classical calamitic mesogens, attachment of the non-mesomorphic perfluorinated alkyl chains to the same carbosilane polyols also yielded original mesomorphic systems. Thus, perfluorinated dendrimers of the zeroth to the third generation having 4, 12, 36, and 108 perfluoalkyl chains were prepared (Fig. 14, R = D) [138, 139]. Whereas G0 was obtained as a crystalline material devoid of mesomorphism (Cr 23 I), G1 and G2 exhibited a smectic phase (G1: G –30 SmA –15 I; G2: G –39 SmX) and G3 a Col_h phase (G –41 Col_h) [140, 141]; no transition to the isotropic liquid was detected for G2 and G3. In this series, mesomorphism clearly results from microphase segregation between the fluorophilic shell and the lipophilic interior of the dendrimer, since no mesogenic promoter is present [142]. The crossover behavior may be due to the increasingly dense packing of the perfluorinated chains at the periphery forcing the dendrimer core to deform and to adopt a more constrained conformation as the generation increased.

Terunuma and coworkers reported the properties of a different type of carbosilane dendrimer ($N_C = 3$, $N_B = 3$) bearing either cyanobiphenyl species or an optically active unit derived from 2-phenylpyrimidine at the periphery (Fig. 15). Only three branches emanated from the central silicon atom, the fourth valency being blocked by a phenyl group leading to 3 (G0), 9 (G1), and 27 (G2) terminal functional units.

All the dendrimers with cyanobiphenyl units (Fig. 15, R = A, $m = 5$) exhibited a single enantiotropic SmA phase, for which the stability was found

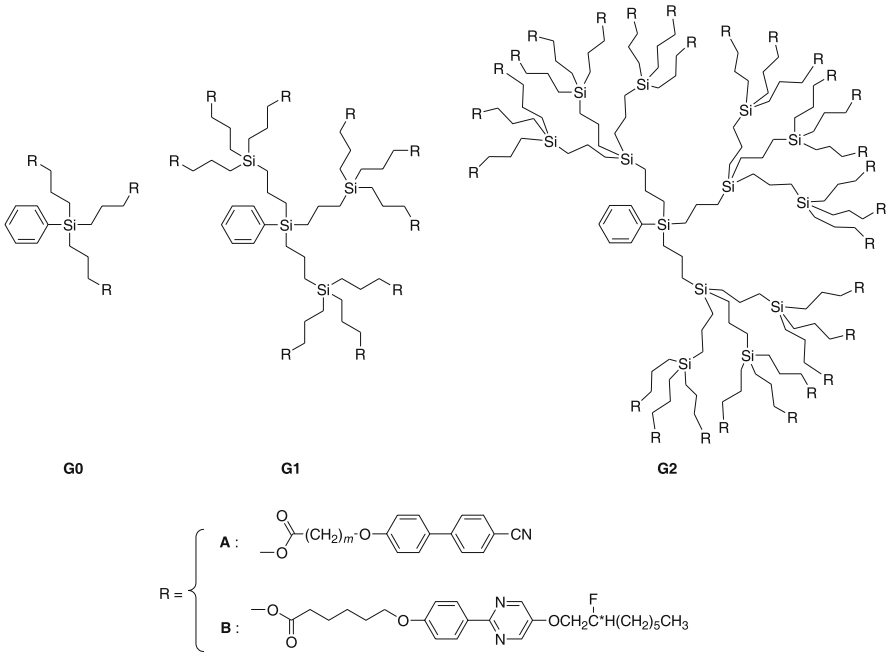

Fig. 15 Carbosilane dendrimers ($N_C = 3$, $N_B = 3$) functionalized by various R groups

to increase with generation number (Table 3) [143], whereas it was not affected to a great extent by the spacer length at a fixed generation (Fig. 15, R = A, $m = 4$–7) [144]. The dendrimers containing the chiral moieties (Fig. 15, R = B) exhibited a broad SmA phase only from room temperature up to around 80, 100, and 110 °C respectively [145]. However, the blends containing 10 wt % of the dendrimer with a non-chiral, liquid crystal material (also derived from 2-phenylpyrimidine), exhibited a broad ferroelectric SmC* phase from room temperature up to ca. 60 °C with additional SmA and N* phases before isotropization at 83–85 °C. No influence of the generation could be felt here, but the mixtures exhibited ferroelectric behavior, with an electro-optical switching time increasing with the generation number as in ferroelectric liquid crystalline polymers.

Table 3 Mesomorphic behavior of the compounds shown in Fig. 15

G*n*	Mesogen A ($m = 5$)	Mesogen B	Blend
G0	G 7 SmA 44 I	SmA 80 I	Cr 5.5 SmC* 62 SmA 71 N* 83 I
G1	G 14 SmA 72 I	SmA 105 I	Cr 7 SmC* 59 SmA 72 N* 85 I
G2	G 15 SmA 115 I	SmA 110 I	Cr 7 SmC* 56 SmA 72 N* 83 I

Let us also mention the only example of a bent-core molecule [146] fixed to the zeroth generation of a carbosilane core (Fig. 16) [147]. Truly speaking, this molecule, abusively referred to as a dendrimer, should be seen as a branched tetramer, since there is no branching, but the concept may be successfully applied for the supermolecules of higher generations (vide infra the case of PPI dendrimers bearing bent core mesogens). This compound exhibits a new type of polar smectic mesophase between the glassy state and the isotropic liquid (G 47 $SmCP_R$ 139 I), this organization resulting from a compromise between both the constraints imposed by the bent molecule and by the carbosilane moiety. By X-ray diffraction and optical microscopy, it was proposed that the molecules are tilted and adapt a polar order within the layers, but both the polar and tilt directions change randomly (no long-range orientational correlation between layers) in such a way that the polarization is cancelled, leading to an optically uniaxial phase. Switching into the ferroelectric organization ($SmCP_F$) can be achieved upon the application of a strong electric field due to the alignment of the polar directors of the layers parallel to the electric field. Once formed, the ferroelectric state remains stable, and spontaneous polarization as high as $P_S = 1400\ nC\ cm^{-2}$ could be measured.

Probably the most complete study on silicon-containing LCDs was that carried out by the group of Shibaev. The dendritic motif is based on a tetravalent core ($N_C = 4$), and a binary branching point ($N_B = 2$) leading to 4, 8, 16, 32, 64 and 128 terminal mesogens from G0 up to G5 (Fig. 17). The link with the mesogenic group is achieved by the hydrosilylation reaction between the peripheral double bonds of the dendrimer and the monosilylated mesogen. The effect of the nature of the mesogen and the generation of the dendrimer has been systematically analyzed.

These mesomorphic carbosilane dendrimers are characterized by a "surface" layer of mesogenic groups on the dendritic macromolecules of regular structures, responsible for the liquid-crystalline states of these compounds. The possibility of the creation of a liquid-crystalline shell around a central nucleus core formed by the soft dendritic matrix opens perspectives for the applications of such compounds. In a first paper [148], only the smallest generation (G1) of carbosilane dendrimer was synthesized and studied, the basic reaction used being hydrosilylation between the mesogen-containing fragments and the allyl groups of the dendritic matrix [149]. The liquid-

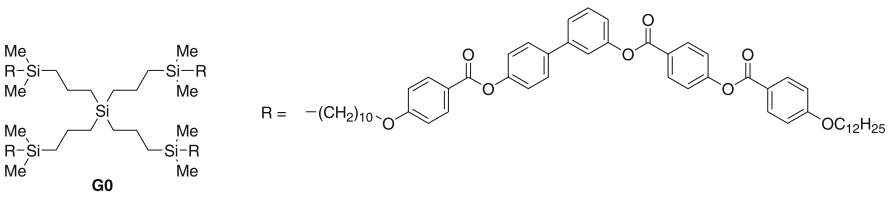

Fig. 16 Molecular structure of the zeroth generation dendrimer bearing a bent mesogen

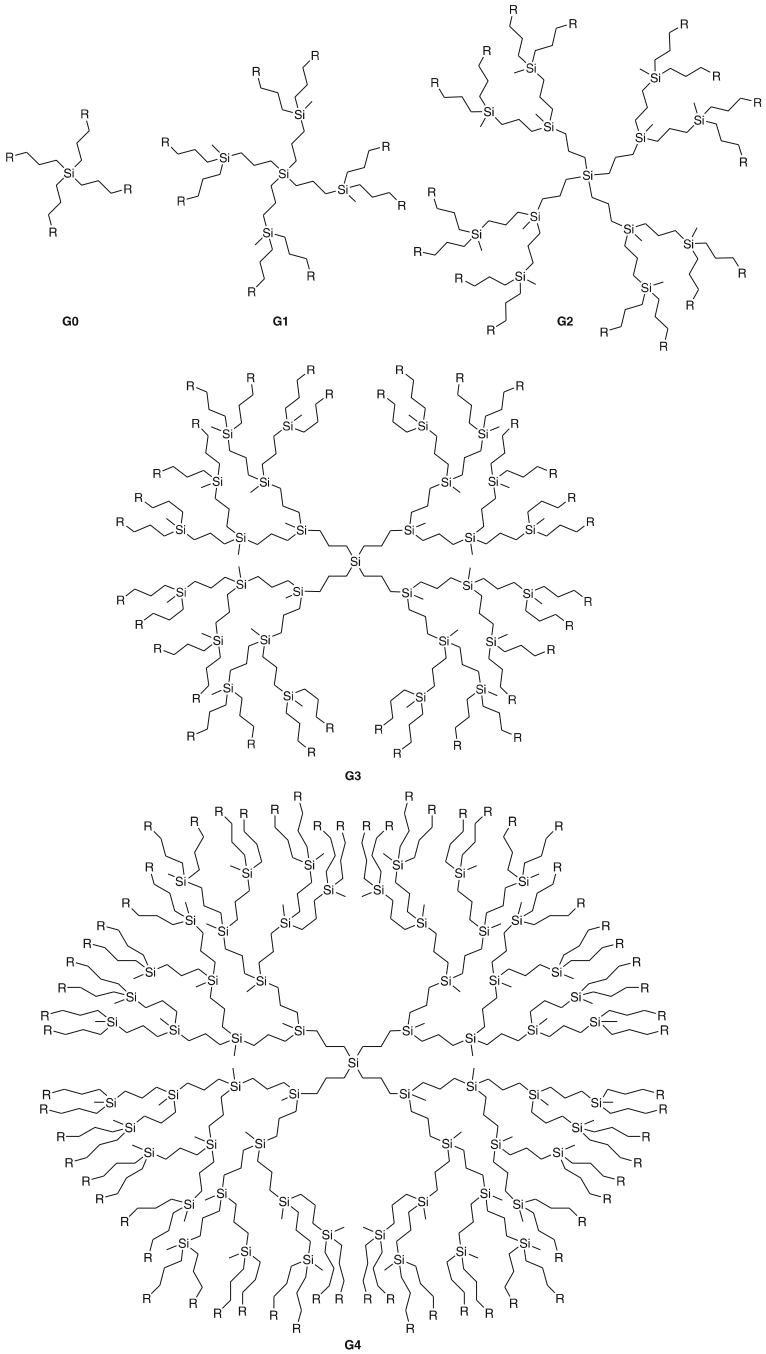

Fig. 17 Carbosilane dendrimer ($N_C = 4$, $N_B = 2$) from G0 to G4 bearing mesogenic R groups (G5 not reproduced here)

crystalline properties of the dendrimers were determined by optical polarizing microscopy in combination with differential scanning calorimetry (DSC) measurements and X-ray diffraction.

The phase behavior of the G1 compounds depends on the chemical nature of the terminal mesogenic groups. In the case of cholesteryl-containing dendrimers, a single smectic A phase was observed above a glassy phase, the glass transition temperature being below room temperature (Fig. 18, R = C: G –15 SmA 100 I). The layer spacing is in the range of 43–45 Å with an intermolecular distance of about 6 Å between the cholesteryl moieties. In the

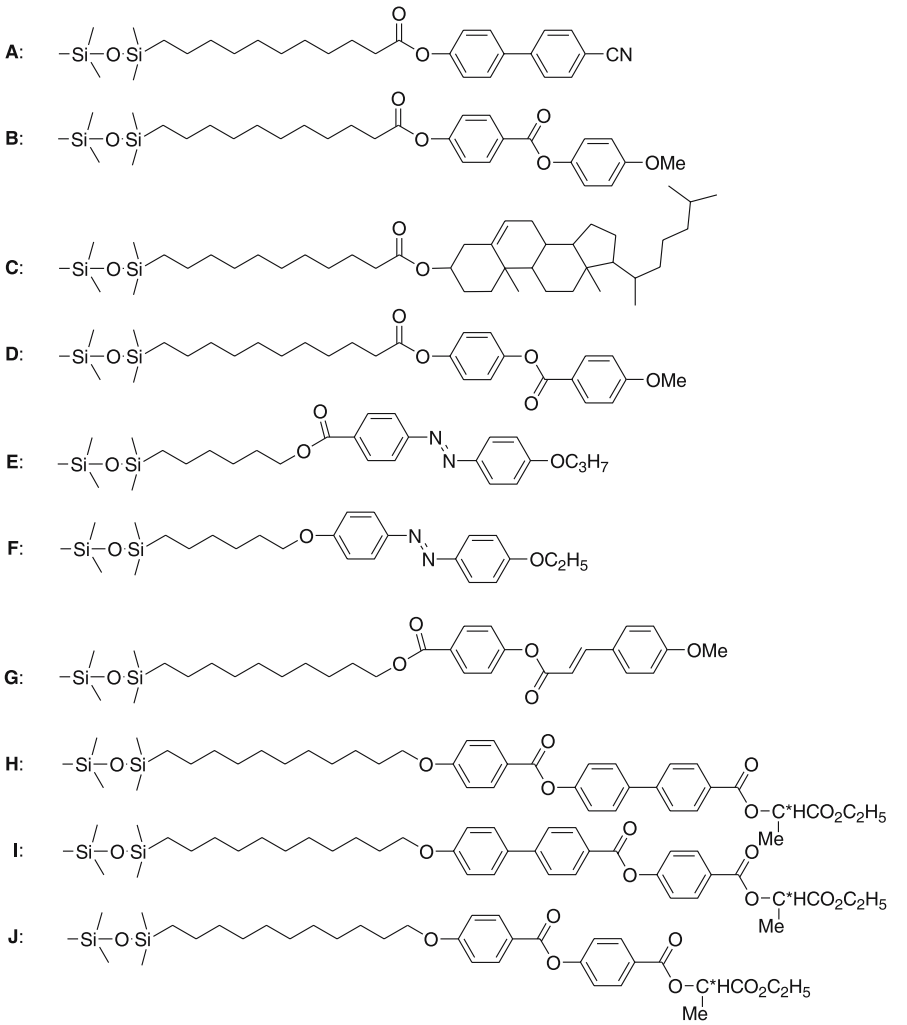

Fig. 18 Various R groups used for carbosilane-siloxy dendrimers shown in Fig. 17

other cases of cyanobiphenyl- (Fig. 18, R = A, Table 4) and methoxy phenyl benzoate-containing dendrimers (Fig. 18, R = B, Table 5), lamellar smectic A and C mesophases were identified with a layer spacing of about 42 Å; in these cases, two additional diffuse bands in the wide angle region of the X-ray diffraction patterns are related first to the intermolecular distance between the mesogenic groups (∼ 5 Å) and to the dendritic matrix itself (∼ 7 Å). Investigations of electro-optical properties of these dendrimers show that the dielectric polarization is proportional to the second power of the electric field in accordance with the Kerr law and that the Kerr constants are close to those of the low molar mass analogues of the corresponding mesogenic groups [150]. This suggests that the freedom in the orientation of the mesogenic groups is one of the most important factors influencing the capability of these compounds to form mesomorphic phases.

The synthesis of higher generations, up to the fifth one, was later described by the authors (Tables 4 and 5) [151, 152]. Following a divergent scheme, the strategy used for preparing the carbosilane dendrimers with terminal mesogenic groups (Fig. 18, R = A and B) involved three main steps: first the synthesis of carbosilane dendrimers with terminal allylic groups, then the modification of mesogens by the introduction of reactive terminal

Table 4 Mesomorphic behavior of the carbosilane dendrimers bearing cyanobiphenyl mesogens [a]

G*n*	R = A
G1	G –22.5 SmC 50 SmA 91.5 I
G2	G –21 SmC 55 SmA 89.5 I
G3	G –22.5 SmC 57 SmA 92 I
G4	G –21 SmA 109 I
G5	G –20 SmA T_X Col_r 121 Col_h 130 I

[a] T_X: transition temperature was not determined

Table 5 Mesomorphic behavior of the isomeric carbosilane dendrimers bearing methoxyphenyl benzoate (B) and anisic acid derivative (D) mesogens

G*n*	R = B	R = D
G1	G 30 SmC 77 I	G 30 SmC 52 SmA 58 I
G2	G 27 SmC 60 SmA 78 I	G 25 SmC 64 SmA 70 I
G3	G 15 SmC 67 SmA 81 I	G 10 SmC 65 SmA 79.5 I
G4	G 15.5 SmC 80 SmA 86 I	G 8 SmC 69 SmA 77.5 I
G5	G 12.8 Col_r 80.2 SmA T_X Col_h 96 I	G 0 M1 50 M2 95 I

groups such as Si – H and finally the attachment of these modified mesogenic groups onto the surface of the carbosilane dendrimers. Structural studies on both series of dendrimers, containing either terminal cyanobiphenyl or methoxyphenyl benzoate groups, show the existence of disordered smectic phases (smectic A and C) up to the fourth generation despite the assumed globular shape of the dendritic core [153], with layers of mesogenic groups alternating with layers formed by the carbosilane dendritic cores and aliphatic spacers. This model is supported by viscosity measurements in toluene and chloroform solutions of dendrimers which indicate that an increase in the generation number entails an increase in the crown size due to uncoiling of the terminal chains in the direction normal to the core surface [154, 155]. It is interesting to note that the layer spacing is almost constant with the low generation materials, and varies slightly for the high generation compounds, always in the range between 40 and 50 Å.

The phase diagram for the system G3 dendrimer (Fig. 18, R = A) and CCl_4, in the temperature range 0–90 °C, and concentration range 1–55 wt % was realized experimentally [156]. It showed two domains of phase co-existence: between 1 and 36.5 wt % of dendrimer, two phases coexist without varying their composition with temperature, and in the concentration range 36.5–55 wt %, the system separates into two phases, one being liquid-crystalline.

Molecular dynamics simulation studies of a third generation carbosilane dendrimer bearing cyanobiphenyl groups (Fig. 18, R = A) in solution have been carried out [157]. An hybrid model was used where the heavy atoms of the dendritic core are represented by Lennard-Jones sites and the mesogenic peripheral units by Gay–Berne potentials. It is shown that in the isotropic phase, the dendrimer adopts a spherical shape, with the alkyl chains (linking the mesogenic groups to the dendritic core) wrapping around the core and the terminal mesogenic units arranged randomly near the surface of the dendrimer. In the nematic and smectic solvents, the dendrimer core adopts a similar structure to the isotropic phase, but the terminal mesogenic units align to lie close to the solvent director. This occurs through a rearrangement of the alkyl chain conformations resulting in the dendrimer forming a rod shape. Such fluctuations in the conformations of the alkyl chains allow the dendrimer as a whole to become elongated along the nematic director and the peripheral mesogenic groups to align with an order parameter approaching that of the solvent. Such an elongation of dendrimers to form rod-shaped structures is consistent with the induction of lamellar phases in the bulk.

Unexpectedly, the fifth generation of the carbosilane LC dendrimers containing 128 terminal cyano groups not only form a lamellar but also supramolecular columnar mesostructures [158]. A smectic A phase exists at low temperature, for which the molecular organization is the same as that of the previous generations with a layer spacing of 53 Å despite the presence of the large number of peripheral mesogenic groups. At higher temperature,

this lamellar mesophase transforms firstly into a rectangular columnar phase, and on further heating into a hexagonal columnar phase. The explanation of this behavior given by the authors is based on a change of the molecular shape. With the increase of the temperature, the carbosilane LC dendrimers become less elongated and their shape more circular, favoring the formation of ellipsoidal columns. Each column consists of the stacking of ellipsoidal molecules, elongated in a direction perpendicular to the columnar axis. Further increase of the temperature leads to a more symmetrical shape of the LC dendrimers which become circular. The columns would then result from the stacking of these quasi-discoid molecules, and the arrangement of the latter into a hexagonal packing (Fig. 19). In both rectangular and hexagonal phases, the surface of the columns is covered by the mesogenic groups while their inner part consists of soft dendritic cores. A similar trend in the mesomorphic properties was observed with carbosilane dendrimers terminated with methoxyphenyl benzoate groups and with the mesogens based on anisic acid derivatives, isomeric system to B, (Fig. 18, R = B and D, Table 5) with little differences in the transition temperatures [159, 160].

The dielectric properties of fourth-generation mesogenic carbosilane dendrimers with alkyloxycyanobiphenyl terminal groups were studied. Permittivity and dielectric loss measurements were performed in the mesophase and isotropic phase in the range of electric field frequencies 1 kHz–100 MHz. A dispersion of permittivities was observed in this frequency range. It was shown that dispersion in the isotropic phase could be caused by two Debye-type relaxation processes. The activation energy of the low-frequency relaxation process decreased as the length of the alkyl chain of terminal dendrimer mesogen groups increased [161].

The analysis of these systems was completed by AFM studies [162, 163]. In particular AFM pictures of a monolayer of the fifth generation of the cyanobiphenyl-containing dendrimer shows patches with a thickness of ~ 3 nm on silicon substrate. These patches consist of individual particles. The

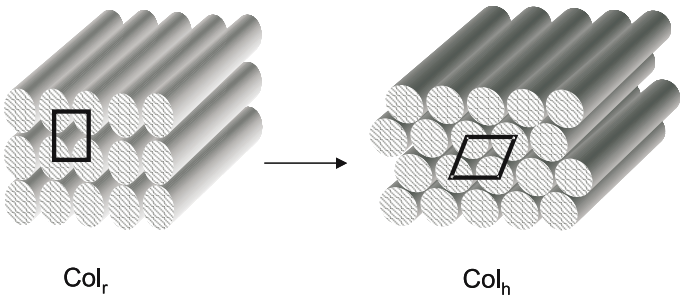

Fig. 19 Schematic diagrams of model structures formed by carbosilane LC dendrimers of the fifth generation (G5)

distance between the particles is close to the estimated size of one individual dendrimer which equals 5.5 nm according to X-ray diffraction data. Using a mica substrate, one can distinguish a rectangular two-dimensional packing. The structural ordering of some of these carbosilane LCDs within surface monolayers was studied, and found to strongly depend on the nature of the substrates (hydrophilic or hydrophobic) [164].

The influence of generation number on the phase behavior shows firstly that the glass transition temperature remains more or less constant and secondly that both the temperature and the enthalpy of the SmC-SmA transition increase whereas the enthalpy of the SmA-I transition temperature decreases with increasing the generation number. The increase of the transition temperatures is explained by a strengthening of the cooperative interactions of the increasing number of terminal mesogenic groups, and the decrease of the enthalpy by the more and more symmetrical shape of the LC dendrimers. According to the authors, these two opposite tendencies compete and result in the appearance of new supramolecular structures with a columnar morphology for the highest generation dendrimer [165].

In order to introduce electro-optical properties such as ferroelectric properties, Shibaev and coworkers first prepared carbosilane dendrimers of generation 1 to 3 with 8, 16 and 32 terminal ethyl-L-lactate-containing mesogenic groups (Fig. 18, R = H, I and J, Table 6) [166–169]. All the dendrimers exhibit a chiral smectic C mesophase above the glass transition in a broad temperature range, leading to ferroelectric properties (Table 6). For these dendrimers, the glass transition temperature does not depend on the generation number and is about –5 °C (Fig. 18, R = H and I) or –17 °C (Fig. 18, R = J). However, the decrease of the anisotropy of the mesogen leads to a strong diminution of the clearing temperature near to room temperature. The spontaneous polarization measurements were only possible at relatively high temperature, i.e. 80 °C, mainly because of the high viscosity of the materials at lower temperature. The highest values of Ps have been found to be around 140 nC cm^{-2}. The increase in generation number leads to a decrease in the value of Ps and to an increase in the switching time.

Table 6 Mesomorphic behavior of the carbosilane dendrimers bearing chiral mesogens (H, I and J)

G*n*	R = I	R = H	R = J
G1	G –5 SmC* 176 SmA 182 I	G –5 SmC* 175 I	G –17 SmC* 47 I
G2	G –5 SmC* 159 SmA 166 I	G –4 SmC* 167 I	G –17 SmC* 46 I
G3	G –5 SmC* 156 SmA 183 I	G –4 SmC* 158 I	G –17 SmC* 44 I
G4	G –4 Col_r 173 I	G – 4 Col_r 160 I	
G5	G –6 Col_r 178 I	G –6 Col_r 162 I	

The analogous dendrimers of higher generation (fourth and fifth, Table 6) exhibit only a rectangular columnar mesophase above the glass transition temperature, always about –5 °C [170]. According to the authors, each column consists of ellipsoidal disks of dendrimers as before, flattened towards the columnar axis in one direction and elongated perpendicular to that direction. The mesogenic groups are located entirely on the surface of the columns, while the inner part of the columns consists of the dendritic cores.

More recently, they also considered photosensitive dendrimers. The interest in such compounds is because of new opportunities provided by such systems in the production of various optical devices and the preparation of materials suitable for optical data storage. Moreover, the development of photoactive dendrimers capable of forming liquid-crystalline phases is particularly interesting, because a low viscosity of dendrimers is expected to induce a fast response of the so-called dendrimers to the action of an external field such as for example light irradiation (photosensitive materials). The first example concerns a liquid crystalline carbosilane dendrimer of first generation with azobenzene terminal groups (Fig. 18, R = E), exhibiting a smectic A mesophase (G –15 SmX 9 SmA 51 I) as for the dendrimers described above with various terminal mesogenic groups [171]. In this case, the azobenzene terminal moiety serves a dual function; on one hand, its rigid anisometric shape ensures the development of a mesomorphic state, and on the other hand, the presence of azo-chromophores ensures that the LC dendrimer is sensitive to light irradiation. It was shown that the $E - Z$ photopolymerization of the azobenzene groups proceeds both in solution and in film under UV irradiation. This process is reversible photochemically and thermally. In addition, it was shown that UV irradiation destroys the smectic ordering and gives rise to a transition to the isotropic liquid, because of the fact that the *Z*-isomer of an azobenzene moiety possesses a low anisometry. A very similar photochemical behavior is observed for the related non-mesomorphic azobenzene-containing dendrimers of higher generations (Fig. 18, R = F, G1, G3, and G5) [172].

The irradiation of the same dendrimer with a linearly polarized light (365 nm) results in an angular dependent E/Z photoisomerization, but the photo-orientation process was not observed practically. A quite different behavior is observed when the film of the dendrimer is irradiated with a linearly polarized green light (488 nm), where a well-pronounced linear dichroism is observed. However, the degree of photo-orientation of the azobenzene groups is rather low, the photo-induced parameter being much lower than the order parameter of the aligned smectic A phase [173]. In contrast, a strong effect is observed in different generations of carbosilane dendrimers where the terminal azobenzene moiety has a very slightly different chemical structure [172]. Under irradiation of the amorphous films by polarized light, a process of photo-orientation of azobenzene groups in the direction perpendicular to the direction of vector *E* of incident light is observed with three mean features.

First with UV radiation, the values of linear dichroism and of the order parameter do not depend on the generation number of the dendrimers. This indicates that a local surrounding of azobenzene groups in these films is similar independently of the molecular weight of the dendrimers. The second feature is the unusual behavior of the order parameter of the azobenzene groups under irradiation. After an increase at the beginning of the irradiation, the order parameter levels off and decreases down to zero, leading to a full degeneration of the orientational order of the system under prolonged light exposure. The third feature is the absence of photo-orientation processes under irradiation of the films by polarized light from an Ar-laser (488 nm).

Another carbosilane dendrimer of first generation containing terminal cinnamoyl groups (Fig. 18, R = G: G –28 SmA 58 I) which undergo *E*/*Z* photoisomerization was prepared according to a new synthetic approach, consisting of the synthesis of the dendrimer with terminal hydroxyl groups, followed by the coupling of 4-methoxycinnamoyl chloride [174]. In the liquid-crystalline phase under UV radiation, the dendrimer undergoes *E*/*Z* isomerization of the cinnamoyl groups, but also photo-cycloaddition leading to the formation of a three-dimensional network. These processes lead to a disordering effect and to an isothermal photo-induced smectic A to isotropic liquid phase transition.

As for the silane-containing dendrimers discussed above, some zeroth generation siloxysilanes were reported (Fig. 20). Again, these branched oligomers cannot be called dendrimers, but the interest of this study was the relationships between the core connectivity (N_C = 2, 3, and 4) and the mesomorphic

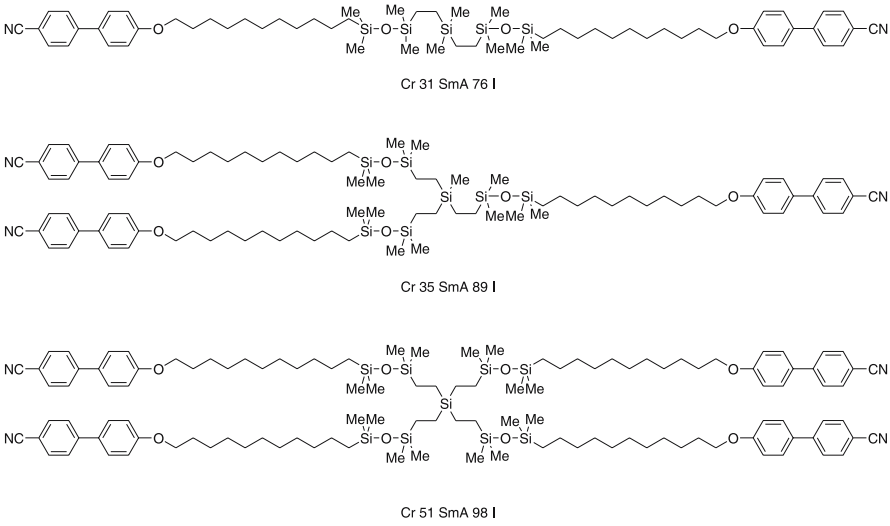

Fig. 20 Effect of the connectivity number of the core of some zeroth generation dendrimers

properties, able to bring useful information once extended to dendrimers. Thus, the linear dimer and the branched trimer and tetramer (Fig. 20) containing several cyanobiphenyl groups were prepared [175, 176]. As the number of mesogenic groups increases, the temperature range and the stability of the SmA phase increases quite steadily, but as expected the nature of the phase was not changed. Likely as the molecule becomes larger, the mesogenic arms have less freedom, and thus certain molecular conformations are more favored than others. As above, the smectic structures consist of a central silicon-containing layer, sandwiched between mesogenic groups, overlapping between layers. The related tetrakis(dimethylsilyl)silane functionalized by pro-mesogenic groups also gives rise to smectic phases [177].

3.1.2
Siloxane Dendrimers

There have been very few families of dendrimers built up around a pure siloxane core. One such dendrimer consisted of a dendritic methylsesquioxane matrix ($N_C = 3$, $N_B = 2$, Fig. 21) to which six terminal cholesteryl groups were attached via undecylene spacers [178]. This G1 compound exhibited a very broad temperature SmA phase (G –1.5 SmA 120 I). The molecules arrange in a single layer smectic phase with complete overlap of the cholesteryl mesogens separated by siloxane layers.

Cyanobiphenyl groups have been attached to tetrakis(dimethyloxy)siloxane to form a branched tetramer or tetrapede (Fig. 22, R = A, G0), which is similar to the siloxysilane derivative just discussed above (Fig. 20). Here again, whatever the spacer length, a smectic mesomorphism was detected, and a substantial increase of the mesophase stability and temperature range were observed as the aliphatic connector length increases; an additional unidentified phase was observed for $n = 9$, SmX (likely SmC) [179]. Lateral attachment of mesogenic groups onto such a tetravalent core led to the formation of a nematic phase above the SmC phase (Fig. 22, R = B, G0) [180].

In contrast to siloxanes, silsesquioxanes exist as ladder- or cage-type nanostructures, and are formed by complete hydrolytic condensation of their

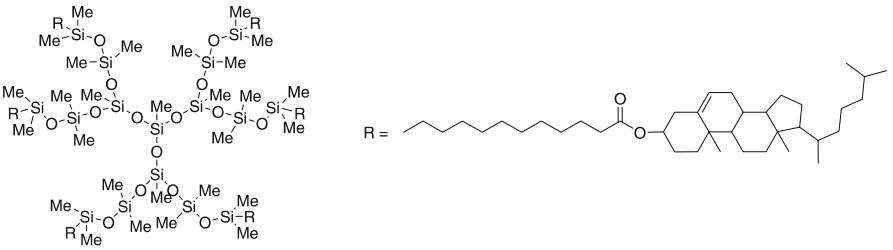

Fig. 21 Chemical structure of the dendritic methylsesquioxane matrix ($N_C = 3$, $N_B = 2$)

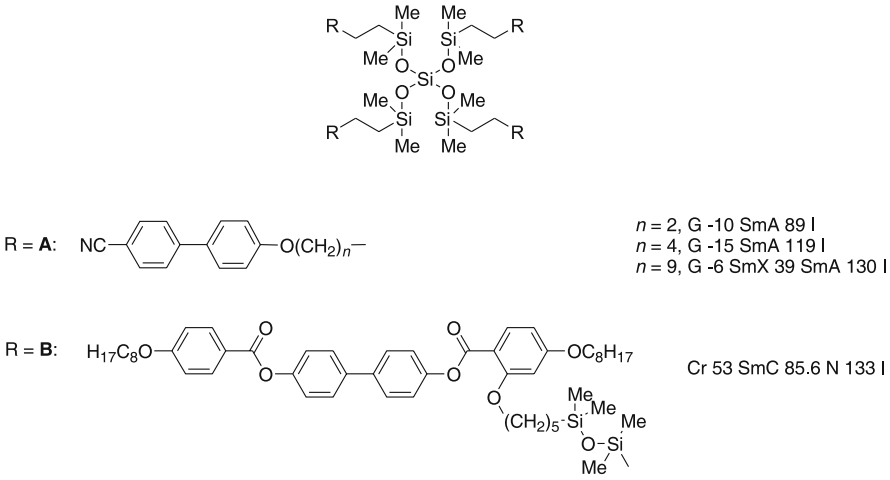

Fig. 22 Tetrakis(dimethyloxy)siloxane bearing four mesogenic groups with end-on and side-on attachment

trifunctional monomers Si_4O_6. Such 3D organosilicon cages are promising in the area of nanocomposites, as when suitably functionalized in the corners, they can be incorporated into organic systems to form hybrid inorganic–organic copolymers with novel properties [181]. The use of these silsesquioxane polyhedral frameworks as initiator cores for liquid crystal dendrimers has only been recently the focus of attention in accordance with the development of efficient syntheses as well as the improvement of the techniques of separation [182]. Such cage-like cores provide a useful central core because they possess several radial primary branches for derivatization, allowing the dense packing limit [183] to be reached at early generations. To start, several polyhedral liquid crystals have been prepared containing cubic cores such as the octa(hydrido)silsesquioxane and octa(dimethylsiloxy)octasilsesquioxane [184–187], and to a lesser extent the hexa(dimethylsiloxy)silsesquioxane [184] with a trigonal prismatic core and the deca(dimethylsiloxy)silsesquioxane [185] with a pentagonal prismatic core functionalized by eight, six, and ten mesogenic side groups (end-on), respectively (Fig. 23). These first generation polyhedral cage-like materials essentially display SmA and SmC phases often directly at the ambient and over broad temperature ranges; the exception are those cuboid materials giving rise to a nematic phase either after partial substitution of the cube [188–190], or by lateral attachment (side-on) of the mesogens [191].

As for the tetramers and dendrimers previously described, the mesogenic arms of the octasilsesquioxane-based materials can arrange parallel to one another; thus these supermolecules can pack together in layers to form a lamellar phase. Molecular simulations in the gas phase at absolute zero confirm this point of view and show that the minimized structure of the

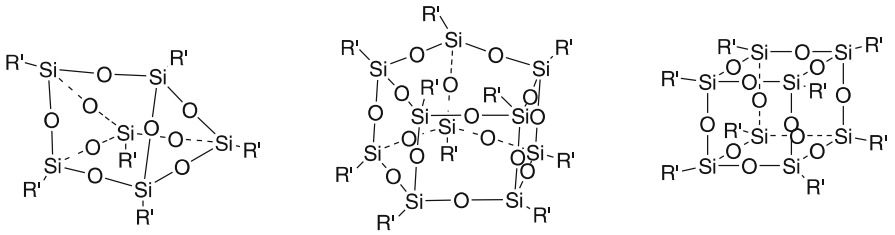

R' = R, R–SiMe$_2$O–, R is a mesogenic group

Fig. 23 Various polyhedral silsesquioxane backbone-based liquid crystals

cyanobiphenyl-substituted octasilsesquioxane is made by the cyanobiphenyl mesogenic arms packed together in a parallel arrangement thereby producing a supermolecular system that has a rod-like shape which is favorable to the formation of smectic A phases. Changing the chemical nature of the cyanobiphenyl groups by other mesogenic groups led to the induction of other smectic phases (eg., SmC) or to chiral phases (when chiral mesogens are attached).

Some dendrimers were eventually obtained by doubling the number of mesogenic groups fixed at each summit of the octa(dimethylsiloxy)octasilsesquioxane cage (Fig. 24). Branching was achieved by using either biforked carbosilane or malonate groups allowing for the preparation of materials containing 16 mesogenic units R (Fig. 24, R = B [192], D [175], F [57, 193] and G [175]). Substituted with cyanobiphenyl groups attached end-on, all first [186] and second generation [175, 192] systems yield to solely smectic phases, with in one case a decrease of the mesophase stability and temperature range on increasing the generation (Fig. 24, R = A → B), whereas the opposite was observed in the other case (Fig. 24, R = C → D). A more drastic change was, however, observed when the mesogens were laterally attached. Indeed, whereas the first generation system strongly promoted chiral nematic phases over broad temperature ranges, starting directly at the ambient [175, 194], the compound of the next generation appears to favor a columnar mesomorphism with both Col_r and Col_h phases being detected; the N* phase existed over a 6 °C temperature range only (Fig. 24, R = E → F). Moreover, in this study, the topology of mesogen attachment was found to strongly influence the mesomorphism (compare the isomeric compounds with R = F and G, Fig. 24). In order to understand the formation of such various mesophases, the authors proposed two extreme but feasible situations. One possibility results from the decoupling of the mesogens and the siloxane-cage thus acting independently, the cuboid core being surrounded by loosely packed mesogens. In the other possibility, the materials act as giant molecular systems, having either rod-like or disk-like shapes. To understand the forma-

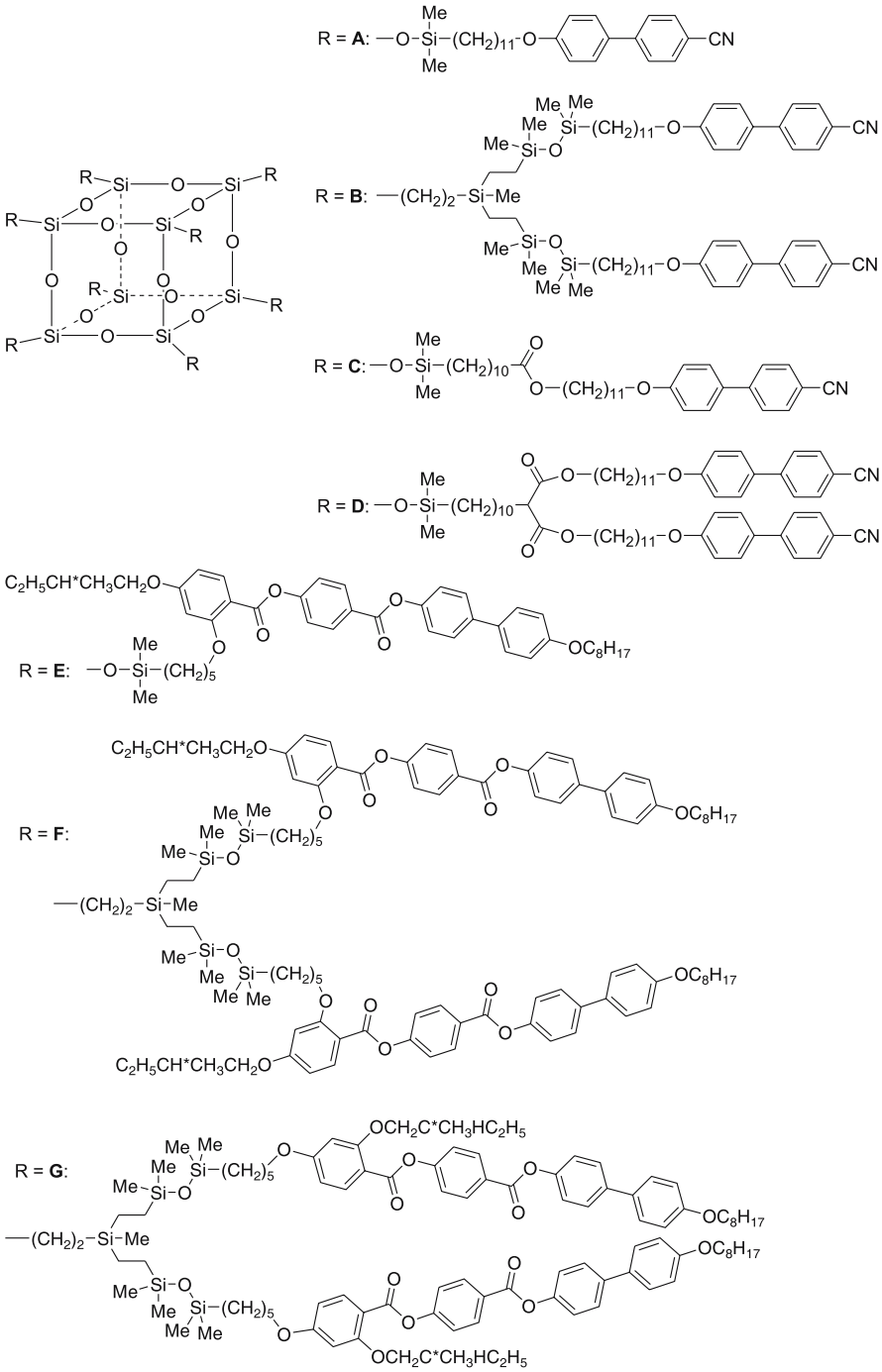

Fig. 24 Octa(dimethylsiloxy)octasilsesquioxane cage-like dendrimers

Table 7 Thermal behavior of the *R*-functionalized octa(dimethylsiloxy)octasilsesquioxane cage-like dendrimers

R	Transition temperatures
A	G –7 SmA 128.5 I
B	G –17.5 SmC 63 SmA 92 I
C	Cr 34.5 SmX 44 SmC 64 I
D	Cr 35 (SmC 30) SmA 96 I
E	G 24 N* 117 I
F	G 5.5 Col_r 30 Col_h 102 N* 108 I
G	Cr 133 SmC* 162 N* 165 I

tion of columnar mesophases, a "cotton-reel" model was proposed in which the dendrimer is assumed to have a cylindrical shape that has approximately the same height as its diameter. The long axes of the mesogenic units are roughly parallel to or slightly tilted with respect to the rotational axis that is normal to the cylinder. It seems that, contrary to the case of side-chain polysiloxane analogues where no columnar mesophase could be observed, the silsesquioxane core assists in the formation of the hexagonal and rectangular disordered structures, presumably through segregation of the siloxane cores from the mesogenic units in distinct columns.

3.1.3 Carbosilazane Dendrimers

Recently, a new dendritic system based on a carbosilazane core ($N_C = 3$, $N_B = 2$) with laterally attached mesogenic units (Fig. 25) [195–197] was synthesized. Depending on the mesogenic unit, these dendrimers exhibit a single, enantiotropic, room temperature nematic phase (Fig. 25, R = A), or in addition to the *N* phase, an additional SmC (G0, G1), or a Col phase (G2) between ca. 50 and 130 °C (Fig. 25, R = B) (Table 8). It is interesting to remark that although the molecular weight of these dendrimers doubles with each

Table 8 Mesomorphic behavior of the carbosilazane dendrimers

G*n*	Mesogen A	Mesogen B
G0	G –26 N 42 I	Cr 73 SmC 74.5 N 130.5 I
G1	G –23 N 40 I	Cr 58 SmC 74.5 N 130 I
G2	G –22 N 41 I	Cr 52 Col_x 73 N 126 I

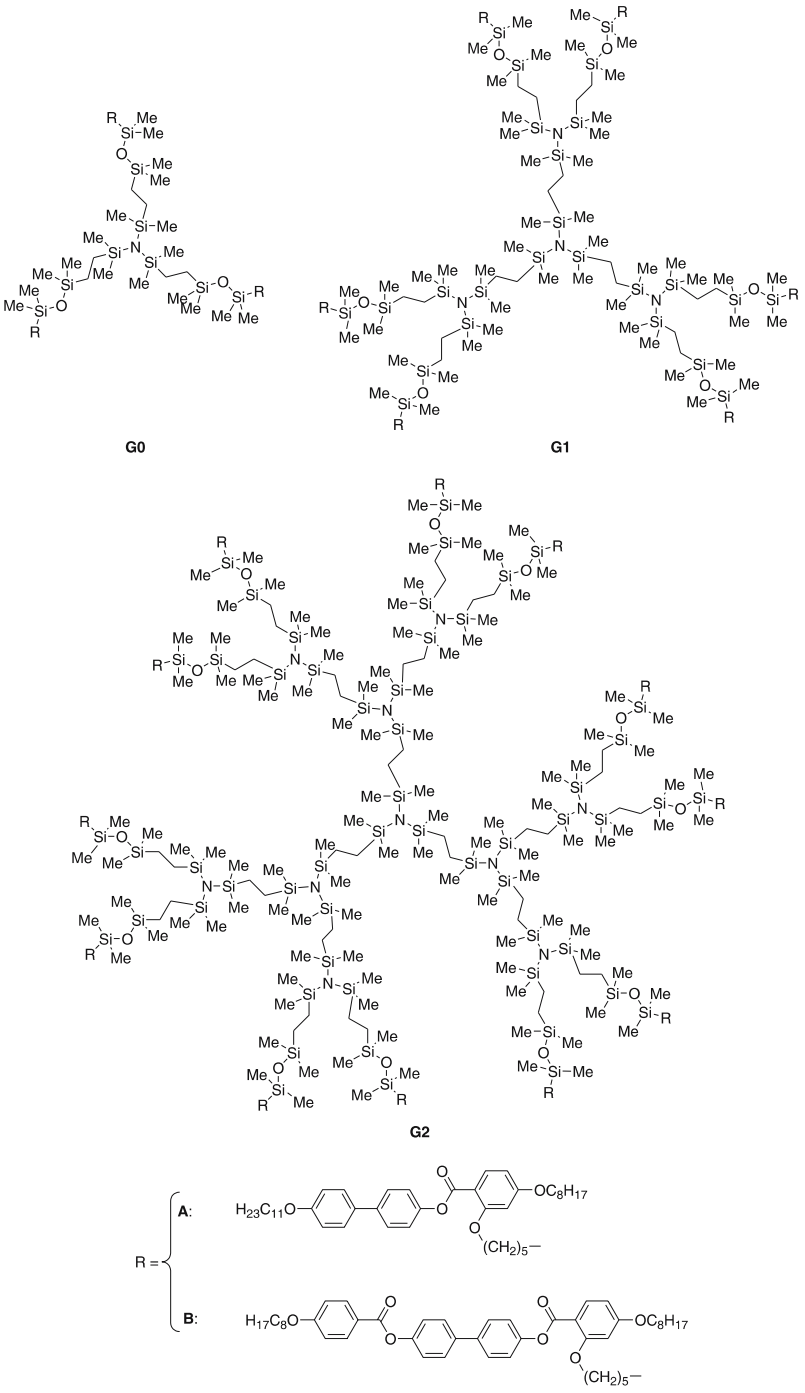

Fig. 25 Carbosilazane dendrimers

subsequent generation, the mesomorphic properties and transition temperatures are similar. This behavior has to be compared with the usual behavior of side-on liquid-crystalline polymers where a strong stabilization of the nematic phase is observed with increasing the degree of polymerization. This indicates that in the case of these nematic dendritic systems, the microphase separation of the silicon- and carbon-rich molecular moieties is not sufficiently pronounced on increasing generation to enhance the stability range of the mesophase. The orientational order and the dynamics of G0 in the nematic phase was analyzed by optical and dielectric studies, and confirmed the complete decoupling between the carbosilazane core and the mesogenic pendant groups [198].

3.2
Polydamidoamine and Polypropyleneimine Dendrimers

The dendritic motif of these systems is based on a tetravalent core ($N_C = 4$) and a binary branching point ($N_B = 2$) leading to 4, 8, 16, 32, 64 and 128 terminal mesogens from G0 up to G5 as was the case for some of the carbosilane dendrimers. These materials are built by the functionalization of the periphery of a pre-formed dendrimer poly(amidoamine) and poly(propyleneimine) (Fig. 26) with units (R) that promote the formation of supramolecular organizations giving rise to liquid crystal mesophases [53–57, 199]. For instance, the introduction of rod-like or disk-like units at the periphery of the original dendrimer leads to dendritic architectures that display liquid crystalline properties. The mesomorphic properties of these LC dendrimers (phase type, transition temperatures and thermodynamic stability) are determined by the enthalpy/entropy balance, the degree of chemical incompatibility of the constituent parts, their size and the structure of the (pro)mesogenic unit itself.

3.2.1
Structure-Property Relationships

In a pioneering work, Meijer et al. [200] described two series of PPI dendrimers functionalized with pentyloxy and decyloxy cyanobiphenyl mesogenic groups (Figs. 26 and 27, R = A and B). All the dendrimers with the pentyl spacer show liquid-crystalline phases above the glass transition temperature (between 10 and 30 °C) and below the isotropic liquid (ca. 130 °C). The dendrimers with the decyloxy spacer also exhibit liquid-crystalline behavior (between 100 °C and 114, 124 and 135 °C for G0, G2 and G4, respectively). X-ray diffraction experiments suggest that all the mesophases observed are smectic A in nature. One striking feature is the almost constant value of the layer spacing whatever the generation number for a given spacer. The authors explained the formation of smectic phases by a microphase separation between the mesogenic rigid units and the flexible dendritic skeleton.

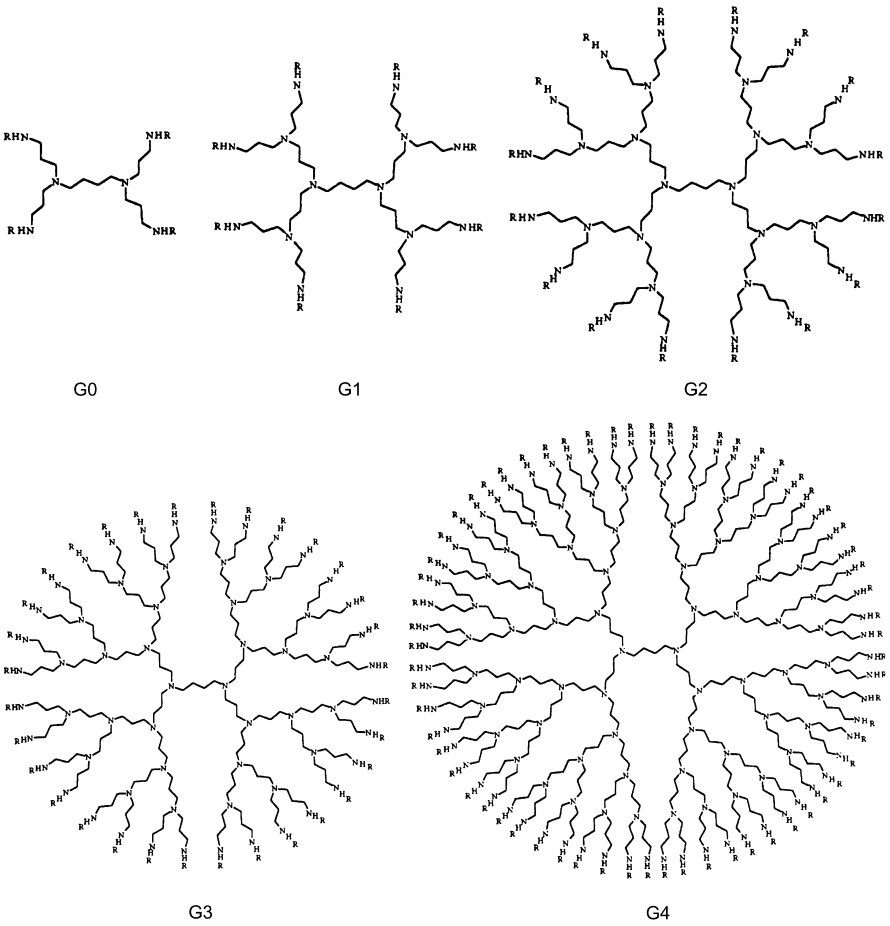

Fig. 26 Representation of the five generations of PPI dendrimers, functionalized by the R group. PAMAM dendrimers are closely structurally related: (i) the segment containing three methylene groups between two consecutive N junctions in the PPI dendrimer is replaced by the $-(CH_2)_2-CONH-(CH_2)_2-$ segment; (ii) the spacer between the two central N atoms is two methylene groups long (rather than four in the PPI)

The arrangement of the mesogenic end-groups is predominantly perpendicular with respect to the layer planes, with the dendritic cores located between these mesogenic sublayers. This orientation of the mesogenic groups is the same as for the low molecular weight cyanobiphenyl molecules which are well known to adopt antiparallel arrangements due to strong dipole–dipole interactions between the terminal cyano groups. The fact that the layer spacing does not vary as a function of the number of peripheral mesogenic units implies that the dendritic core should be in a pronounced distorted conformation, which seems to indicate an extension which occurs only in two

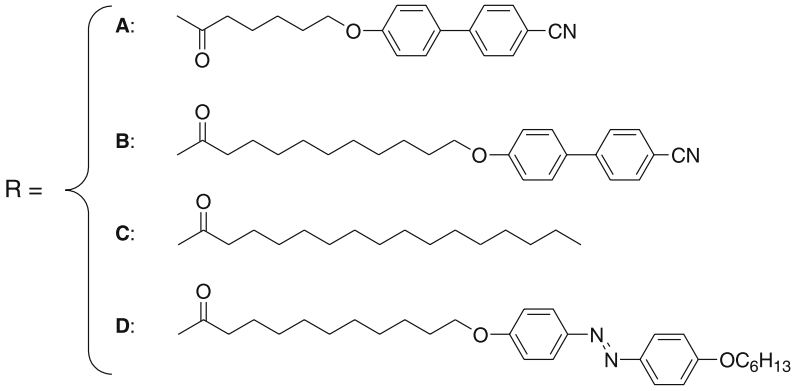

Fig. 27 Functional mesogenic groups used by Meijer

dimensions in a plane parallel to the smectic layers with increasing generation number.

The flexibility and thus the possibility of distortions of the PPI core was confirmed by the study of the self-assembly of amphiphilic dendrimers based on PPI dendrimers of five different generations with up to 64 end groups modified with long hydrophobic chains or azobenzene moieties (Fig. 27, R = C, D) [201, 202]. These molecules are able to arrange themselves in Langmuir monolayers in which the dendritic core is in contact with the water subphase and the alkyl chains are all pointing toward the air, forming a hydrophobic layer. Calculations showed that the shape of the dendritic core is distorted with an axial ratio of 1 : 2.5 for the first generations to approximately 1 : 8 for the three highest generations of dendrimers. Let us also remark that such dendrimers of the fourth generation (Fig. 27, R = B and C) were used as additives in a classical nematic matrix in order to develop electro-optical switches based on light scattering [203].

Note that this behavior is in marked contrast to that of the zeroth to the second generation of related PAMAM and PPI dendrimers ($N_C = 3$, $N_B = 2$) with 4′-cyanobiphenyl hydrogen glutarate that did not produce any mesomorphic behavior, except a lyotropic nematic phase in 80 wt % *N*,*N*′-dimethylformamide (DMF) solutions containing lithium bromide [204, 205].

Similarly, the functionalization of the G0, G1 and G2 PPI dendrimers with cholesteryl groups through carbamate linkage appeared to be the right strategy to induce mesomorphism in these systems [206]. They all exhibit a glass transition between 63 and 78 °C, and after a rich thermal history, all melt into birefringent fluids at ca. 149–162 °C, identified as a SmA phase. G0 then clears at 170 °C, whereas both G1 and G2 clear at 210 °C.

In another pioneering work, Lattermann et al. [207, 208] have also considered poly(propyleneimine) dendrimers (Fig. 26) of different generations but substituted with the non-mesogenic 3,4-bis(decyloxy)benzoate groups. Re-

markably, mesomorphic behavior was observed in the four first generation compounds (the G4 dendrimer was thought to be devoid of mesomorphism). Induction of mesophases was because of the chemical incompatibility between the dendritic core and the peripheral substituents. Contrary to the behavior of conventional non-mesomorphic and mesomorphic linear polymers the melting temperatures of these dendrimers decrease with increasing molar mass. The observed mesophases are all hexagonal columnar in nature, monotropic for G0, and enantiotropic for G1, G2 and G3 (G0: Cr 100 (Col_h 69) I; G1: Cr 100 Col_h 102 I; G2: Cr 76 Col_h 124 I; G3: Cr 60.5 Col_h 107.5 I). Recently, the G4 derivative was found to exhibit also a Col_h phase, and on cooling an additional monotropic cubic phase [209]. The lattice parameters of these hexagonal columnar phases did not correspond to the diameter of flat, two-dimensional, disk-like molecules, as determined from molecular modeling, even if a total interdigitation of the terminal aliphatic chains is assumed which is, on the other hand, not probable at all when taking into account the extremely dense packing of the alkyl chains in the outer shell. Thus, the formation of a columnar phase by a stacking of conventional flat disks can be excluded and the model of a spheroid (oblate or globular) structure of the dendrimer which can be accepted in solution is not valid in the liquid-crystalline phases. Consequently, the authors described the organization of the columnar phase of their dendrimers as resulting from the piling of three-dimensional cylindrical segments consisting of a polar core surrounded by an apolar shell. The corresponding thickness of the dendrimeric cylinder segments has been estimated to be around 10–12 Å, whereas their diameter has been determined by X-ray diffraction to be in the range of 40–50 Å. Such an anisotropic deformation of the polymeric structure is thought to be driven by the microphase separation in polar and apolar regions along the hexagonal columnar lattice. The G3 dendrimer bearing 4-decyloxybenzoate groups exhibits a transient SmA phase. Induction of lyotropic polymorphism was achieved in binary mixtures of some of these dendrimers bearing 4-decyloxybenzoate, 3,4-bis(decyloxy)benzoate and 3,4,5-tris(decyloxy)benzoate groups respectively with chloroform, cyclohexane, *n*-hexane, decane, decanol, THF, DMSO [209]. Some of these dendrimers were complexed with copper(II), and EPR spectroscopy was successfully applied for the determination of the structure and geometry of copper(II) coordination sites within the liquid crystalline dendrimers [210].

More recently, a systematic study of the properties of side-chain LC dendrimers has been undertaken on these PPI dendrimers and also on PAMAM systems by Serrano et al. [211]. In these dendrimers, the mesogenic group is connected to the dendritic scaffold by an imine linkage. In all cases, it was found that the enthalpic gain of the mesogenic units arranged as in a classical liquid crystalline mesophase dominates over the entropic tendency of the dendrimer core to adopt a globular isotropic conformation. The flexibility of the dendritic PAMAM and PPI cores allows the macromolecule to adopt

a microphase-separated molecular conformation which gives rise to various types of liquid crystalline supramolecular organizations. The chemical structure of the (pro)mesogenic units (shape, number of terminal alkoxy chains) determines the type of mesophase formed (nematic, lamellar, columnar).

LC dendrimers obtained by functionalization of the various generations of commercial amino-terminated PAMAM and PPI dendrimers with mesogenic units bearing one terminal alkoxy chain, namely 4-alkoxybenzoyloxysalicylaldehyde (Fig. 28, R = L_1), display as expected smectic mesophases and a nematic phase for G0 (Fig. 29) [212]. In this case and in agreement with the first suggestions of Meijer et al. [200], the molecular model proposed consists of cylinder-like shaped dendrimers in which the dendritic core occupies the central slab and the lateral mesogenic units are arranged parallel to each other, extending up and down from the molecular dendritic matrix (Fig. 30). This model explains the mesogenic behavior of these PAMAM and PPI derivatives since the dendrimeric supermolecules can be considered as large rods that would be ordered parallel to each other promoting the supramolecular order typical of smectic mesophases (Figs. 30 and 35).

In this type of supramolecular organization, the dendritic core deforms strongly with increasing generation number, since the layer spacing remains

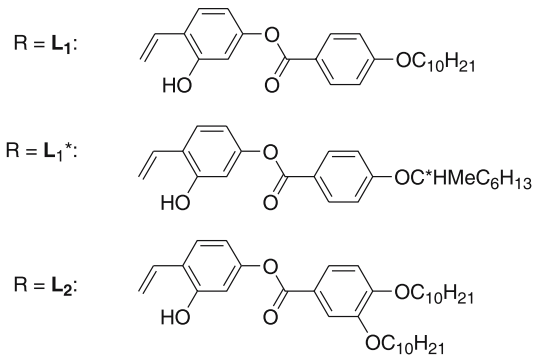

Fig. 28 Structure of the L_1, L_1* and L_2 mesogenic groups

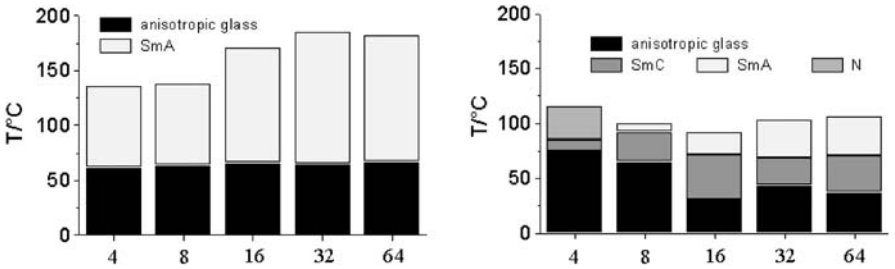

Fig. 29 Mesomorphism of PAMAM (*left*) and PPI (*right*) dendrimers functionalized by L_1

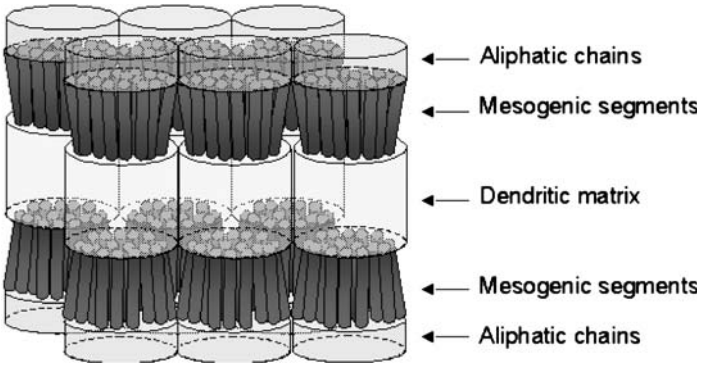

Fig. 30 Schematic representation of the molecular model for dendrimers with one-terminal-chain mesogenic units. Model for the Smectic A supramolecular organization (here G3-L_1 dendrimer)

around 4–5 nm whatever the molecular weight (Fig. 31). This deformation takes place in two dimensions in a plane parallel to the smectic layers. Systematic calculations performed from X-ray diffraction and volume data indicate that the diameter of the dendrimer cylinder increases from 1.3 nm up to 6 nm when going from the lowest generation up to the fourth one containing 64 peripheral mesogenic units. These results were further confirmed by MD calculations.

The same dendritic matrices functionalized with mesogenic units bearing two terminal alkoxy chains (3,4-dialkoxybenzoyloxysalicylaldehyde, Fig. 28, R = L_2) exhibit solely a hexagonal columnar mesophase (Fig. 32) [213, 214].

These dendrimers cannot be arranged in a molecular cylindrical model as that proposed for the smectic phases, since the cross-sectional area of the terminal chains is larger than the area occupied by the mesogenic units. In

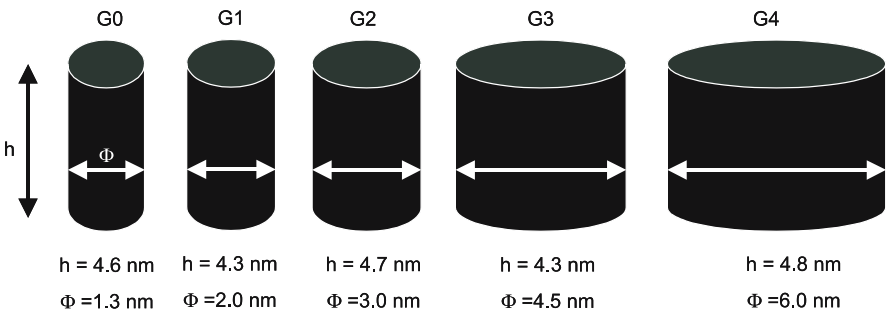

Fig. 31 Variation of the size of the elementary dendrimer cylinder as a function of generation number (G*n*). *Φ* is the diameter and *h* the height of the cylinder (i.e. lamellar periodicity)

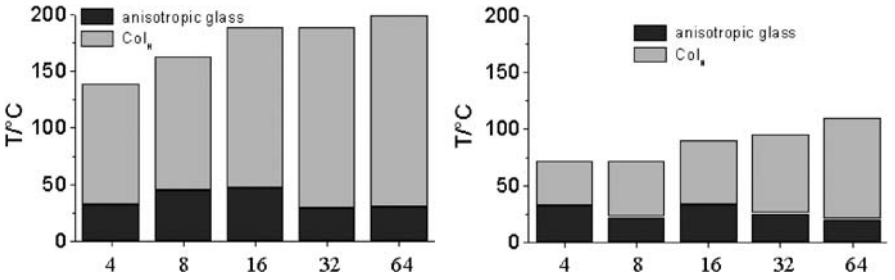

Fig. 32 Mesomorphism of PAMAM (*left*) and PPI (*right*) dendrimers functionalized by L_2

this case, the dendrimers tend to adopt a different and more stable conformation, so that the mesogenic units can be accommodated optimally. The most probable conformation consists of a disk-like radial arrangement that allows the filling of the space in three distinct regions corresponding to the central core, the rigid part of the mesogenic units and the terminal chains (Fig. 35). Therefore, the dendritic molecules fill up thick disks or disk equivalents: for the low generations, two or three molecules are needed to form a complete disk, and from the second generation onwards, just one molecule constitutes a disk, whose thickness depends on the generation number (Fig. 33). These molecular disks self-assemble into supramolecular cylindrical columns which are arranged according to a hexagonal symmetry.

This proposed model was further justified by MD simulation which reproduces the paving of the hexagonal lattice of the dendrimers in a flattened wedge conformation. The result of the calculation evidenced a good filling of the available volume. An enhancement of the micro-segregation over the entire simulation experiment time was also observed, contributing to the stabilization of the structure. Furthermore, the compensation of the molecular

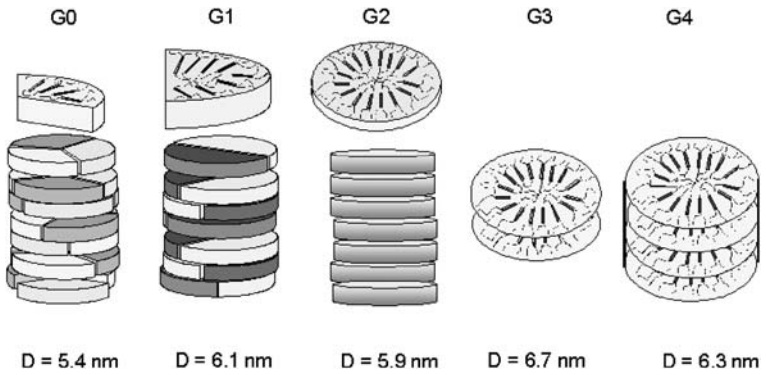

Fig. 33 Schematic representation of the molecular model for the dendrimers bearing the L_2 mesogenic unit. Model for the columnar supramolecular organization (*D*: intercolumnar distance)

areas at the dendritic/mesogen interfaces implies the tilt of the peripheral rigid segments with respect to the radial directions (Fig. 34).

It is interesting to note that the diameter of the columns does not vary significantly with the generation number. Indeed, it varies irregularly between 5.3 nm and 6.7 nm, despite the fact that the molecular weight of one single dendrimer varies between 2660 up to 48 500 Daltons when going from the lowest generation up to the fourth generation. In other words, this clearly indicates that the dendritic core deforms strongly in one main direction corresponding to that of the columnar axis, whereas the mesogenic units are arranged radially (Fig. 35) to ensure efficient lateral interactions within and between columnar slices. Similarly to the case of lamellar phases described above, systematic calculations performed from XRD and volume data indicate

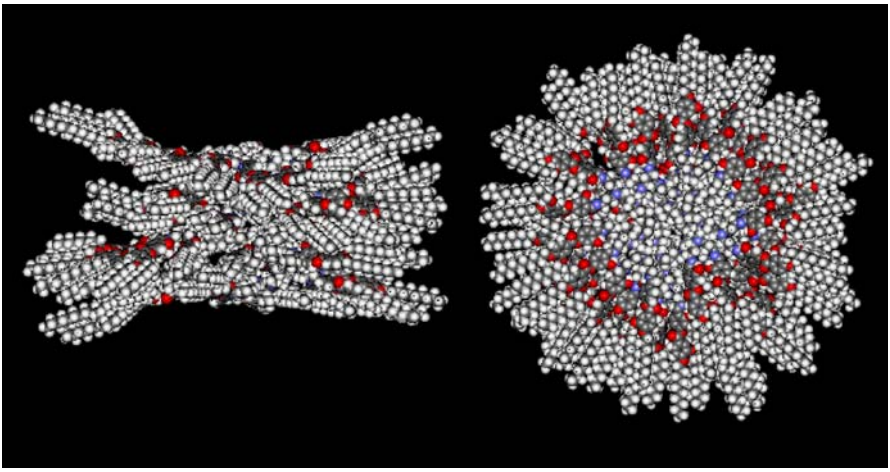

Fig. 34 Modelization of the self-organization of the G4-L_2 dendrimer into columns

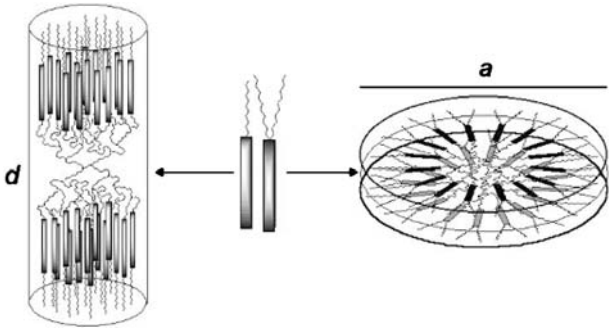

Fig. 35 Relationship between dendritic core deformation and mesogen type and the conformation of the side-chain liquid crystalline dendrimers

that the highest generation dendrimer (containing 64 peripheral mesogenic groups) can fill the equivalent of a disk 1.9 nm thick, whereas the second generation dendrimer containing 16 peripheral mesogenic groups alone fills a disk 0.5 nm thick. It has been found that, whatever the generation, there is on average 16 mesogenic units over 0.5 nm along the columnar axes.

To conclude this part, let us emphasize that both lamellar and columnar mesophases can be obtained with dendrimers, even with those of high molecular weight, the stability of the corresponding phases being ensured by lateral interactions between the (pro)mesogenic units and by a significant deformation of the conformation of the dendritic core. The difference in the symmetry of the mesophase is only related to a small difference in the molecular design of the peripheral mesogenic groups. Those with only one terminal end-chain produce lamellar mesophases by the lateral expansion of the dendritic matrix within the layer (prolate deformation), whereas those with two terminal end-chains lead to columnar mesophases by stretching of the matrix along the columnar axis (oblate deformation) (Fig. 35). Let us point out also that the dimensions (a few nanometers) of the elementary dendrimer cylinder can be tuned according to the generation number, but the fundamental dimensions of the mesophase structure (layer spacing for the lamellar phases and intercolumnar distance for the columnar phases) do not depend on the size of the dendrimer itself.

In the field of liquid crystals, it is well known that many of the materials displaying a columnar mesophase are constituted of disk-like (discotic) molecules, but very little attention has been paid to LC dendrimers containing discotic mesogenic units, for example based on hexa-substituted derivatives of triphenylene. The latter are also of special interest because of their photoconductive properties. A series of PPI-based dendrimers that incorporate discotic triphenylene mesogenic units (with decyloxy side-chains) at their periphery has been prepared and their properties investigated [215]. All the dendrimers except that of the zeroth generation (Cr 61 Col_r 79 I) show a hexagonal columnar mesophase over a wide temperature range (between ca. 40–50 °C and 110–115 °C). The XRD characterization of this mesophase reveals that its parameters are, here also, practically independent of the dendritic generation considered. In the model proposed by the authors, the flexible dendritic part adopts a cylindrical arrangement with the four generations having a similar diameter but their height increasing. Once more, the interactions between the mesogenic units determine the supramolecular structure and the dendritic central core adopts the elongated conformation necessary to allow this molecular arrangement.

Side-chain LC dendrimers exhibiting the nematic mesophase, which is the most disordered liquid crystalline phase, can also be achieved by the appropriate choice of the mesogenic unit(s) attached to the dendrimer central core. For example, side-chain PPI-derived dendrimers containing mesogenic units of type L_1 (Fig. 28) but with short terminal alkoxy chains (ethoxy, butoxy

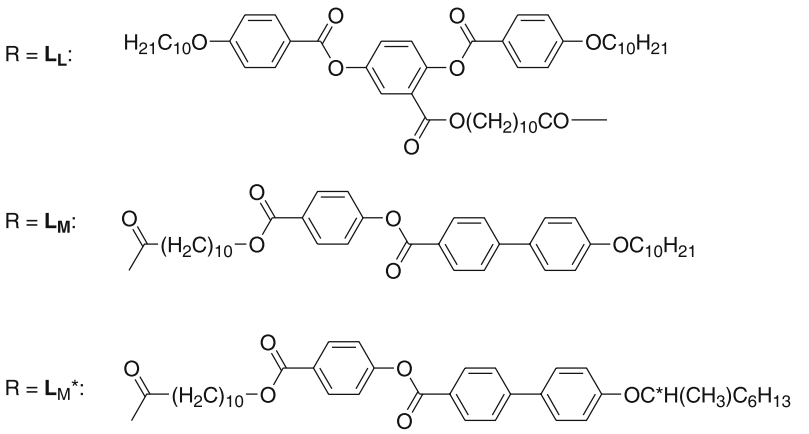

Fig. 36 Structure of the mesogenic groups for end-on and side-on dendrimers

and pentoxy) or mesogenic units attached laterally (Fig. 36, L_L, amide linkage), have been prepared in a similar approach to that employed in side-chain liquid crystal polymers [216, 217]. In this case, the side-by-side molecular arrangement typical of lamellar phases is disfavored, thus promoting a nematic order. For the end-on dendrimers, the clearing temperature range decreases with increasing generation number G0 to G3 (from ca. 120 to 70–80 °C), and then increases for G4 (to ca. 100 °C). No influence of the chain length was detected. Typically, the average temperature range of the nematic phase for the latter compounds phase remains almost generation independent (between ca. 25–30 °C and 70–80 °C), and decreases for the G4 dendrimer (G 14 N 53 I). Nematic or lamellar phases (SmC and SmA) have also been obtained with the third generation of PPI liquid-crystalline co-dendrimers containing various proportions of two types of pro-mesogenic units, i.e. one being laterally attached (Fig. 36, L_L) and one terminally attached (Fig. 36, L_M) [218] through an amide linkage. Decreasing the proportion of the side-on mesogens with respect to the end-on one contributes rapidly to the suppression of the nematic phase at the expense of the smectic phases (SmA and SmC). In these cases, ^{2}D NMR experiments carried out on one of these co-dendrimers have proved that the symmetry of the nematic phase is uniaxial, in contrast to the biaxial nematic phase observed for some side-on-polymers [219].

As described above, the presence of one or two terminal alkoxy chains in the chemical architecture of the mesogenic units induces a drastic modification in the thermotropic behavior of the dendrimer (from lamellar to columnar structures). The introduction of both types of mesogenic units (Fig. 28, L_1 and L_2) in different concentrations within the same dendritic structure, i.e. random co-dendrimers, should present a greater possibility of tuning the symmetry of the mesophase exhibited by the material. A series of such G3 co-dendrimers was synthesized, in which both types of mesogenic

units were introduced in various proportions [220]. The study of the phase diagram (Fig. 37) obtained for these PAMAM co-dendrimers revealed that, for intermediate compositions, two other mesophases (SmC and Col_r) appeared between the smectic A and the hexagonal columnar phases of the two homodendrimers, respectively. Co-dendrimers with a small content of the two-terminal-chain comonomer exhibit a smectic C phase below the smectic A phase. The appearance of the tilted smectic mesophase is a consequence of the increase in the total number of terminal chains for a constant size of the pre-dendritic matrix. The tilt of the molecule affords a larger area of the ideal cylinder base, which allows the accommodation of all the terminal chains (Fig. 38). Larger contents of the two-terminal-chain comonomer in the co-dendrimers favor the occurrence of a rectangular columnar mesophase. As the number of terminal chains increases, their accommodation within a cylindrical rod-like structure becomes unlikely. This elementary dendritic cylinder is deformed into some kind of parallelepiped structure, which in turn promotes the existence of a rectangular columnar mesophase (Fig. 38).

Thus, depending upon the relative concentration of each of the two monomers, orthogonal and/or tilted lamellar mesophases, or else rectangular and/or hexagonal mesophases can be obtained.

The molecular dynamics of the co-dendrimer G3-$(L_1)_{16}$ – $(L_2)_{16}$ in its two phases, i.e. a low temperature Col_r phase and a high temperature SmA phase, was studied by ^1H NMR relaxation [221]. In the high frequency range, the motions appear similar in both phases and are ascribed to reorientations of the dendritic segments, whereas in the low frequency ranges, notable differences in the dynamics between the columnar and layered phases were observed, and were discussed in terms of elastic deformations of the columns and layer undulations.

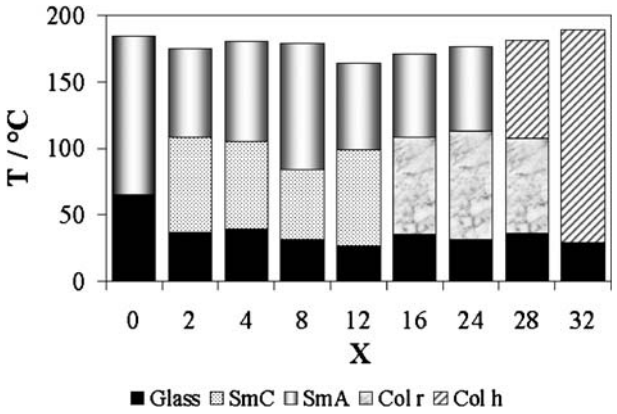

Fig. 37 Phase diagram of the co-dendrimer G3-$(L_1)_{1-x}$-$(L_2)_x$ (X: proportion of L_2 mesogens)

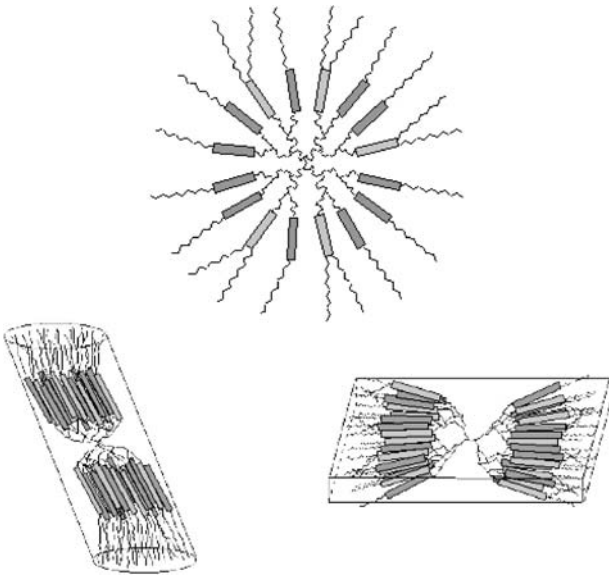

Fig. 38 Schematic representation of the molecular model for codendrimers with one- and two-terminal-chain mesogenic units (SmC and rectangular columnar phases)

As mentioned above, other PPI co-dendrimers have been obtained by mixing in their structures terminal- and laterally attached pro-mesogenic units using a dendritic matrix bearing 32 terminal amine groups [218]. It is shown that there is a gradual evolution from a nematic phase to an orthogonal lamellar phase through the appearance of a tilted smectic C phase (not present in the homodendrimers) when increasing the proportion of terminally attached mesogenic units. These studies confirm that the mesomorphic behavior of such block co-dendrimers could be modulated and controlled by a simple modification of the ratio of two pro-mesogenic units present around the dendritic core.

3.2.2
Tuning the Dimensions of the Nano-Dendritic Object

In order to further investigate the influence of the structure of the mesogenic units on the mesomorphic behavior of the dendrimers, bulky units have been introduced at the periphery of the third and fourth generations of amino-terminated PAMAM and PPI (Fig. 39, L_3, L_6, L_9), with the aim of achieving cubic mesophases, since the increased volume around the dendritic core could in principle force the dendrimer to adopt a globular conformation [199, 222].

However, all the dendrimers prepared showed only a hexagonal columnar mesophase, even those bearing the largest mesogenic units containing

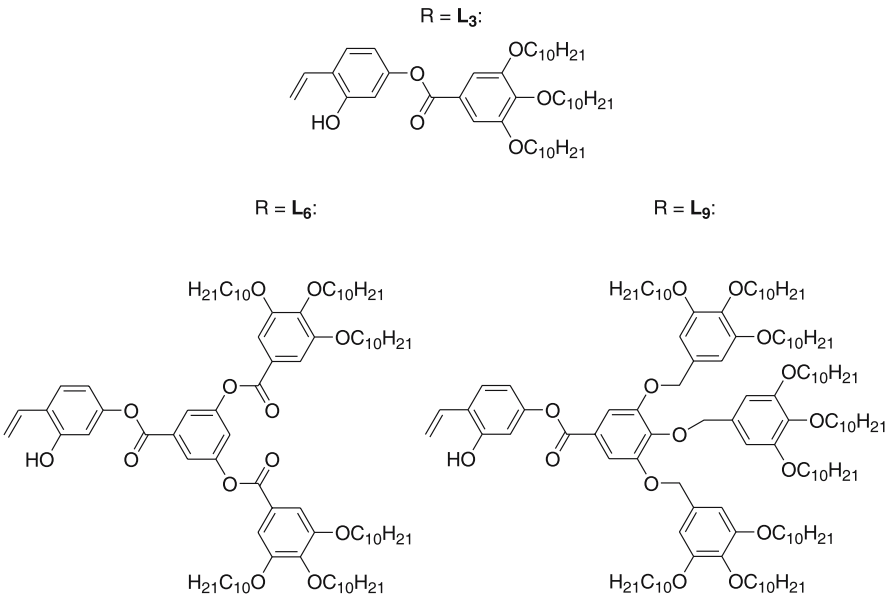

Fig. 39 Chemical structure of the bulky mesogenic units

nine terminal chains each. A model of organization of these dendritic supermolecules, deduced from X-ray diffraction results and theoretical calculations made thereof, was proposed. This molecular model implies a cylinder, whose inner part is occupied by the dendritic core and the bulky mesogenic units spreading around it, as shown in Fig. 40.

The dendritic core adopts an extended conformation which is possible due to the great flexibility (conformational freedom) of the PAMAM and PPI skeletons. In this way, the molecular model of thick disks proposed for the LC dendrimers with two-terminal chain mesogenic units is transformed into a model consisting of a long cylinder, which is the result of the axial elonga-

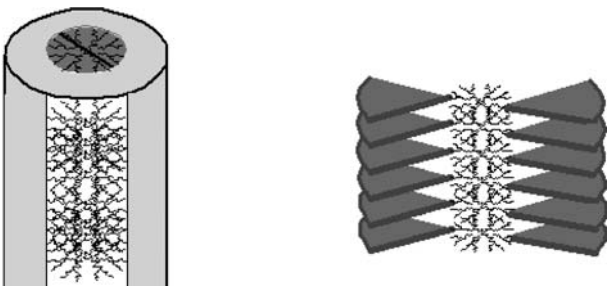

Fig. 40 Molecular model for the LC dendrimers with bulky mesogenic units

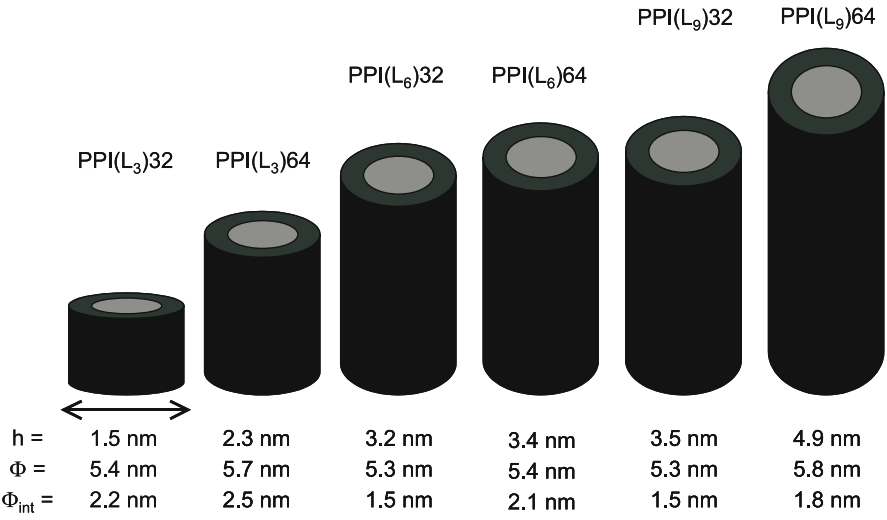

Fig. 41 Variation of the size of the elementary third and fourth generations dendrimer cylinder with bulky mesogenic groups. L_3, L_6 and L_9 are for the bulky groups containing 3, 6 and 9 terminal aliphatic chains, respectively. *h* is the height of the cylinder, Φ the diameter, and Φ_{int} is the internal diameter corresponding to the dendritic part only

tion of the oblate structure caused by the extended conformation adopted by the dendritic core in order to accommodate the bulky units around it. X-ray diffraction investigations show that the diameter of the cylinder is about the same whatever the generation and the bulky peripheral group (Fig. 41). But more detailed calculations indicate that the internal diameter of the cylinder corresponding to the dendritic core decreases when the bulkiness of the peripheral group increases, for example going from 2.5 down to 1.8 nm in the case of the fourth generation dendrimers, in agreement with an additional elongation of 2.6 nm of the dendritic core along the columnar axis. This example also emphasizes another way to tune the dimensions of the nano-dendritic objects by molecular engineering involving bulky peripheral groups. Note that other PPI dendrimers of the zeroth, second and fourth generation functionalized in the termini by anisotropic oligo(*p*-phenylene vinylene) units bearing three terminal dodecyloxy chains and lateral methylbutoxy side chains were reported to exhibit a lamellar mesomorphism between ca. 50–70 (melting) and 160–180 °C (clearing) [223].

3.2.3 Theoretical Aspects

A theoretical approach to identify the key topological and statistical ingredients for the description of the self-organization and of the mesomorphic behavior of such dendritic supermolecules has been developed [224–226].

The model is based on convex deformable hard body supermolecules that can interconvert between spherical and cylindrical states. In other words, the dendrimer is considered to be a deformable object that can exist in a certain number of conformational states governed by the intra-dendrimer interactions. Then, these objects are assumed to interact with one another as a whole in a way that is dictated by inter-dendrimer segmental interactions. It is shown that isotropic, nematic, smectic and columnar phases can be generated and that there is a strong thermodynamic selection of conformations according to their packing efficiency in each of the mesomorphic phases. In this model, the smectic and columnar phases are mainly stabilized by the anisometry of the global shape of the predominant supermolecular conformations. A second theoretical approach has been to consider directly the interactions among the dendritic segments in a pair-wise manner and to impose on the intra-dendritic pairs the configurational constraints dictated by their connectivity within the same dendrimer [227]. With this approach, the ensemble of dendrimers reduces to an ensemble of mesogenic dimers with spacers of different lengths corresponding to the different branch paths within the dendritic scaffold. This segmental approach is more suitable for the description of the mesomorphic properties that are sensitive to the ordering and to the motion of dendritic segments rather than of the dendrimer as a whole.

3.2.4 Chiral Properties

In order to get ferroelectric properties, a series of chiral PPI co-dendrimers bearing chiral and achiral terminal chains has been investigated [228]. Such an approach has been chosen to mimic the situation occurring in classical mixtures of low molecular weight liquid crystals using chiral dopants. It is shown that the presence of small quantities of the chiral mesogen unit (the chiral monomer is L_1* and the co-monomer is L_1; Fig. 28) favors the formation of the smectic C* ferroelectric phase and that this mesophase disappears only when the ratio of chiral terminal groups is larger than 75%. The stability of this smectic C* phase increases from the zeroth to the fourth generation of co-dendrimers. Unfortunately, ferroelectric behavior is revealed to be very poor. Switching was detected only in the small dendrimers (G0 and G1) and in co-dendrimers bearing a small number of chiral mesogenic units. Similarly, a third generation of PPI liquid-crystalline co-dendrimers containing various proportions of two types of pro-mesogenic units (Fig. 36; L_L, L_M^*) show a modulated SmC (or modulated SmA) and a N* (or N) phase for low contents of L_M^*, a SmC* for a ratio 40 : 60 of L_L/L_M^*, and a single SmA phase for a higher content of L_M^* [218].

Four PPI dendrimers of the zeroth and first generations containing bent-core molecules at the periphery were recently reported (Fig. 42, Table 9) [229]. These dendrimers exhibit a relatively high viscosity which is unfavorable for

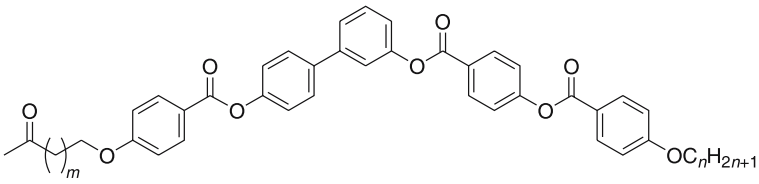

R = **B1** (n = 12, m = 3), **B2** (n = 16, m = 9)

Fig. 42 Structure of the bent mesogens

Table 9 Mesomorphic behavior of the dendrimers bearing bent-mesogens

Gn	Mesogen B1	Mesogen B2
G0	I 151 Col_r 104 Cr	I 144 SmX 113 Cr
G1	I 162 Col_r 120 Cr	I 149 SmX 122 Cr

detailed investigation of the physical properties. No switching and thus ferroelectric behavior could be observed for any of the dendrimers.

3.2.5 Amphiphilic PPI Dendrimers

The alkylation of PPI dendrimers of the third and fourth generation has been undertaken by reaction of all the amino end groups of the parent dendrimers with *n*-dodecyl isocyanate. While mesomorphism was not induced in these compounds, their corresponding protonated homologues were shown to exhibit thermotropic cubic phases of $Ia\bar{3}d$ symmetry [230]. This is attributed to the enhancement of the amphiphilic character and the subsequent "nanophase" segregation of the two incompatible parts. The proposed structure consists of 24 nearly spherical, multicationic dendrimeric entities located in the axes constituting the skeletal graph of the gyroid, while the aliphatic chains are located on each side of the minimal surface [231–234].

G0 to G4 generation amphiphilic PPI dendrimers with facial amphiphilic carboxylic acids were prepared (Fig. 43). Some of these ionic systems show a sequence with unconventional liquid crystalline phases, depending on the dendrimer generation, the structure of the facial amphiphilic acid and the external conditions (temperature and concentration) [235]. For example, different square columnar phases, as well as a channelled layered phase, i.e. a mesophase combining a layer structure with a hexagonal organization of columns have been observed (Table 10). The supramolecular dendrimers thus formed represent a new class of mesomorphic materials, whose properties can be tailored by the dendrimer generation and dendrimer-to-mesogen ratio. A single SmA phase is formed when there is no spacer (A0)

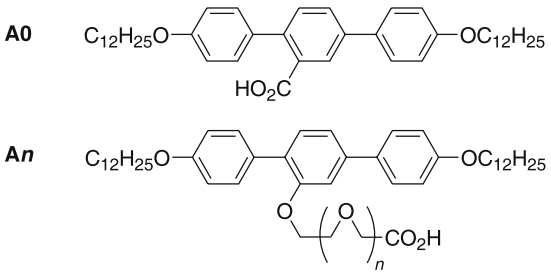

Fig. 43 Structure of the facial amphiphilic mesogenic side-groups A0 and A*n*

Table 10 Mesomorphism of the facial mesogen-containing dendrimers

G*n*	A0	A3	A4
G0	SmA 155 I	Col_h 87 I	Col_{squ} 109 I [a]
G1	SmA 159 I	Col^a_{squ} 116 I	Col_{squ}-*p4mm* 123 I
G2	SmA 165 I	Col^a_{squ} 125 I	Col_{squ}-*p4mm* 124 I
G3	SmA 167 I	Col^a_{squ} 124 I	
G4		Col^a_{squ} 117 I	Col_{squ}-*p4mm* 116 I

[a] Two co-existing columnar mesophases Col_{squ} with *p4mm* and *p4gm* symmetries

or when the amphiphilic spacer is short (A2) between the terphenylene and the dendrimer, whereas for the other materials with A3 and A4, solely Col_h and Col_{squ} phases were observed (Table 10). A dimorphism of two different columnar phases, with two different square 2D lattices (*p4mm* and *p4gm*), was observed for all the blends of the G*n*-A3 series, except for G0-A3, which leads to a Col_h phase only. As for the blends G*n*-A4, exclusively the *p4mm* square columnar phase was found for all generations except the G0 which showed the two square columnar phases (Table 10).

Ionic liquid crystals derived from the protonation of PPI dendrimers with a cholesteryl-based carboxylic acid led to materials exhibiting mesomorphic properties, which are dictated by the degree of protonation of primary amino groups [236]. G0 to G4 systems exhibit a glass transition at ca. 36–38 °C. At higher temperatures, they become birefringent fluids, followed by another transition at ca. 90–110 °C into a second mesophase. Both mesophases were identified as SmC* and SmA phases, respectively. They all decompose before clearing at 150 °C, the onset of the degradation. The mesophase stability was considerably reduced compared to the covalent systems [206].

Non-covalent thermotropic liquid crystal dendritic systems have been achieved recently by converting the amphiphilic surface of the dendrimers ($-NH_2$) into a hydrophobic shell (alkanoate chains). Tomalia et al. reported on the "non-aqueous lyotropic" behavior of supramolecular complexes re-

Table 11 Mesomorphism of the ionic dendrimers

G*n*	[PPI-H^+]·[$^-O_2CC_{17}H_{35}$]	[PPI-H^+]·[$^-O_2CC_{13}H_{27}$]	[PAMAM-H^+]·[$^-O_2CC_{17}H_{35}$]
G0	Cr 67 SmA 116 I	Cr 27 SmA 116 I	Cr 55 SmA 99 I
G1	Cr 55 SmA 134 I	Cr 28 SmA 125 I	Cr 71 SmA 130 I
G2	Cr 56 SmA 131 I	Cr 34 SmA 127 I	Cr 63 SmA 126 I
G3	Cr 48 SmA 127 I	Cr 11 SmA 73 I	Cr 53 SmA 130 I
G4	Cr 68 Col_{tet} 102 I	Cr 5 Col_h 78 I	Cr 62 SmA 133 I
G5			Cr 63 SmA 140 I

sulting from ionic interactions between the second generation of a PPI dendrimer ($N_C = 3$, $N_B = 2$, $Z = 12$) terminated with amino groups and octanoic acid [237]. The presence of a lamellar phase was detected by polarized light optical microscopy and X-ray diffraction for acid/dendrimer molecular ratios of 30 to 13. Similar ionic liquid crystal systems of PAMAM and PPI dendrimers (from G0 to G4) and long chain carboxylates were obtained recently [238–240]. All of the dendrimers, in approximately a 1 : 1 stoichiometry (primary amine groups : carboxylic acid groups) show lamellar phases (G0-G5) [238, 240], except for the highest generations of PPI dendrimers (G4) which exhibit columnar phases with hexagonal or tetragonal bidimensional symmetries, namely Col_h or Col_{tet} phases, depending on chain length (Table 11). It is also interesting to remark that such ionic dendrimers do not have aromatic mesogenic groups in their structure, which indicates that the ionic interactions play a key role in the formation of these thermotropic mesomorphic phases. For the PAMAM G3 dendrimer, the increase of stearic acid ratio with respect to primary amine groups leads to the transformation of the mesophases from SmA (for 0.11–1.5 ratio) to a columnar phase (for an acid/amine ratio of 2.33) [239].

PPI dendrimers (G1 to G4) functionalized on the periphery by pyridyl moieties (obtained by reacting 3-pyridyl isothiocyanate with the $-NH_2$ endgroups) form hydrogen-bonding supramolecular complexes when mixed with 3-cholesteryloxycarbonyl-propanoic acids [241]. The complexes are birefringent glasses at room temperature. Above the glass transition temperature (ca. 49–57 °C), they turned into viscous birefringent fluids, characterized as SmA phases. In all cases the isotropization could be reached, as the complexes decomposed at ca. 140 °C.

3.2.6 Photoactive PPI Dendrimers

In view of obtaining photo-responsive surfaces, photo-active Langmuir–Blodgett films based on the fourth generation PPI dendrimer, randomly sub-

stituted with palmitoyl- and azobenzene-containing alkyl chains, have been prepared (Fig. 27, R = C and D). The co-dendrimer thus obtained has a random functionalized shell with 32 functionalities on average [201, 202, 242]. This partial modification of the dendritic surface gives rise to materials which can be processed into stable Langmuir and Langmuir–Blodgett films where the dendrimer anchors the azobenzene units and hence prevents microphase separation of the azobenzene moieties, thereby facilitating reversible *cis-trans* isomerization.

In many of the PPI dendrimers described above, the mesogens are linked to the dendritic scaffold through an amide linkage. There is only one report concerning the same type of dendrimers coupled with rigid mesogens by ester linkages which show also smectic phases. These are obtained by using the zeroth and first generation PPI dendrimers and ω-(4′-cyanobiphenyloxy)alkyl acrylate [243, 244]. They all show ordered smectic phases (probably SmE) between ca. –10 °C and 90 °C. The advantage of such an approach is to cover the dendritic scaffold with a number of mesogen groups that is twice larger for identical generation than in the cases discussed above, i.e. 8, 16, 32, 64 and 128 groups for G0 to G4 (as in Fig. 26, but the NHR terminal functionality is replaced by a NR_2 functional end). A whole family of such dendrimers was synthesized, bearing peripheral 2,3-difluorobiphenyl mesogenic units [245]. Whereas the SmE-to-SmA phase transition is generation-independent (around 50 °C), a net enhancement of the mesophase stability is observed with generation (the clearing temperature increases linearly from 70 to 95 °C from G0 to G4).

3.3
Dendrimers with Polyether Dendritic Cores

Third-generation amphiphilic monodendrons extended by linear polyethylene oxide chains have shown to self-assemble into various supramolecular architectures. Thus, the AB-block copolymers with $n = 31$ (Fig. 44) melted at 63 °C from a crystalline lamellar into a $Pm\bar{3}n$ micellar cubic phase (clearing at 93 °C), whereas increasing the polyethylene oxide chain ($n = 96$) modifies substantially the phase sequence as a function of temperature: Cr 63 Col_h 114 Cub-$Ia\bar{3}d$ 190 lamellar 226 I; the cubic phase is likely continuous [246]. With an intermediate polyethylene oxide chain length ($n = 62$), the AB-block material melts from a crystalline lamellar phase into a Col_h phase (clearing at 175 °C) [247]. The dendrons themselves are not mesomorphic [248]. Here, mesomorphism clearly results from microphase segregation between the chemically incompatible parts, namely hydrophobic dendrons and hydrophilic linear polymer. Ionic conductivity of ion-doped samples was monitored in these different phases. It appears that it is strongly correlated to the mesophase behavior. Thus, charge transport has been measured in a nanostructured material in which the conducting medium is confined to either mi-

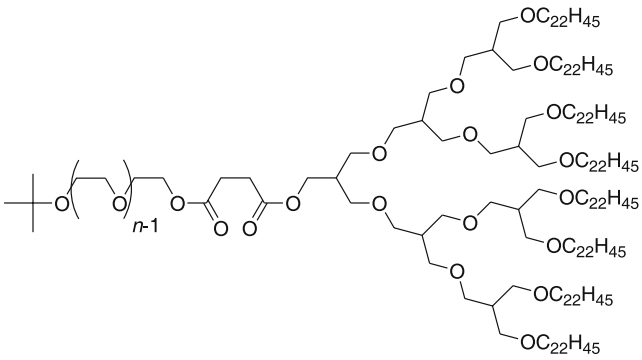

Fig. 44 Structure of the extended amphiphilic monodendrons with a polyether core

celles, infinite cylinders, lamellae or even bicontinuous networks throughout the entire macroscopic sample. This can be of importance in devices such as ion conductors, photovoltaic or electroluminescent cells.

Other dendritic frameworks were used, but did not always yield to mesomorphic systems. For instance, the polyalkylarylether dendrimers functionalized by azobenzene mesogens failed to show any liquid crystalline property despite the mesomorphic side-group promoter [249].

3.4
Dendrimers with Polyester Dendritic Cores

Hult and coworkers reported the first ferroelectric LCDs by attaching chiral mesogens onto a polyester dendritic core [250]. This dendritic core is quite original and is built by various generations of 2,2-bis(hydroxymethyl)propionic-based monodendrons that are coupled in the last stage of the reaction to 1,1,1-tris(hydroxyphenyl)ethane (Fig. 45, $N_C = 3$, $N_B = 2$) [251, 252]. The zeroth (G0), first (G1), second (G2) and third generation (G3) dendrimers end-capped with 3, 6, 12 and 24 mesogenic units (Fig. 45, R = A) were found to exhibit a SmC* phase (Table 12) [253, 254]. As the generation was increased, additional smectic mesophases could be observed for G2 and G3 among others, a SmA phase, and two unidentified tilted smectic phases M1 and M2; at the same time, the stability of the mesophases was enhanced. Moreover, once these compounds were placed into a surface-stabilized ferroelectric cell, all showed ferroelectric behavior upon the application of an external electric field, but electro-optical measurements did not reveal any cooperative effect since neither the spontaneous polarizations nor the tilt angles were found to be influenced by the generation number (at the same reduced temperature, $Ps \approx 35\ nC\,cm^{-2}$ and $\theta \approx 25°$). Similarly, the second harmonic generation and the dielectric relaxation processes [255] seemed insensitive to the increasing generation number.

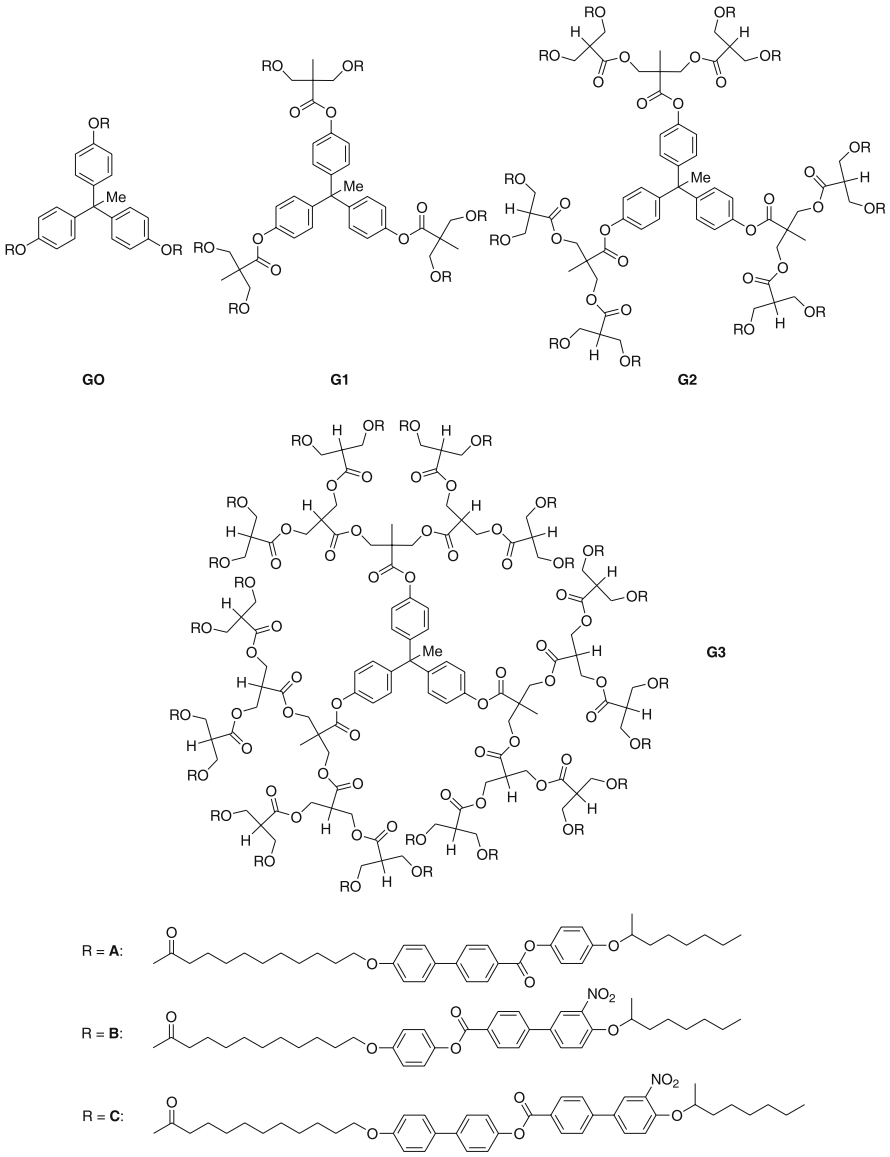

Fig. 45 Structure of the dendrimers with a polyester ramified core

The mesomorphic properties of the G2 dendrimer were substantially modified by the grafting of mesogenic units containing a nitro group (Fig. 45, R = B, C) [256]. In both cases, the two unidentified phases disappeared, and only the SmC* and SmA were observed (Table 12). For the dendrimer bearing the B moiety, the mesophases appeared at much lower temperatures than for the dendrimer functionalized by A groups, whereas for the compound bear-

Table 12 Mesomorphic behavior of the dendrimers with a polyester core

G*n*	R	Phase sequence
G0	A	Cr 77 SmC* 135 I
G1	A	Cr 82 SmC* 124 I
G2	A	Cr 84 SmC* 91 M1 121 M2 127 SmA 150 I
G2	B	G 34 SmC* 69 SmA 82 I
G2	C	G 70 SmC* 152 SmA 208 I
G3	A	Cr 84 SmC* 107 M1 130 M2 134 SmA 151 I

ing C groups, the liquid crystalline phases were substantially stabilized due to the elongation of the mesogenic core. Moreover, the crystalline phase of G2-A is suppressed to yield a glassy state instead in G2-B and G2-C.

4 Main-Chain Liquid-Crystalline Dendrimers

Regarding the dendrimers considered in this part, the branching points are no longer single atoms (C, N, Si) but consist of anisotropic molecular moieties instead. These units are linked together through long and flexible alkyl spacers and form therefore the dendritic matrix; the differentiation between side-chain and main-chain occurs at the first generation onwards (Fig. 46). The mesogenic groups are now present at every level of the dendritic hierarchy, and the dendrimers are forced to adopt constrained and regular structures. As such, the anisometric branches do not radiate isotropically as in side-chain dendrimers, but, on the contrary, favor preferentially an

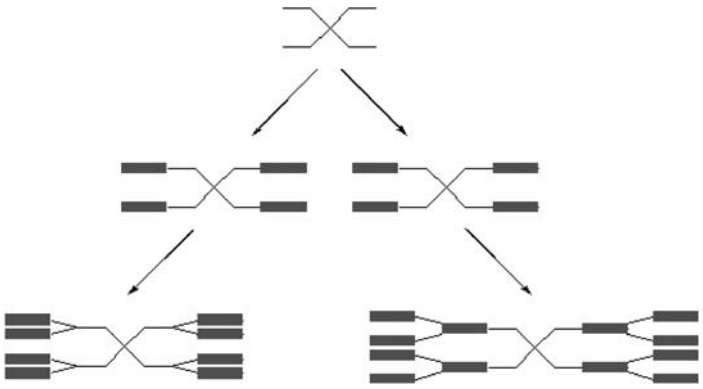

Fig. 46 Schematic of the structural difference between side-chain (*left*) and main-chain (*right*) dendrimers

anisotropic order by a gain in the enthalpy of the system in order to produce the most stable structure.

These main-chain dendrimers may represent an interesting alternative for the development of original molecular materials having a new architecture. Shibaev et al. foresaw the elaboration of such compounds, but have not yet reported on their synthesis and physical properties [151]. Up to now two families of such systems have been identified, namely the willow-like and the octopus dendrimers.

4.1 Willow-Like Dendrimers

The study of the so-called willow-like dendrons and dendrimers echoes a previous important study by Percec on non-regular hyperbranched polymers, another class of cascade macromolecules but distinct from the purely dendritic systems. Indeed, in the original study, Percec et al. synthesized cascade macromolecules by a random self-polymerization of tri-functionalized AB_2 mesogenic monomers derived from biphenylene, naphthalene and terphenylene moieties [67, 69]. These hyperbranched polymers exhibited a single nematic phase and did not crystallize on cooling; depending on the basic mesogenic unit, the nematic temperature range varied from 20 to ca. 80 °C. Because of such a statistical mode of construction [74–77], these hyperbranched macromolecules were characterized by a randomly branched structure with a high, and non-controllable degree of branching and broad molecular weight distributions. Despite these interesting results, they later synthesized regular dendrimers, based on the terphenylene monomer unit free of these imperfections [257–261]. Thus, the four generations of monodendrons (DH1-4) and the corresponding dendrimers (G1-4) resulting from the attachment of DH1-4 onto a tribenzoic acid were obtained by convergent methods with polydispersity indices close to unity (Fig. 47). All the monodendrons and dendrimers were mesomorphic and formed both enantiotropic nematic and smectic phases; only DH1 exhibits a single monotropic nematic phase (Table 13). Note that the corresponding hyperbranched system exhibited a single nematic phase (G 50 N 132 I). On average, the isotropization temperature increases with the generation as well as the stability of the nematic phase, but this effect is very much diluted for the third and fourth generation of both the monodendrons and dendrimers which exhibit an almost identical mesophase temperature range. The nature of the smectic phase is not clear, but on the basis of X-ray diffraction, a SmI or SmF phase (or the more ordered ones SmJ or SmG) seems most likely.

In these systems, the formation of both the nematic and smectic phases is attributed to a particular chain conformation implying that all the sub-units lie parallel to each other to give an overall rod-like shape, rather than a disk-like or spherical shape. This is possible since the racemic AB_2 monomer pos-

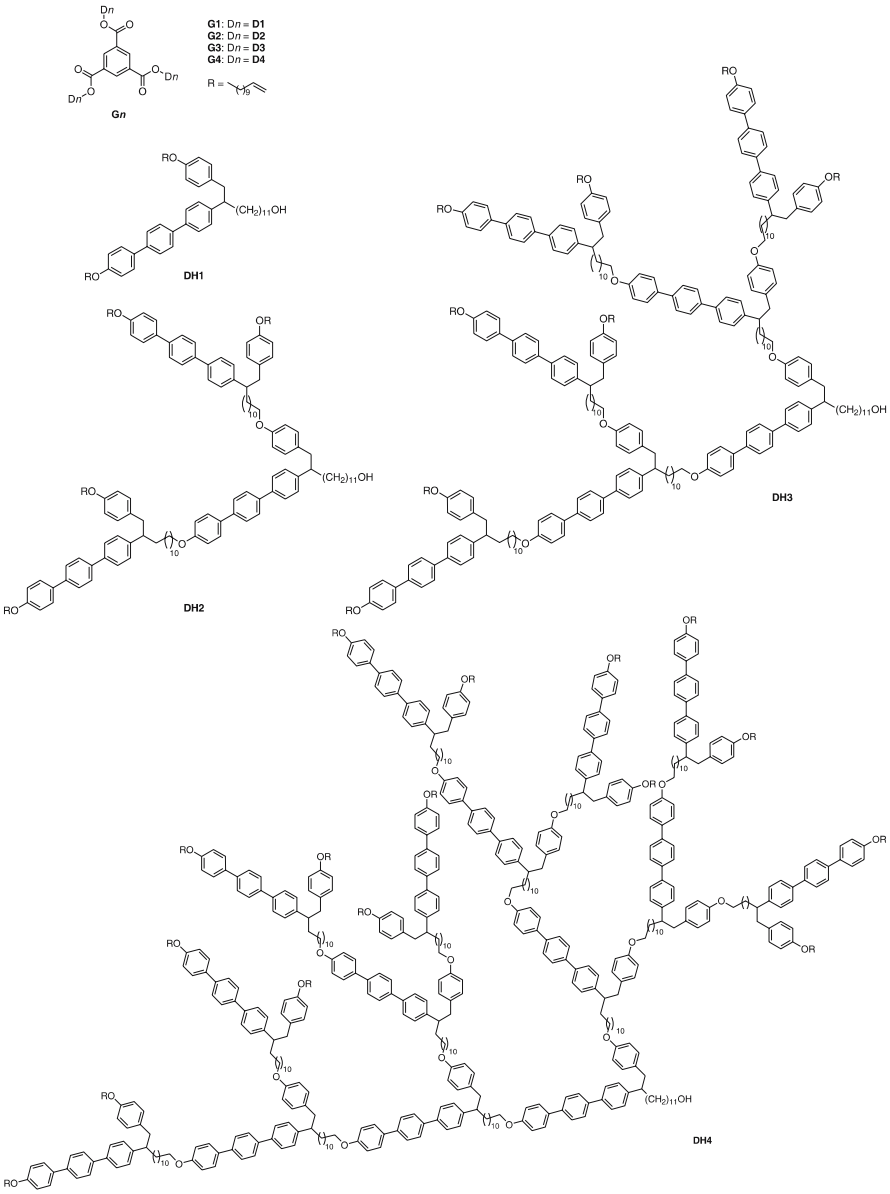

Fig. 47 Structure of the willow-like dendrons (DH*n*) and dendrimers (G*n*)

sesses a carbon linkage between the terphenylene and phenylene units, which exhibits conformational flexibility. Amongst the stable conformational isomers, the *anti* isomer has an extended conformation and leads to mesogens aligning in a parallel fashion, whereas the *gauche* isomer produces a kink in

Table 13 Mesomorphic behavior of the willow-like dendrimers (dendrons and dendrimers)

DH*n*	Dendrons	G*n*	Dendrimers
DH1	Cr 66 (N 54) I	G1	G 5 Cr 32 S 45 N 73 I
DH2	G 58 S 61 N 92 I	G2	G 20 S 42 N 96 I
DH3	G 52 Cr 63 SmX 69 N 105 I	G3	G 53 S 66 N 106 I
DH4	G 63 SmX 73 N 110 I	G4	G 49 S 70 N 108 I

the chain, resulting in a decrease of the temperatures. The subtle combination of both of these conformations of the monomeric sub-units allows for the induction of both smectic and nematic phases at rather accessible temperatures.

A series of polynorbornenes containing the second generation dendron D2 as a side group ($R = C_{11}H_{21}$), with different degrees of polymerization were also synthesized [262, 263]. They exhibit a nematic (over 2 °C), two SmA and a hexatic B phase on cooling from the isotropic liquid (which occurs at around 100 °C).

4.2 Octopus Dendrimers

For the octopus dendritic materials, a modular synthesis was elaborated for the preparation of the branches. Each constitutive part was prepared separately and later assembled selectively together. The anisotropic units selected were a tolane- or stilbene-based moiety, because of both their thermal stability and chemical versatility. Such poor mesogenic segments, despite their intrinsic anisotropy and rigidity, were also chosen in order to test whether mesomorphism could be induced solely by the dendrimerization process [264]. The dendritic branches, bearing mesogenic moieties and functionalized by a focal acid group, were coupled to a small tetra-podand core unit, bearing four amino groups, to yield the final dendrimer (Fig. 48).

Homolithic (Fig. 48, X = Y) [264, 265] and heterolithic (Fig. 48, $X \neq Y$) [264] dendrimers were synthesized and all of them were liquid crystalline. In such systems, mesomorphism was induced by the precise assembling of these non-mesogenic units within the dendritic frame. Moreover, the mesophase stability was found to greatly depend on the localization of the various units within the heterolithic systems (Fig. 51). Indeed, the principles of the modular construction can be applied here for the preparation of regular co-dendrimers made of at least two basic building blocks which can be arranged in a very controlled manner, alternated or segmented (Fig. 49). Only the former has been prepared to date. The possibility of creating such polyfunctional and discrete dendritic structures with the ability to self-organize

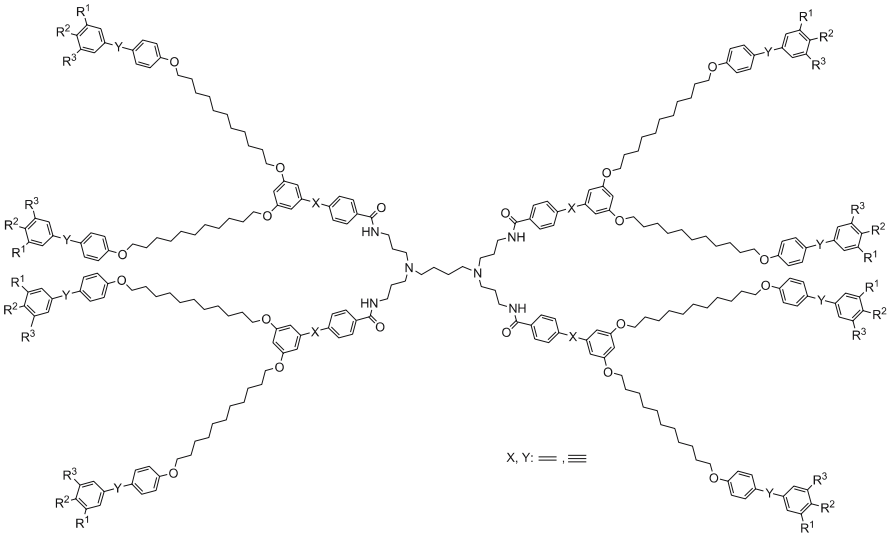

Fig. 48 Example of octopus LCD of the second generation (R^1, R^2 and R^3 stand for $OC_{12}H_{25}$ or H)

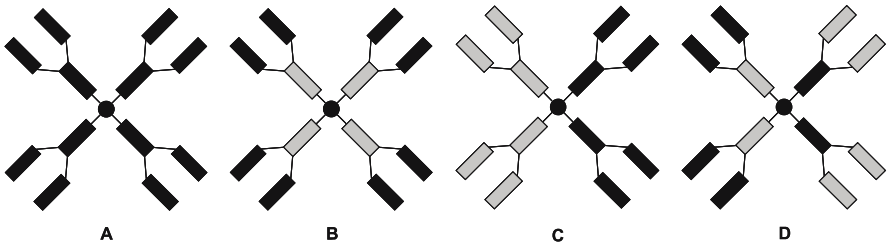

Fig. 49 Schematic representation of homolithic (**A**) and heterolithic alternated (**B**), segmented (**C**) and alternated-segmented (**D**) octopus-like dendrimers

into mesophases is an attractive strategy in the field of material science for the elaboration of multicomponent systems.

The dendrimers bearing only one aliphatic end-chain at the extremity of the outer tolane unit exhibit a smectic behavior (Fig. 48, $R^2 = OC_{12}H_{25}$, $R^1 = R^3 = H$). The X-ray diffraction patterns are characterized by the presence of 3–4 orders of reflection corresponding to a well-defined lamellar stacking. On the basis of these X-ray patterns, a high-temperature phase has been assigned as a disordered smectic A phase, whereas the other, low-temperature phase (due to an extra in-layer order) as a hexatic smectic B phase, the layer spacing being rather large, in the range 10–12 nm (homolithic derivative: SmB 101 SmA 121 I; heterolithic derivative: SmB 109 SmA 132 I). This confirms the prolate conformation of the dendrimers in both smectic phases with

the peripheral anisotropic units being almost perpendicular to the layer normal direction. In this case, the morphology of the smectic phases generated by such multiblock molecules is quite unique in that it possesses a two-level molecular organization, each being dependent on the other. It consists of an internal sub-layer made of tilted rigid segments with no correlation of the tilt, flanked by outer slabs inside which the mesogenic groups are arranged perpendicular to the layer (Fig. 50). Molecular modeling supports this view of strongly segregated multilayer structures, with interfaces between the various molecular parts. Obviously, these interfaces are not so well defined due to thermal fluctuations. Nevertheless, let us point out that because of this peculiar structural feature, such layered mesophases cannot exactly be described as purely SmA or SmB phases, and were referred to as "supersmectic" phases [264].

As for the other set of dendrimers bearing two (Fig. 48: $R^1 = R^2 = OC_{12}H_{25}$, $R^3 = H$, $X = / \neq Y$; $R^1 = R^3 = OC_{12}H_{25}$, $R^2 = H$, $X = Y =$ double bond: Col_h 42 I) or three aliphatic chains (Fig. 48: $R^1 = R^2 = R^3 = OC_{12}H_{25}$, $X = Y =$ double bond: Col_h 84 I) at the extremity of the outer tolane or stilbene part, they all exhibit a columnar mesophase with a hexagonal symmetry (Fig. 51) [264, 265]. The formation of columnar mesophases in non-discotic systems, and particularly with polycatenar mesogens [266, 267], is a consequence of the mismatch between the surface areas of the aromatic cores and the cross-section of the aliphatic chains, resulting in the curvature of all the interfaces, as has been discussed with SC-LCDs bearing polycatenar endgroups. In the present case, in order to compensate the discrepancy between the cross sections of both the anisometric segments and the chains, one can also imagine the former to be tilted and distributed in a "splay" fashion, with respect to the columnar axis, also resulting in the curvature of the in-

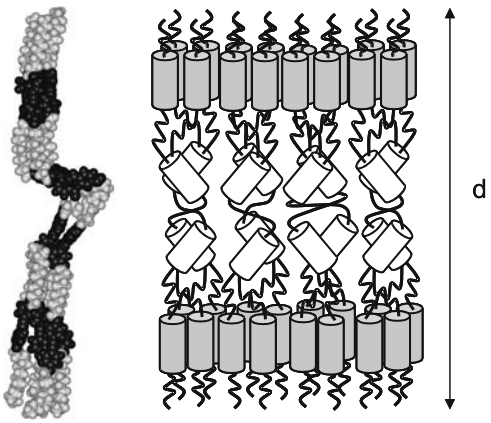

Fig. 50 Snapshot of the molecular conformation of the octopus dendrimers with 8 terminal chains and model for their molecular organization in smectic layers

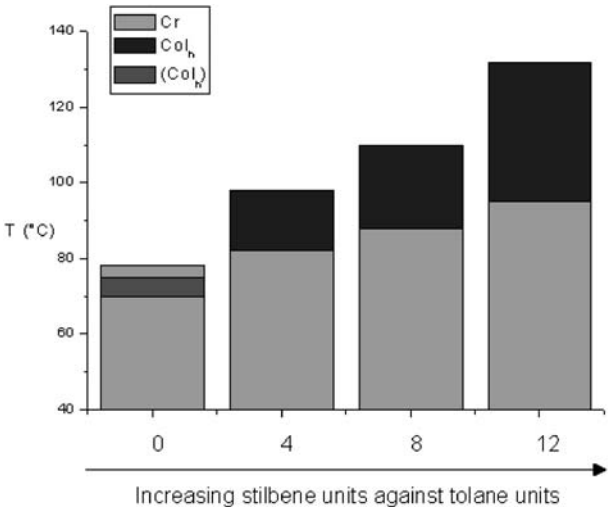

Fig. 51 Diagram showing the evolution of the mesophase stability from tolane-rich (*left side*) to stilbene rich (*right side*) octopus LCDs ($R^1 = R^2 = OC_{12}H_{25}$, $R^3 = H$)

terfaces [268, 269]. Indeed, the parameters of the hexagonal lattices obtained experimentally, $a = 9–10$ nm, correspond fairly well to the diameter of the dendrimers in a flattened conformation, ranging between 10 and 11 nm as estimated by MD simulation (Fig. 53). It is therefore highly probable that the octopus preferably adopts an oblate shape within the columns that is a flattened or wedge-like conformation with the anisotropic blocks lying more or less in the 2D hexagonal lattice plane, rather than a prolate conformation (cylindrical) as in the smectic systems.

As for the dendromesogens described by Percec et al. [79–85], where columnar structures are generated from the self-assembling of the most stable molecular conformations having either a wedge-like or half-disk shape, the mesophase formation of these dendrimers results from the self-assembling process into disks and columns of octopus molecules necessarily adopting pre-defined shapes. The overall molecular conformations of the dendrimers in the mesophase are driven by the steric congestion of the terminal aliphatic chains and depend on the segregation between the different constitutive blocks. In the present case, one ($R^1 = R^2 = R^3 = OC_{12}H_{25}$) or two ($R^1 = R^2 = OC_{12}H_{25}$, $R^3 = H$) molecular conformations likely predominate to satisfy the geometrical requirements. The supramolecular disks or columns thus result from the molecular association of two or three dendrimers (depending on the aliphatic chain substitution) in the appropriate conformation, as depicted in Fig. 52; and these columns are packed in a hexagonal lattice. Moreover, considering the diblock, alternated chemical nature of these octopus dendrimers, an *onion* morphology for the columns is most likely probable (Fig. 53) [264].

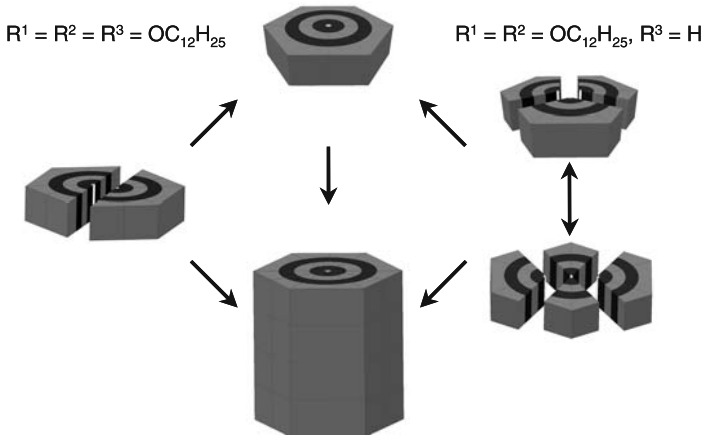

Fig. 52 Schematic representation of the self-assembling and self-organization processes of octopus-like dendrimers into the Col_h phase

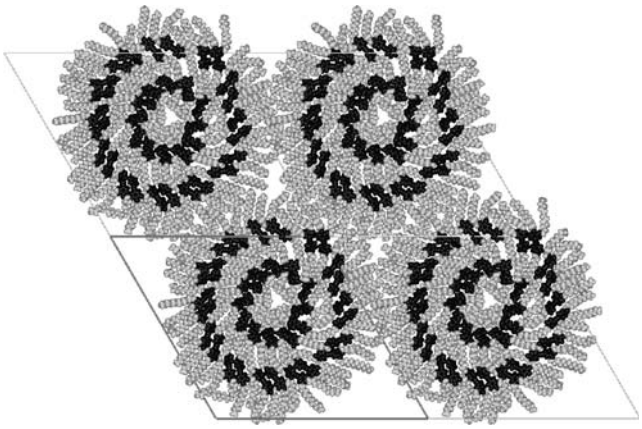

Fig. 53 Snapshot of the molecular conformation in the Col_h phase of a 16 chains octopus LCD

This model of an onion internal structure of the columns was supported by molecular dynamics on the homolithic stilbenoid system (Fig. 48, X = Y :=; $R^1 = R^2 = OC_{12}H_{25}$, $R^3 = H$). It showed good segregation at the molecular level by means of interlocked crowns of stilbenoid units belonging to the same generation, such crowns being stabilized by intermolecular interactions. Each crown was separated by neutral aliphatic coronas.

For these dendrimers, the morphology of the mesophase is thus determined by the number of alkyl chains grafted on the peripheral mesogenic group, i.e. the change in the number of terminal chains per end group modifies the relationships between the hard parts and the soft parts, and

consequently the molecules will adopt either a *parallel* (prolate) or *flat* (oblate) conformation. The formation of the smectic lamellar phases is the result of the parallel disposition of the mesogenic groups on both sides of the focal tetravalent core, the dendrimer adopting the shape of a giant elongated multipede (vide infra), and then organizing into layers. In contrast, the grafting of additional terminal chains at the periphery prevents such a parallel disposition of the pro-mesogenic groups, which are forced into a radial arrangement around the central moiety: the dendrimer can adopt the shape of a flat-tapered object and self-arrange into supra molecular columns.

To complete this analysis, the variation of the core connectivity number and the effect on the mesomorphism was studied [270]. Three new second generation main-chain dendrimers (with the same heterolithic branch: Fig. 48: $R^1 = R^2 = OC_{12}H_{25}$, $R^3 = H$, $X = / \neq Y$) were prepared from various amido-cores of zeroth generation and with different multiplicities: 1,4-diaminobutane ($N_C = 2$), tris(2-aminoethyl) amine ($N_C = 3$) and PAMAM-G_0 ($N_C = 4$); the latter was also prepared for the possibility to rigidify the core by additional hydrogen-bonds (amido groups) and the consequent effects on the mesophase stability. They all exhibit a broad Col_h phase. The transition temperatures and mesophase stability were found to be influenced by the nature and the connectivity number of the core (Fig. 54).

Since the overall number of peripheral chains per dendritic molecule is changed, while the lattice parameter of the Col_h phases remains roughly similar, the number of dendrimers self-assembling into columns is different in order to keep the total number of radiating chains constant as shown in Fig. 55.

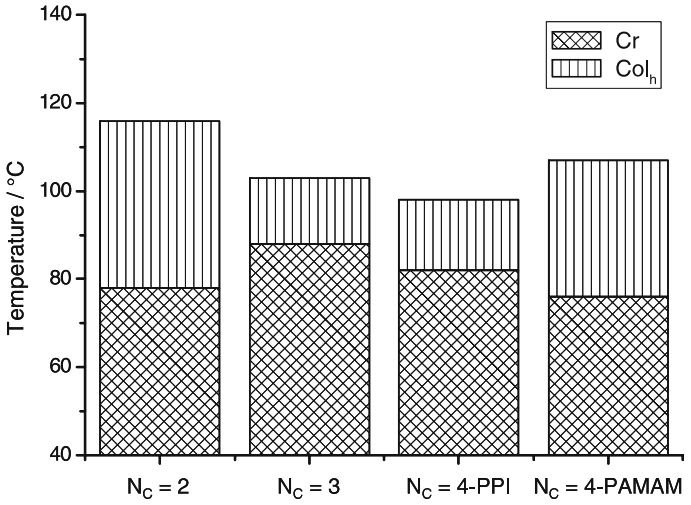

Fig. 54 Evolution of the mesophase stability from $N_C = 2$ to $N_C = 4$

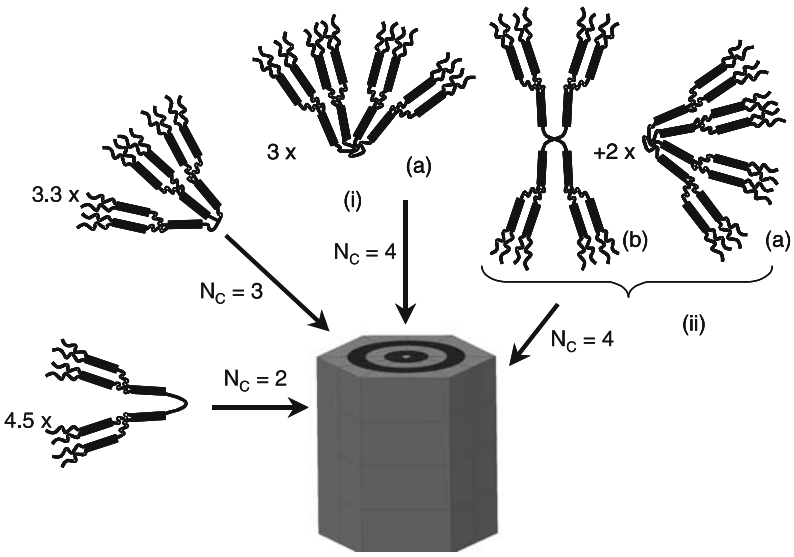

Fig. 55 Self-assembling and self-organization process into columns for the octopus dendrimers with various core connectivity numbers

5
Shape-Persistent Liquid-Crystalline Dendrimers

The so-called "shape-persistent LC dendrimers" represent an unusual and original family of dendrimers [271]. The particularity of these systems is the nature of the dendritic matrices, which are completely rigid and highly conjugated, and are different from the dendrimers described previously since they have the potential to be intrinsically mesogenic. Adequately functionalized by terminal aliphatic chains, they can behave as large, disk-shaped mesogenic molecules right from early generations potentially showing columnar mesomorphism. Because of their expanded and electron-rich core, such dendrimers should find many applications in materials science owing to their interesting photochemical and photophysical properties, and to their readily attainable nanoscale dimensions [271].

Pesak and Moore [272] described a convergent scheme for the synthesis of three generations of shape-persistent tolane-based dendrimers functionalized at the periphery by oligo(ethylene oxide) chains (Fig. 56). All the dendrimers, existing as stiff glasses at room temperature, were mesomorphic on heating, exhibiting wide temperature-range hexagonal columnar phases with clearing points increasing dramatically with the generation number (Table 14). Surprisingly, preliminary data for the dendrimer of the fourth generation indicated that this compound was amorphous.

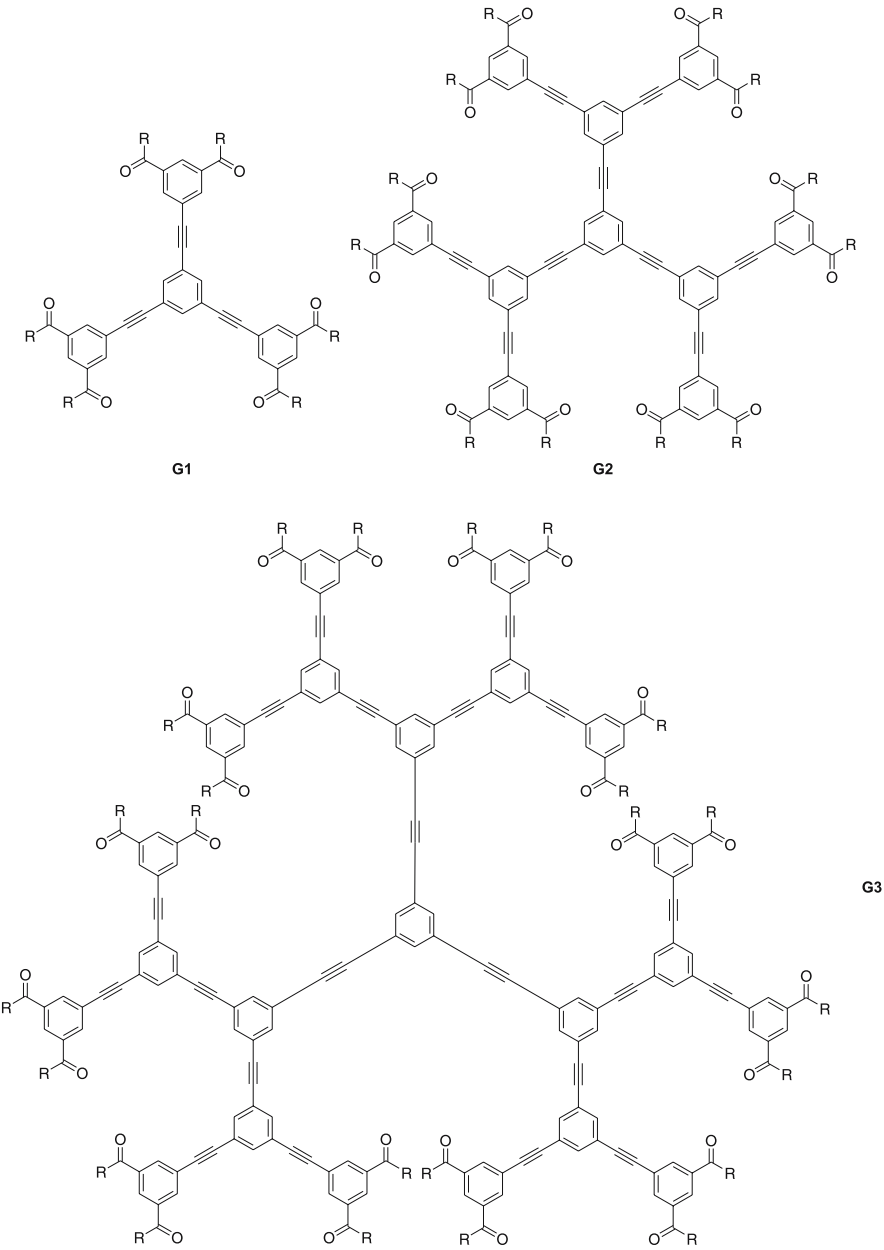

Fig. 56 Chemical structures of the tolanoid-like dendrimers (R = $O(CH_2CH_2O)_3Me$)

Stilbenoid-like dendrimers possessing an analogous molecular structure were reported by Meier to be mesomorphic too [273]. The five generations of stilbene-based dendrimers (Fig. 57) [274, 275] and the first two gener-

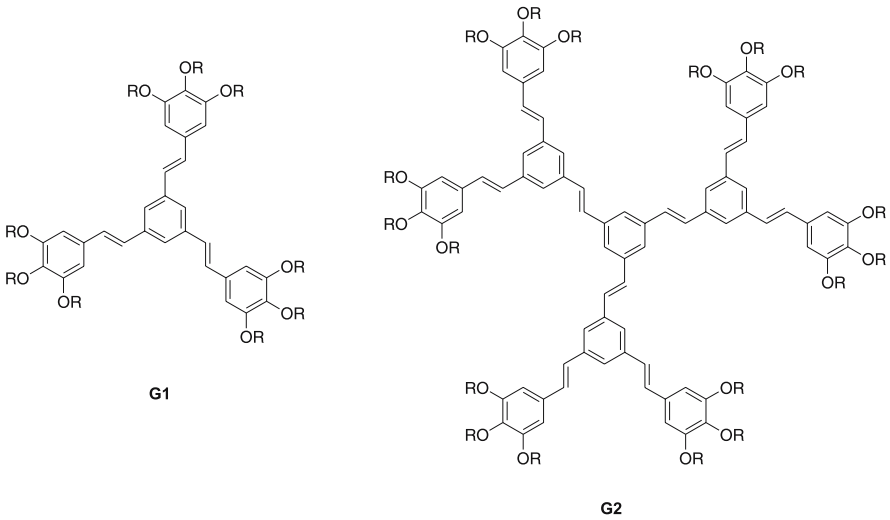

Fig. 57 Chemical structures of the stilbenoid-like dendrimers (R = OC_3H_7, OC_6H_{13}, $OC_{12}H_{25}$)

ations of distyrylbenzene-based dendrimers (Fig. 58) [276] were synthesized by a convergent scheme based on the Wittig–Horner reaction, which allowed an *E*-configuration with double bonds to be obtained. It was found that only generations G1 and G2 showed columnar mesophases as long as the alkoxy chains were long enough (R = OC_6H_{13}, $OC_{12}H_{25}$), whereas higher generations (not drawn here) failed to exhibit mesomorphism (Table 14). The unusual phase sequence Col_h-to-Col_o was attributed to the presence of several conformers whose distribution is temperature-dependent, leading to distortion of the columnar structures of the Col_h phase at high temperatures. Note that the elongation of the dendritic arms results in a huge stabilization of the mesophases. An interesting temperature-dependent ^{2}D NMR study carried out on the neat phases of the stilbenoid dendrimers (Fig. 57), selectively deuterated in specific positions, showed different molecular and segmental motions in the crystalline, liquid crystalline and isotropic phases [277]. It particularly revealed that G1 adopts an average planar shape, despite the significant deviation of the styryl arms from the molecular plane, whereas in contrast G2 does not show large angle motions. These motions are correlated with the photophysical properties of the materials (fluorescence, photochemistry and photo-oligomerization).

In these series of compounds, X-ray diffraction studies revealed that the inter-columnar distance significantly increases between G1 and G2, and then remains constant for G3, whereas the unit cell parameter *c* (representing the stacking periodicity between adjacent molecules in the column) nearly doubles on the passage from second to third generation. Molecular model-

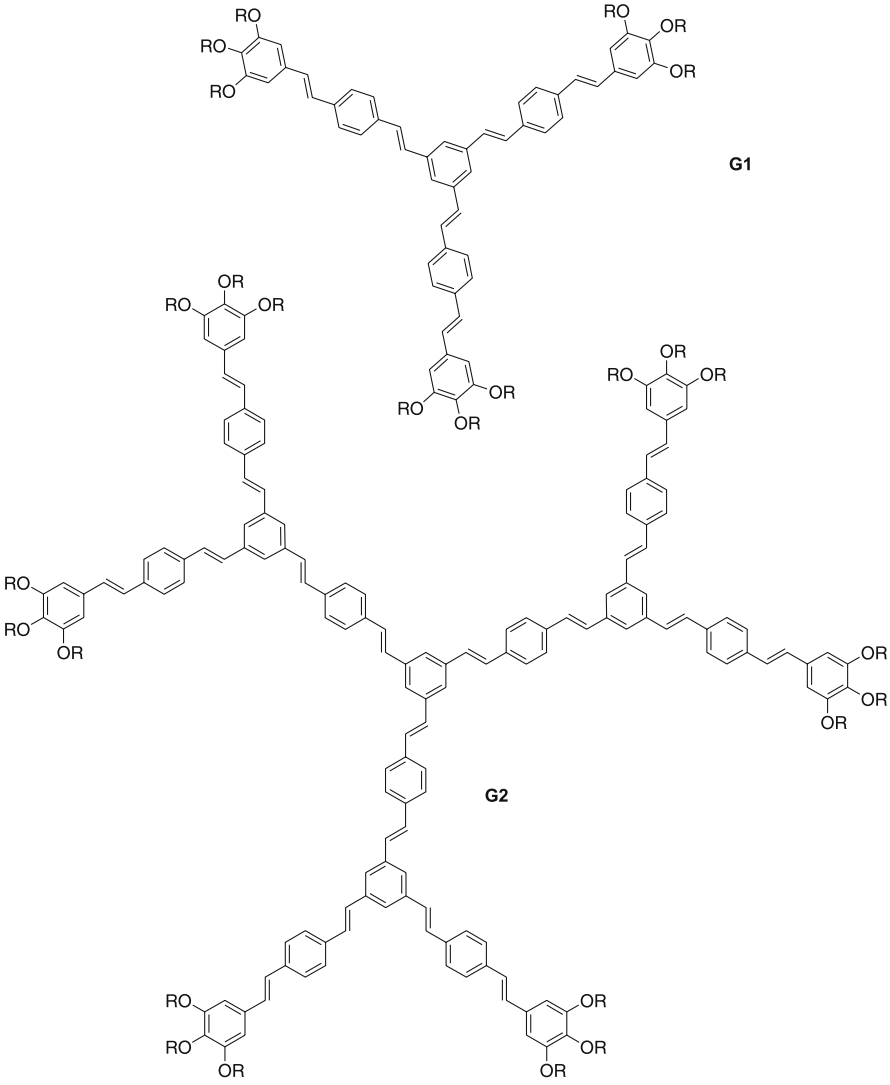

Fig. 58 Chemical structure of elongated distyrylbenzene-based dendrimers (R = OC_3H_7, OC_6H_{13}, $OC_{12}H_{25}$)

ing showed that in fact the dendrimers of the first and second generation have a planar conformation without any steric hindrance. In contrast, such a purely planar conformation is impossible for the largest dendrimers because of overcrowding of the terminal chains preventing as such a regular arrangement. For these compounds, the expansion of the molecule occurs in the molecular plane for the first generations to form megadisks and the growth expands out-of the molecular plane for higher generation numbers to

Table 14 Mesomorphism of the shape-persistent dendrimers

G*n*	Tolanoid dendrimers	Stilbenoid dendrimers ($R = OC_{12}H_{25}$)	Elongated Stilbenoid dendrimers ($R = OC_{12}H_{25}$)
G1	G –58 Col_{ho} 41 Col_h 62 I	Cr 38 Col_h 75 I	G 21 Col_h 108 I
G2	G –58 Col_{ho} 31 Col_h 181 I	Cr 11 Col_h 32 Col_o 99 I	G –27 Col_o 195 I
G3	G –52 Col_h 191 I		

form cylindrical objects. The stability of the columnar mesophases of these large unimolecular disks, which are formed by their face-to-face stacking is primarily enhanced in consequence to the increasing interactions between successive macrodisks. Then, the mesomorphic properties are lost once this out-of plane growth becomes too important because of steric repulsions and strong distortions of the molecular shape.

Structurally related dendrimers of the elongated stilbenoid systems based on a 1,3,5-triazine star-shape of the first generation having styryl or higher oligo(phenylenevinylene) arms were also prepared [278]. The four materials exhibit a liquid crystalline phase (still unidentified) with increasing phase stability on lengthening of the arms (clearing temperatures 109.5, 96.0, 233.3, and > 300 °C for mono-, di-, tri- and tetra(styrylbenzene) systems, respectively).

Other related dendrimers of the first [279] and second [280] generation based on the 1,3,5-triazine unit and tolane arms were also reported by Lee and Yamamoto. The dendrimers of the first generation bearing two chains exhibit a Col_h phase as expected. Surprisingly, the members of the second generation also showed a Col_h phase between 130 and 150 up to 170–230 °C, despite of the grafting of only one terminal chain per peripheral arm.

6
Liquid-Crystalline Metallodendrimers

Metallomesogens are metal complexes which exhibit liquid-crystalline properties, forming the same type of mesophases as found in purely organic materials. They may have a covalent (neutral) or an ionic character, and a large number of thermotropic [281, 282] and lyotropic [283] metal-containing liquid crystals have been reported. Metallomesogens are becoming a very important class of mesogenic materials, as new properties may be expected on the introduction of metals into a liquid-crystalline material. In addition, they offer wider possibilities for structural variations than simple organic materials as, for example, several types of coordination geometry can be envisaged

through the metal and by the use of polydentate ligands. This may in turn lead to new mesophases or new types of molecular organizations, which could eventually form the basis for new effects and devices.

While in general the vast majority of dendrimers prepared are purely organic systems, there has been some interest in the synthesis of dendrimers containing transition metals [34–40]. Indeed, their incorporation within a dendritic structure may find many applications in various areas of science as for example efficient catalysts because of the high concentration of active sites, electro-active molecules due to the multiredox centers, sensors due to their multivalent and selective binding ability, or as molecular antennas due to their particular photo-physical properties. These properties can be tuned and modulated depending on the location of the active moieties within the dendrimer: the metals can be incorporated at the core, throughout the structure or at the periphery of the dendrimer. Some interesting aspects concerning these "supra-supermolecular" systems have been discussed elsewhere [34–40, 48–52].

Only a few studies have looked at metal-containing liquid crystalline dendrimers. In these examples, the metal is either located at the core or in the branches of the dendrimer. The first report of a metallomesogen with a dendritic architecture can be backdated to 1993, though they were not described as such. Serrette et al. [284] prepared a first generation of "Fréchet–Percec" dendritic branch, which they then grafted around several coordinative salen-units varying in spacer length (Fig. 59: Y = – CH_2CH_2 –, – $CH_2CH_2CH_2$ –, – CH_2CMe_2 – CH_2 –). Induction of mesomorphism was observed upon complexation to the oxovanadyl metal ion (Table 15), probably due to the rigidification of the central chelating part, since the flexible ligands themselves were devoid of liquid crystalline properties. Infrared spectroscopy further revealed the formation of linear chain structures for complexes with Y = propyl and dimethylpropyl, whereas the complex with Y = – CH_2CH_2 – was

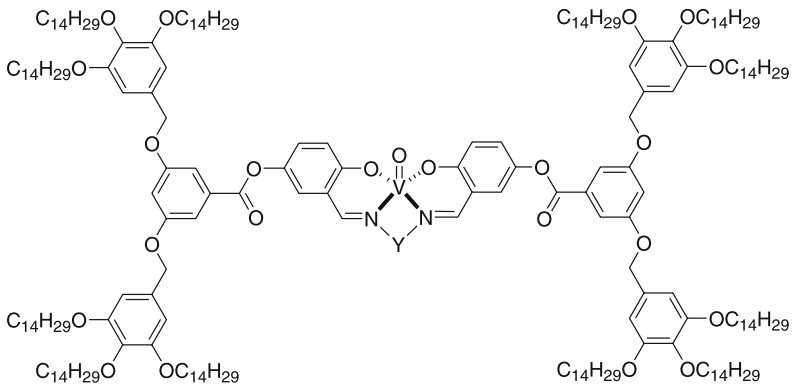

Fig. 59 Structure of the dendritic oxovanadyl complexes

Table 15 Thermal behavior of the dendritic oxovanadyl complexes as a function of the spacer Y

Y	Mesomorphism
$-CH_2CH_2-$	Col_{r1} 119.5 Col_{r2} 156 I
$-CH_2-CH_2-CH_2-$	Col_{h1} 36 Col_{h2} 97.5 Col_r 151 I
$-CH_2-CMe_2-CH_2-$	Col_h 55 Col_r 108 I

monomeric; it nevertheless displayed the largest mesomorphic range. The high-temperature mesophase was identified as a Col_r (*c2mm*) mesophase in all cases, and two of the complexes exhibited the Col_h-to-Col_r phase sequence (Table 15). The destabilization of the hexagonal structure at the expense of the rectangular phase was thought to be due to the bulkiness of the terminal groups and to their spatial requirements, and the driving force for the Col_h-to-Col_r transition may then be linked to the formation of linear chain structures. These could limit the lateral diffusion of the cores, and force the stacking of the core with limited conformational options.

Another series of related mesomorphic metallodendrimers, having the metal located at the core of the dendrimer, were also reported [285]. The dendritic ligands were obtained by condensation of the corresponding 1,3-dione with aminopropanol, and the dicopper complexes were then formed by the reaction with copper(II) acetate (Fig. 60). These ligands, also based on the first generation "Fréchet–Percec" dendron motif, were not themselves mesomorphic, but upon complexation, mesophases were observed whose sta-

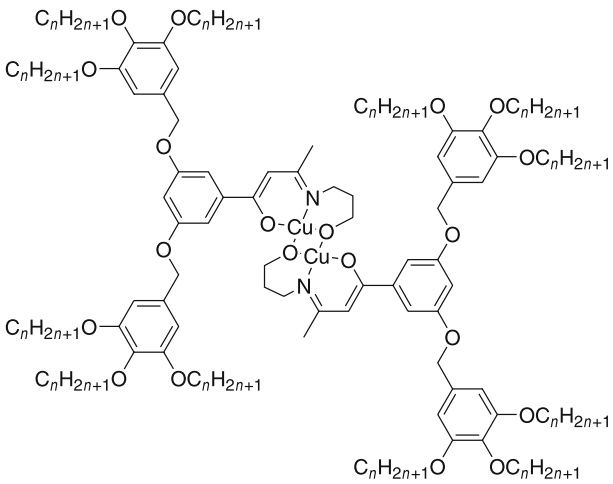

Fig. 60 Structure of the dicopper dendritic complexes

bility was found to be dependent on the number of chains and on their length. Induction of mesomorphism is also likely due to the rigidification of the chelating unit as above. The systems having one and two chains per terminal phenyl groups were not mesomorphic, but those with three chains showed a Col_h phase. The occurrence of the mesophase depended strongly on the chain-length. Thus, short- and long-chain derivatives (n = 5, 14 and 16) were not mesomorphic, whereas the intermediate chain length compounds (n = 6–9, 10, 12) displayed a Col_h phase with transition temperatures sensitive to the chain-length (between 80–100 °C for the melting temperature and 100–120 °C for the clearing temperature). The more circular core of the dicopper complexes with respect to that of the oxovanadyl ones just discussed above may explain the observation of only the Col_h phase for the latter.

Metallomesogens with branched, dendrimeric ligands L1 and L2 derived from tris(2-aminoethyl)amine were reported in 1996 by Stebani et al. (Fig. 61) [286]. This series of metallomesogens of the type $[MX_2(Li)]$ (i = 1 or 2) was obtained subsequently to the complexation of L1 and L2 with various metal salts, $CoCl_2$, NiX_2 (X = Cl, NO_3), CuX_2 (X = Cl, SCN and NO_3) and $ZnCl_2$. Depending on the metal, the complexes could be obtained with two possible coordination geometries, either with the trigonal bipyramidal mode giving rise to pentacoordinated ionic complexes ($[MXL]^+[X]^-$) (Fig. 61a) or

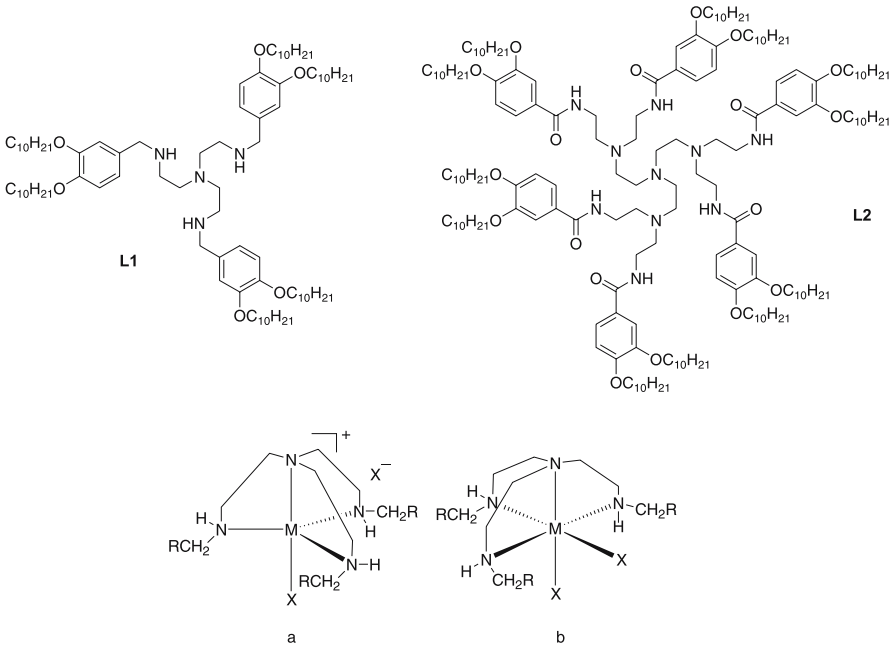

Fig. 61 Dendritic ligands L1 and L2, and the corresponding metal complexes in the trigonal bipyramidal (**a**) and octahedral (**b**) geometry

as the neutral octahedral complexes ([MX_2L]) (Fig. 61b). The distinction between these two modes of coordination was elucidated by infrared and UV/Vis spectroscopy: the copper(II) and cobalt(II) complexes adopted the trigonal bipyramidal structure and the nickel(II) complexes were octahedral, whereas it was not possible to determine the structure of the zinc(II) complexes. A Col_h phase was observed for quasi all the complexes with L1 between 40–60 °C and 65–85 °C, and up to 120 °C for the zinc(II) complex (Table 16), the exception being [$Ni(NO_3)_2$(L1)] which melted directly to the isotropic liquid at 46.5 °C.

Dendrimer L2 was itself mesomorphic, showing a monotropic Col_h phase, Cr (79.5 Col_h) 98.5 I, [287] which upon complexation to $CuCl_2$ became enantiotropic (Table 16). By UV/Vis spectrum, the complex was found to adopt a trigonal bipyramidal structure as [CuCl(L1)]Cl. Thus, a dendritic effect could be observed in this series in that the stability of the mesophase increased considerably with the dendrimer size; the complex [CuCl(L1)]Cl cleared at 75 °C whereas the clearing point of the complex [CuCl(L2)]Cl was 140 °C.

In these three series of dendrimers, the metal was located as the central node of the macromolecule, and induction of mesomorphism was systematically observed on complexation to the metal ion. When coordinated, the dendritic core is likely to lose its flexibility, its conformation being locked by the metal center, and thus the molecule adopts a molecular shape approximating that of a disk.

A quite different approach was used by Serrano et al. So far, whatever the generation number, the number of metallic centers was constant and equal to one, because the unique coordinative site was located at the center of the dendrimer and the metal was embedded within. Here, dendrimers based on the zeroth- and first-generation of PPI dendrimers and end-functionalized by four or eight coordinating 4-(alkoxybenzoyloxy)salicylaldimine were con-

Table 16 Mesomorphism of the metallodendromesogens

Dendrimers	Transition temperatures
[CoCl(L1)]Cl	G 56 Col_h 85.5 I
[$NiCl_2$(L1)]	G 40 Cr 47 Col_h 64.5 I
[$Ni(NO_3)_2$(L1)]	G 36 Cr 46.5 I
[CuCl(L1)]Cl	G 41 Col_h 75 I
[CuSCN(L1)](SCN)	G 41 Cr 48.5 Col_h 75 I
[$CuNO_3$(L1)](NO_3)	G 36 Cr 47.5 Col_h 79 I
[$ZnCl_2$(L1)]	G 60 Col_h 126 I
[CuCl(L2)]Cl	G 49 Col_h 140 I

sidered as potentially multicoordinative organic ligands [288]. Whereas all the organic dendromesogens were found to possess a smectic mesomorphism [213], the complexation of copper(II) affected strongly the mesomorphic properties of the corresponding complexes. Indeed, mesophase formation was either suppressed in some of the corresponding metallodendrimers (Fig. 62, G0: $n = 10$, mp: 179 °C; G1: $n = 10$, mp: 110 °C; $n = 14$, mp: 80 °C), or the mesophase temperature ranges strongly reduced for the mesomorphic complexes (Fig. 62, G0: $n = 14$, Cr 163 SmC 197 I; $n = 18$, Cr 167 SmC 187 I; G1: $n = 18$, Cr 35 SmC 108 I). Interestingly, the transition temperatures were raised upon complexation for the zeroth generation dendrimers, while for the first generation systems, the temperature interval was similar for the ligand and complex. By X-ray diffraction, the unique mesophase was identified as a SmC phase. The structure of the smectic phases of the dendritic ligands is explained by a parallel arrangement of the mesogenic units extending up and down from the molecular center. However, the complexation of copper(II) resulted in the breaking of this parallel arrangement, and in the opening of the branches, allowing as such interdigitation of the molecules located in neighboring layers. This model is in agreement with the diminishing of the layer

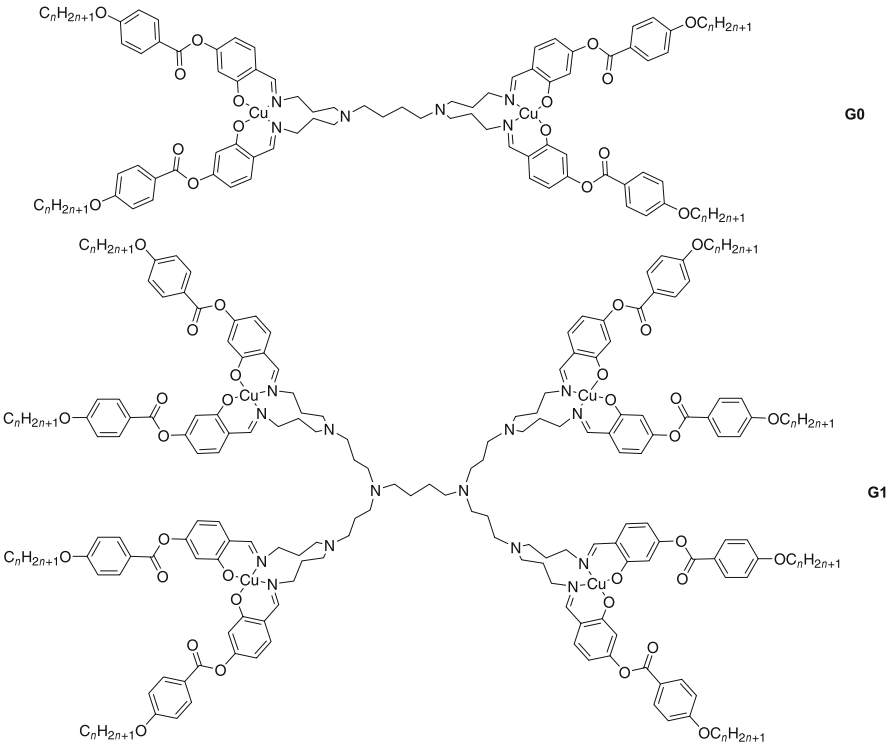

Fig. 62 Dimetallic and tetrametallic dendrimers

periodicity and with the increasing molecular area of the complexes compared to those of the ligands.

Deschenaux and co-workers have designed liquid-crystalline dendrimers based on aromatic polyester cores containing ferrocene [289] for the purpose of designing dendrimer-based molecular switching devices. All of the dendrimers were prepared by a convergent and iterative synthetic methodology leading to precisely monodisperse macromolecules. The dendrimers shown in Fig. 63 [290] and Fig. 64 [291–293] possess respectively 6 and 12 terminal groups (i.e. ferrocene units), each including a cholesteryl mesogenic promoter. Both dendrimers bearing a cholesteryl unit form an enantiotropic smectic A phase (G 47 SmA 150 I, and G 52 SmA 169 I). The other dendrimer (Fig. 64, R = B), for which the ferrocene unit is located at the periphery of the dendrimer, shows an unidentified smectic phase (SmA or SmC) between 119 and 256 °C. The higher temperatures observed for this compound are likely due to the elongated calamitic core unit used to promote the mesophase formation. The SmA mesophase was unambiguously determined by X-ray diffraction on powder and aligned samples. The structure of the mesophase can be explained by the formation of layers containing the dendrimer cores, with interdigitation of the mesogenic units from layer to layer.

A mixed [60]fullerene-ferrocene dendrimer (Fig. 65) was also found to be mesomorphic, showing a room temperature smectic A phase which cleared at 157 °C (no glass transition temperature was detected) [294, 295]. The mesophase was only slightly destabilized upon the addition of C_{60} when com-

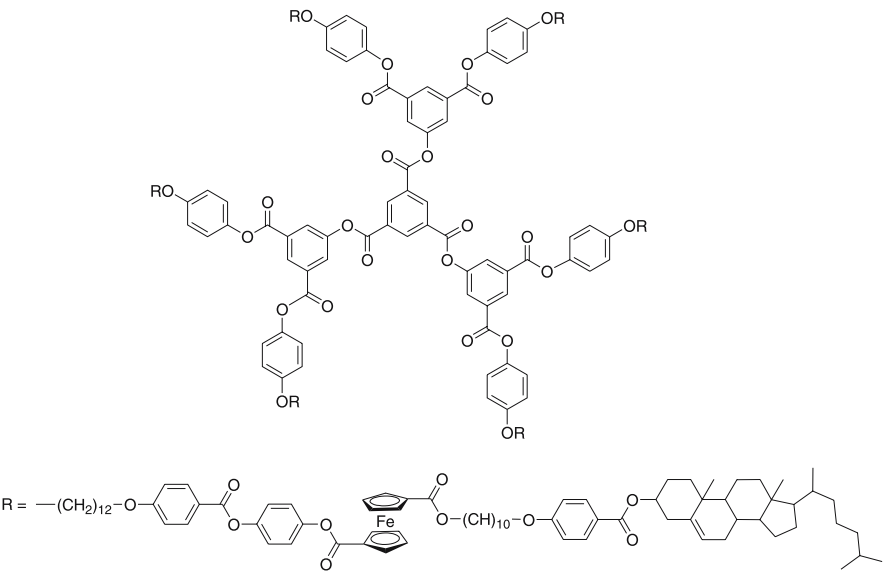

Fig. 63 Structure of the ferrocene-containing dendrimer with six mesogenic arms

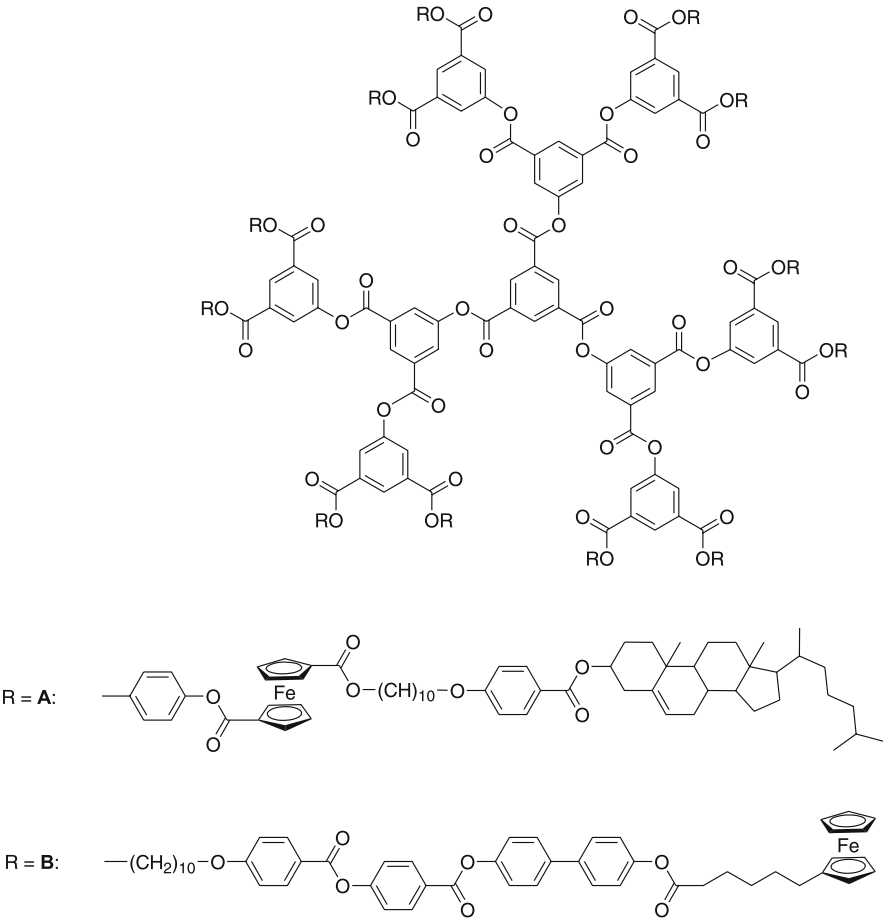

Fig. 64 Structure of the ferrocene-containing dendrimers with twelve mesogenic arms

pared to its malonate ferrocene-containing liquid crystalline dendrimer precursor (Fig. 65, SmA 169 I), probably because both species possess a similar size, and C_{60} is embedded within the dendritic matrix. The zeroth generation was also mesomorphic (SmA 118 I) [296]. This result showed that the association of fullerene (electron-acceptor unit) and ferrocene (electron-donor unit) within the same structure may be an attractive strategy to elaborate liquid-crystalline switches [297] based on the photo-induced electron transfer occurring from ferrocene to fullerene [298].

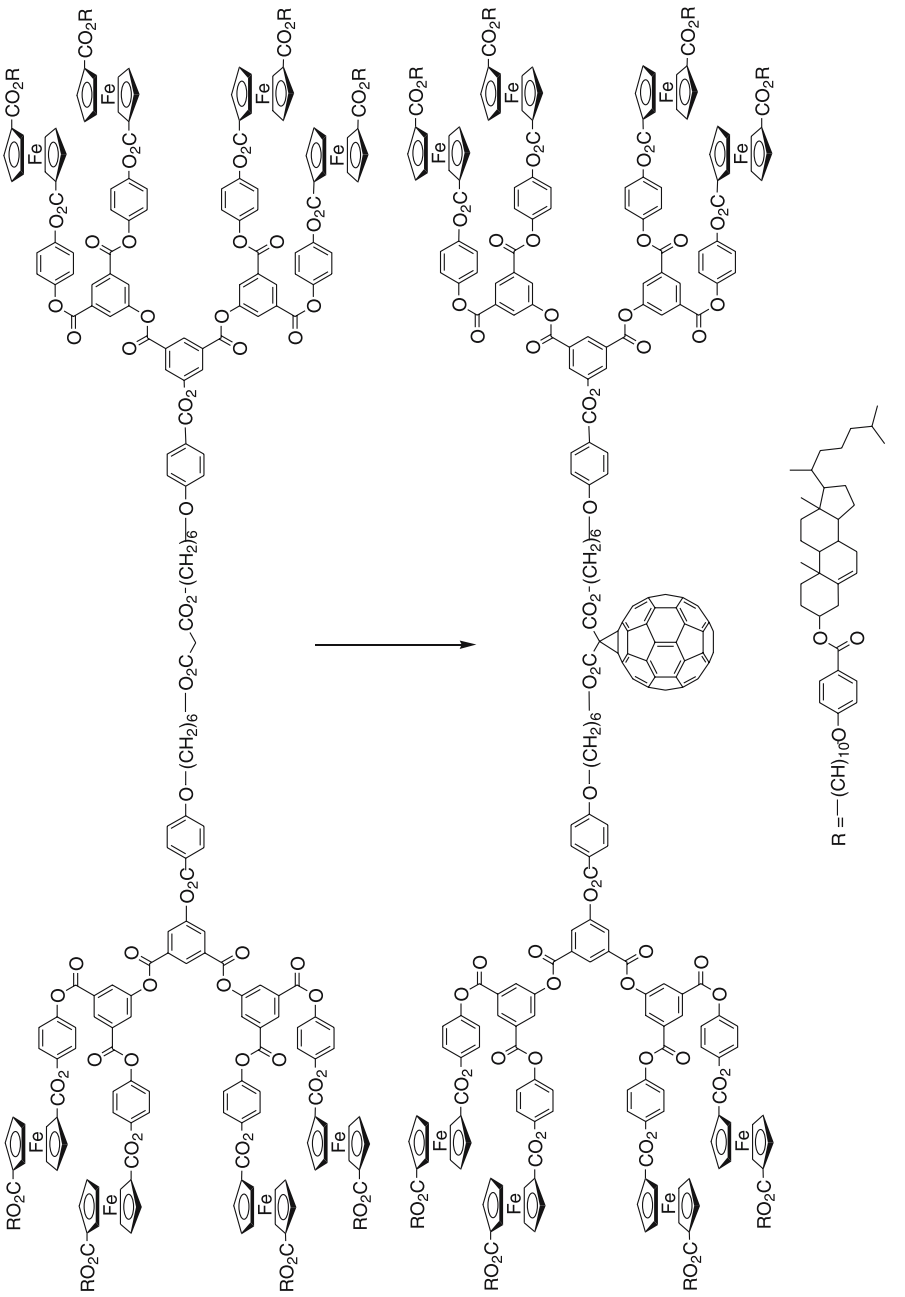

Fig. 65 Structure of the mixed [60]fullerene-ferrocene-containing dendrimer and of its precursory malonate

7
Liquid-Crystalline Fullerodendrimers

Following the work described above, Deschenaux and co-workers engaged in a more systematic study of the elaboration of fullerene-containing thermotropic dendrimers [299, 300] and on the understanding of how such a sphere-like structure could be inserted within liquid crystals in order to ultimately control the properties through dendrimer generation. The use of mesomorphic dendritic addends to functionalize C_{60} was thought to be a suitable solution to avoid aggregation of C_{60} units (decreasing the unfavorable interactions), and thus to favor the formation of mesophases.

An addition reaction of malonate-based dendritic addend onto C_{60} led to a new series of methanofullerodendrimers (Fig. 66) [301]. In such systems, C_{60} is buried within the large dendritic branches, and as a consequence the supramolecular organization of these fullerodendrimers is independent to the change of the generation number of the dendritic carapace (for G2, G3 and G4) and is similar to that of the corresponding malonate species. The mesophase stability was, however, slightly enhanced with generation for both systems (Fig. 67). The only drastic change concerned G1 where the nematic phase was suppressed and replaced by the SmA phase upon the insertion of C_{60}.

The G0 analogues (Fig. 66, G*n* = R) were also found to be mesomorphic, Cr 97 SmA 153 N 162 I and G 29 SmA 142 I, for the malonate and C_{60} adduct, respectively. The supramolecular organization of these dendrimers was deduced from a detailed X-ray diffraction analysis and molecular simulation. For G0, both arms of the molecules are folded towards the same direction, and then the structure consists of a head-to-tail arrangement of such conformers. As for G1, the molecule adopts a V-shape (constituted by pairs of mesogenic groups), and arranged in a head-to-tail fashion favored by the antiparallel packing of the polar end groups. For both structures, lamellae interact through a layer of fullerene. For the next system, G2, the branching part begins to have significant lateral extension with respect to the layer normal, and the two branches extend on both sides of the C_{60} nucleus. Then, for G3 and G4, the structure is solely governed by the polar cyano groups. The central part of the layer is constituted by the fullerene moiety embedded in the large dendritic segments, and the layer interface is formed by partially interdigitated mesogenic groups. In all cases mesophases are likely stabilized by dipolar interactions (antiparallel arrangement of the cyanobiphenyl units).

The corresponding G1 and G2 hemi-dendritic systems were also prepared for comparison (Fig. 68) [301]. Similar trends were observed in that the SmA phase was preferred to the nematic phase, suppressed upon the insertion of C_{60}. The same type of supramolecular organizations is suggested. Interestingly, the mesomorphic temperature range was strongly reduced in the hemi-dendrimers compared to that of the corresponding dendrimers. It was

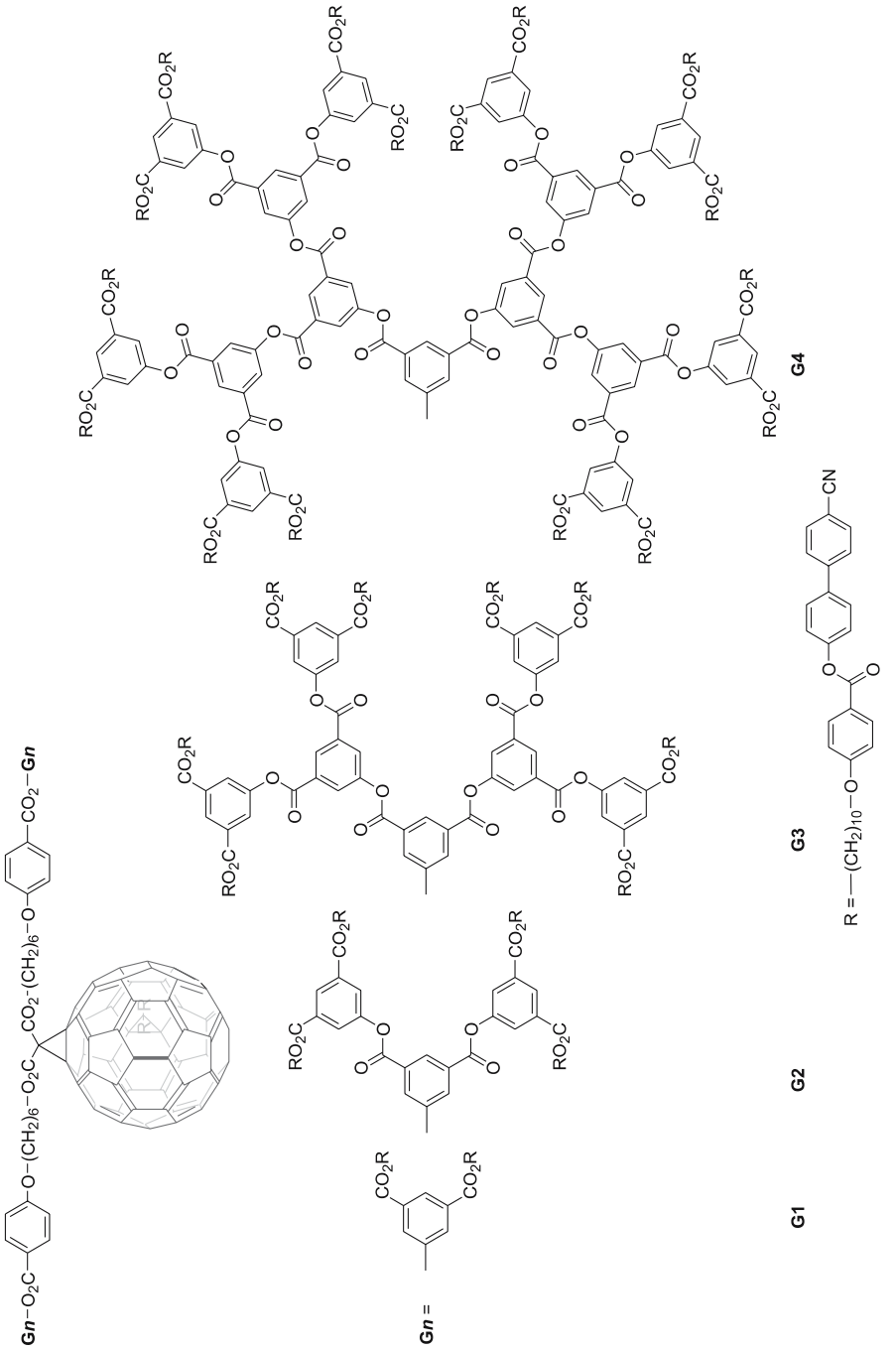

Fig. 66 Liquid crystalline malonate dendritic addends and corresponding methanofullerodendrimers

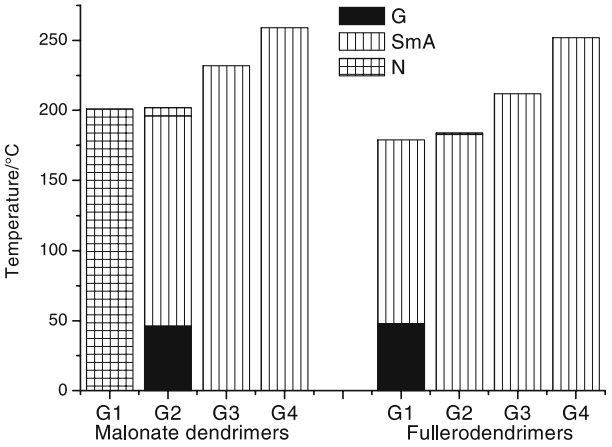

Fig. 67 Mesomorphic behavior of the malonate and corresponding methanofullerodendrimers

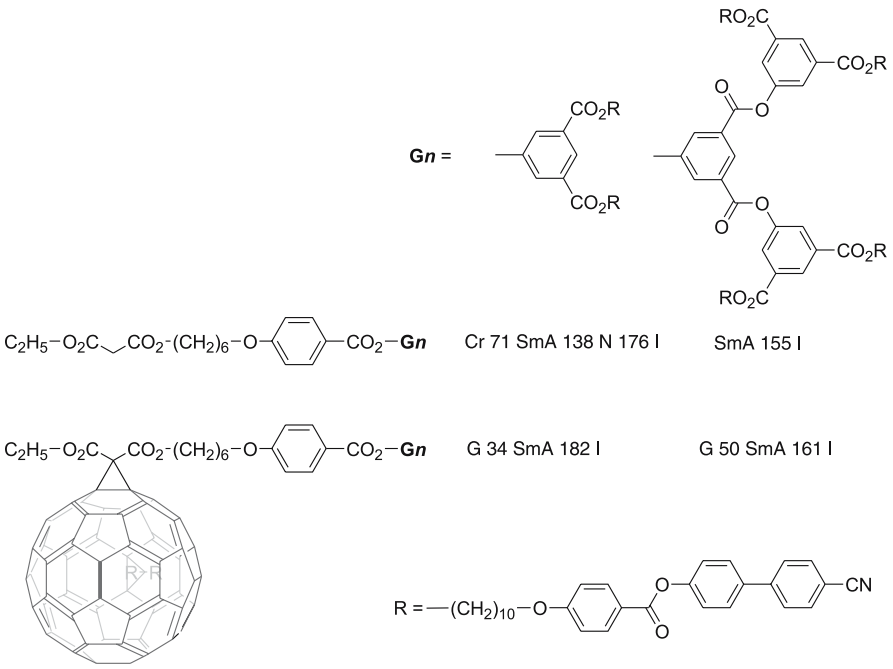

Fig. 68 Hemidendritic malonate and methanofullerene systems

also shown by the electro-optical Kerr effect and hydrodynamic methods that the hemidendrimers are more sensitive than dendrimers to the incorporation of fullerene in their structure (viscosity, shape changes) [302, 303].

Let us note that two homologues of the malonate addends and of the corresponding methanofullerene derivatives described above (Fig. 66) were also prepared with chiral pendant mesogenic groups, laterally attached (Fig. 69). Both the G1 [304] and G2 [57] fullerodendrimers were found to show a chiral nematic phase (Fig. 69, G1: G 26 N* 69 I; G2: G 24.3 N* 80.6 I), and are the first C_{60} derivatives that possess a chiral mesophase; the G1 C_{60}-free malonate was also mesomorphic (G 20 N* 113 I).

As for the silsesquioxane cages (Fig. 24, vide supra) [182], covalent adducts of [60]fullerene offer multiple possibilities for the design of highly functionalized derivatives. In particular, C_{60} can be used as an original initiator core or template for the construction of dendritic systems with high and variable connectivity number with various controllable geometries of attachment. Though, more appropriately referred to as polypedes [57], hexakis(methano)fullerene with 4 (Fig. 70B) [305] and 12 (Fig. 70A) [306] mesogenic groups derived from cyanobiphenyl proved to be mesomorphic. The hexa-adduct malonate difunctionalized in the two poles of the sphere exhibited a transient nematic phase (Cr 85 N 157 I), i.e. observed during the first heating only, while the hexa-adduct functionalized in the six apical positions of C_{60} showed an enantiotropic SmA phase (G 80 SmA 133 I). Unfortunately, no higher generations based on these poly-adducts of C_{60} have yet been reported.

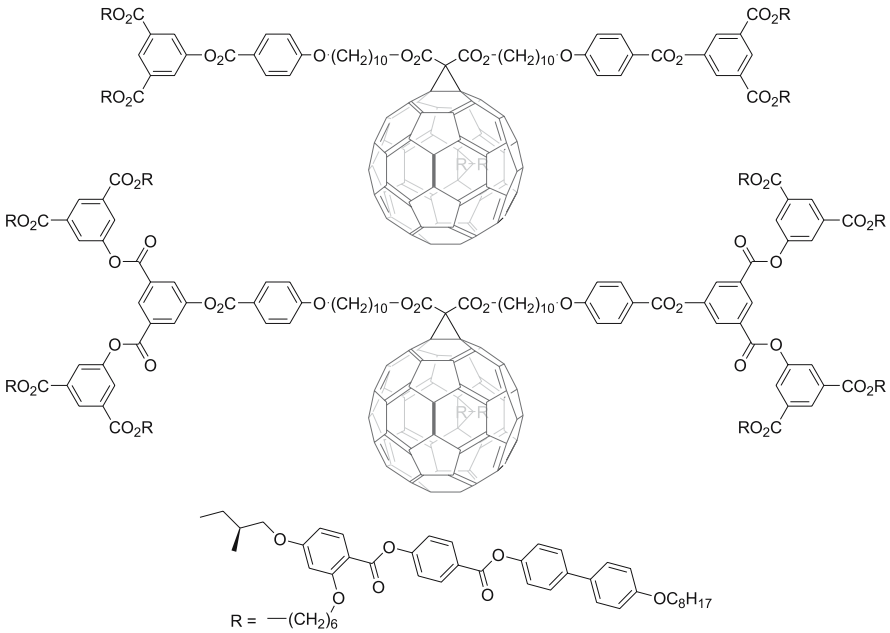

Fig. 69 First C_{60} derivative showing a chiral nematic phase

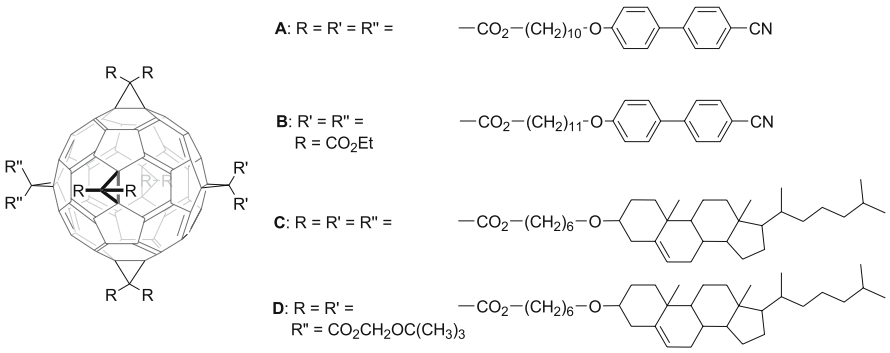

Fig. 70 Liquid crystalline hexakis(methano)fullerene materials

Following a judicious design and challenging chemistry, two novel hexaadducts bearing 12 (Fig. 70C) and 10 cholesteryl units (Fig. 70D), respectively, were reported by Felder-Flesch et al. [307] and found to be mesomorphic. They both exhibit a similar mesomorphic behavior, with a broad temperature SmA phase, quite different to that of the malonate mesogenic promoter for which a chiral nematic phase was observed (G 67 N* 88 I). On heating, a glass-to-SmA phase transformation is observed just above room temperature, followed by the transition to the isotropic liquid at 165 °C and 180 °C for the C and D systems, respectively. The supramolecular organization of these species within the smectic layer consists of an overall smectic bilayer structure in which one of the active moieties (C_{60}) is confined in a central sub-layer sandwiched by two outer-layers of cholesteryl groups; each single layer is separated by thin films of molten aliphatic chains. Moreover, and because of the quasi-spherical structure of C_{60}, the latter likely pave the sub-layer according to a 2D hexagonal arrangement (deduced from XRD and MD). The selected design, i.e polyaddition of cholesteryl moieties on the carbon sphere used as a spherical template to create new 3D architectures, then seems to be a method of choice to obtain stable anisotropic materials and prevent the C_{60} aggregation tendency. This approach should allow the preparation of a wide variety of fullerene hexaadducts, symmetrical or non-symmetrical and with a variable and controlled number of active pendant mesogenic units.

There has been one derivative of bis(methanofullerene) carrying two dendritic wedges (Fig. 71) that was claimed to show a mesophase between 40 and 70 °C, though the phase was not identified; the precursor itself displayed a nematic phase (Cr 48 N 63 I) [305].

Fulleropyrrolidines constitute an important family of C_{60} derivatives that have the advantage over the methanofullerene systems in that they lead to stable reduced species, allowing the development of fullerene-based redox molecular switches. In order to promote mesomorphism in such a mono-adduct structure, Deschenaux et al. decided to modify the C_{60} derivative by the use

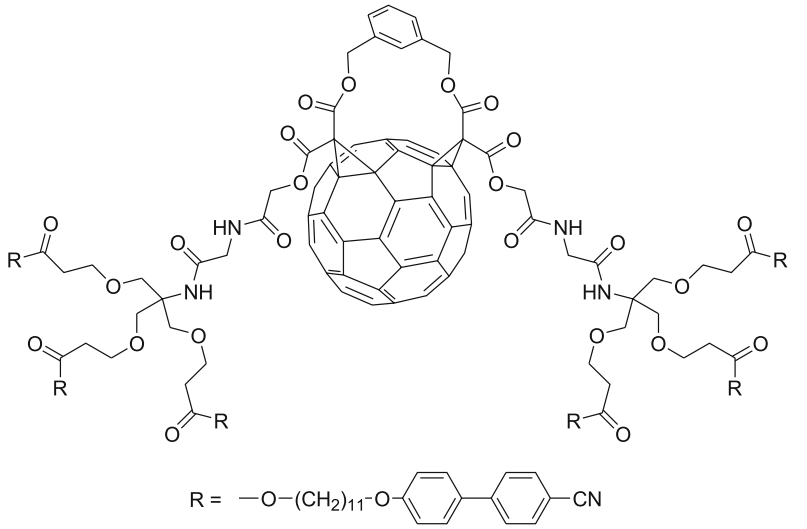

Fig. 71 Structure of the bis(methanofullerene) with dendritic wedges

of a dendritic addend bearing several cyanobiphenyl groups. Four generations of fulleropyrrolidines were prepared (Fig. 72) [308]. This appeared to be the right strategy since, with the exception of the first fulleropyrrolidine derivative that was found to be non-mesomorphic (Fig. 72, G1: Cr 178 I), all the other fullerene-based dendrimers gave rise to a SmA phase (Fig. 72, G2: G 44 SmA 168 I; G3: G 51 SmA 196 I; G4: G 36 SmA 231 I), the stability of which was found to increase with the generation number. The precursory aldehydes and alcohols showed essentially a broad SmA phase, except those of the first generation which showed a nematic phase above a crystalline phase. As for the molecular organization within the SmA phase, the G2 molecules are oriented in a head-to-tail fashion within the layers, and for each molecule the mesogenic groups point in the same direction interdigitating with mesogenic groups of adjacent layers. For the higher generation dendrimers, G3 and G4, the mesogenic units are positioned above and below the bulky dendritic cores, and interdigitation occurs between layers; C_{60} is now hidden in the dendritic core and has no influence in the supramolecular organization as was the case for the methanofullerodendrimers discussed above.

The first synthesized mesomorphic fulleropyrrolidine, G2, (Fig. 73A) [309] was chosen as a representative reference for a systematic variation of the R group in order to evaluate the effects on the mesomorphic properties. When R = H (Fig. 73B) [308], the compound exhibited a broad temperature range SmA phase (SmA 161 I). Modification of the R group by oligophenylenevinylene conjugates (OPV) led also to similar results (Fig. 73C: G 50 SmA 171 I, D: G 50 SmA 169 I) and indicated that the overall behavior is dominated by

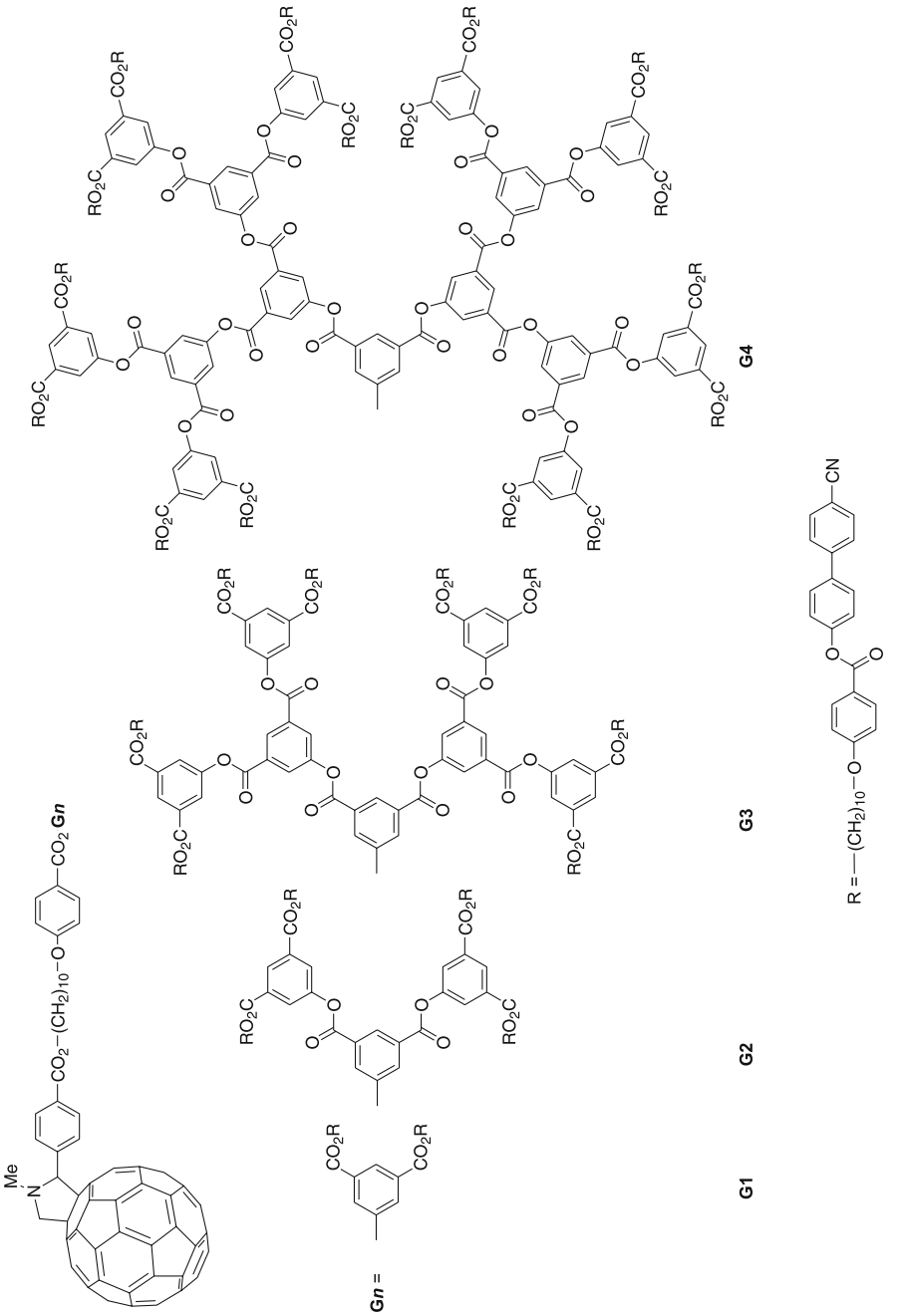

Fig. 72 Structure of the dendritic liquid-crystalline fulleropyrrolidines

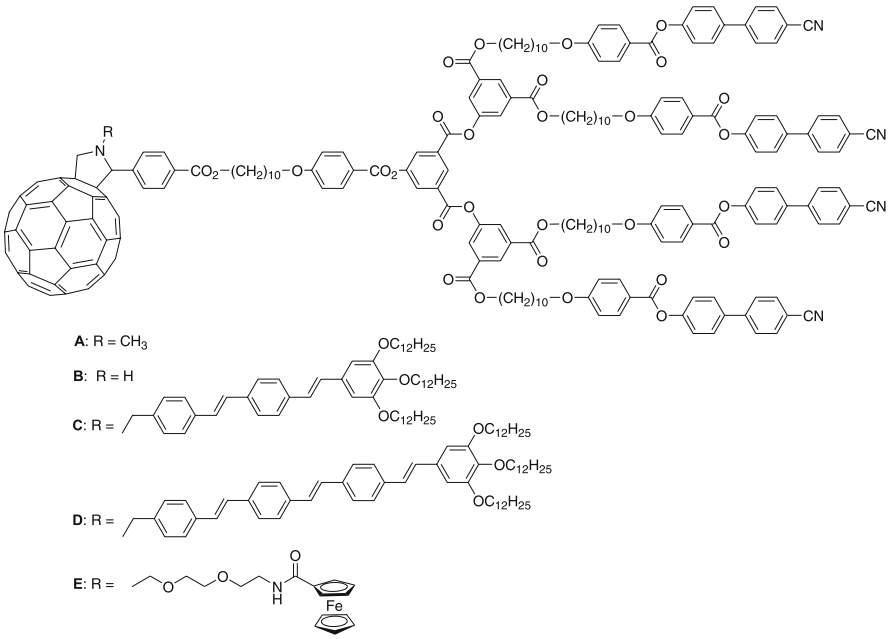

Fig. 73 Fulleropyrrolidine dendrimers of the second generation with various R groups

the dendritic framework [310]. Preliminary luminescence measurements in solution revealed a strong quenching of the oligo(phenylenevinylene) fluorescence by the C_{60} moiety, indicating that these donor-acceptor systems appeared suitable candidates for photovoltaic applications. Second-generation fulleropyrrolidine bearing a ferrocene unit (Fig. 73E) showed a SmA phase between 40 and 135 °C [311]. For this compound, photo-induced electron transfer was observed (through space mechanism) with a lifetime of the charge-separated state of 560 ns in THF. The association of Fc and C_{60} within a liquid-crystalline architecture could be an interesting method for the elaboration of supramolecular switches.

8 Polypedes

The molecular design of these materials is based on a central focal point to which mesogenic units are linked, so that restricted molecular topologies and limited molecular flexibility are induced [57]. They represent a class of materials intermediate between low molecular weight liquid-crystalline compounds and dendritic systems, and can be described as supermolecular entities or giant molecular systems made up of covalently attached

(end-on or side-on) identifiable molecular units (Fig. 74). These architectures once adequately functionalized may then self-organize into mesomorphic supramolecular assemblies with unusual morphologies. When all of the grafted units are the same, they can be considered as a first step of dendritic architectures (zeroth generation) or a polypedal supermolecule. Alternatively, if the mesogenic units are different to one another, they are referred to as multipedal supermolecules (Fig. 74) [57]. This approach also provides the access to several potentially interesting multicomponent structures and materials.

The most simple molecular topology of such systems reported so far is a tetrahedral supermolecule obtained by reacting tetrakis(dimethylsiloxy)-silane with alkenyloxy-cyanobiphenyls (Fig. 22), as discussed previously. Such tetramers exhibit smectic A liquid crystal phases [179]. For such end-on materials, microsegregation at the molecular level favors the formation of the smectic A phases in preference to the nematic phase exhibited by the mesogenic monomers themselves. The use of different polyhedral siloxane systems (Fig. 24) or the C_{60} polyhedron as the template for multi- and polypedal hexakis(methano)fullerenes (Fig. 70) substituted with a large number of terminally attached mesogenic groups confirm the same tendency to the formation of smectic A phases (vide supra).

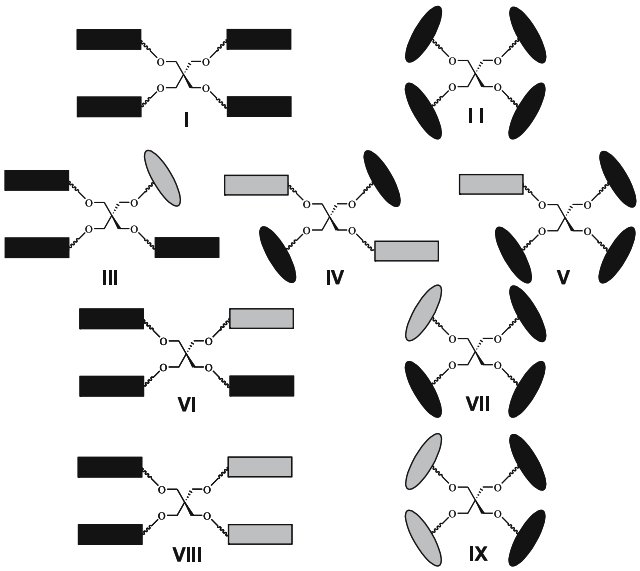

Fig. 74 Schematic representation of LC polypedes (all the mesogenic units are identical) and LC multipedes (either containing two different mesogenic units or two mixed end-on/side-on attachments)

The concept of multipedal liquid crystals was recently further developed by Saez and Goodby [312] who provided an elegant strategy to design tetrameric liquid crystalline polypedes and multipedes around a PE central core (Fig. 75) [57]. Liquid-crystalline materials were previously obtained with a PE central core to which were attached covalently mesogenic sub-units. Despite the large tetrahedral unit, PE was proved not to be particularly detrimental to the formation of mesophases, with a necessary condition, however, being that the peripheral units are strong liquid-crystalline promoters (e.g. calamitic, discotic, conical) and that the attachment is end-on [96–98, 313–322]. In this study, they used two types of mesogenic units, i.e. cyanobiphenyl and biphenyl benzoyloxybenzoate types (Fig. 75, R = A, B, C). The topology of attachment to the core (end-on for the cyanobiphenyl and side-on for the biphenyl benzoyloxybenzoate to yield the various structures I, II, III, and V, Fig. 74), and the chemical nature of the connection between PE and the mesogen (ether, ester and tetramethyldisiloxane moieties) have been used to tailor the mesomorphic properties. The pure cyanobiphenyl derivative (Fig. 75, type I, R = A) exhibits a smectic A phase, whereas all the other oligomers (Fig. 75, II, III, V) exhibit a chiral nematic phase. A chiral nematic phase was induced by the lateral attachment of the chiral phenylbenzoate unit to the core. The stability of the mesophases for the polypedes and multipedes is reported in Table 17.

Complementary dendritic hexamers based on a central scaffold made up of linked pentaerythritol and tri(hydroxymethyl)amino methane units have been found to also exhibit liquid-crystalline properties. This star-shaped scaffold was used to create supermolecules containing two different hemispheres, referred to thereafter as "Janus" supermolecular liquid crystals (Fig. 76) [323, 324]. One of the hemisphere contains three cyanobiphenyl end-groups, whereas the other lobe consists of three chiral phenyl benzoate mesogenic moieties laterally attached. The type of mesophase observed (N*

Table 17 Mesomorphic behavior of the tetrameric polypedes and multipedes

Compound type	Transition temperatures
Tetrapedes (Fig. 75)	
I (R = A)	G –34.3 SmA 21.1 I
III (R = A, R′ = C)	G –20 N* 18.6 I
V (R = B, R′ = A)	Cr 36.2 N* 58.8 I
II (R = B)	Cr 55.8 N* 79.7 I
Hexapedes (Fig. 76)	
R = A, R′ = B, $n = 9$	G –2.8 SmC* 33.8 N* 60.8 I
R = B, R′ = A, $n = 4$	G –7.9 N* 38.2 I

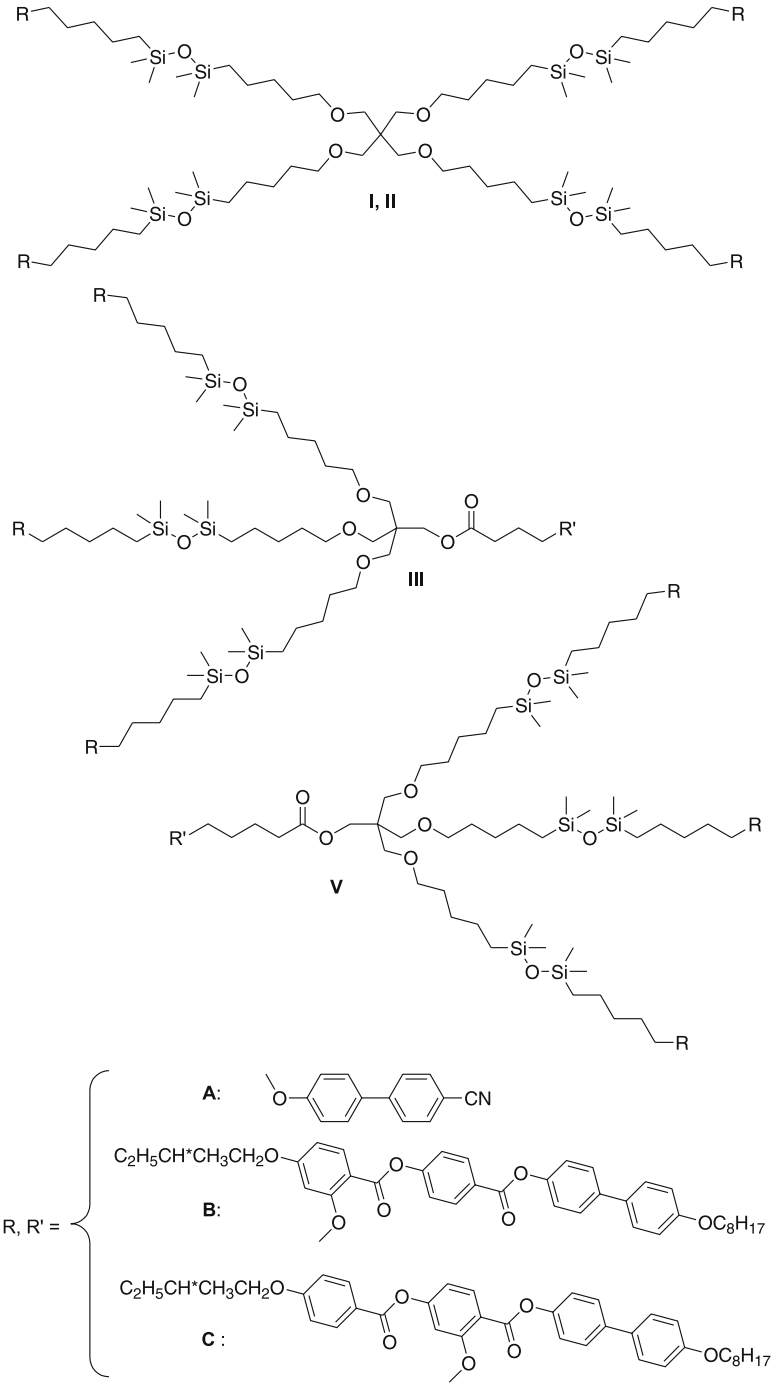

Fig. 75 Supermolecular liquid crystalline tetrapedes and multipedes

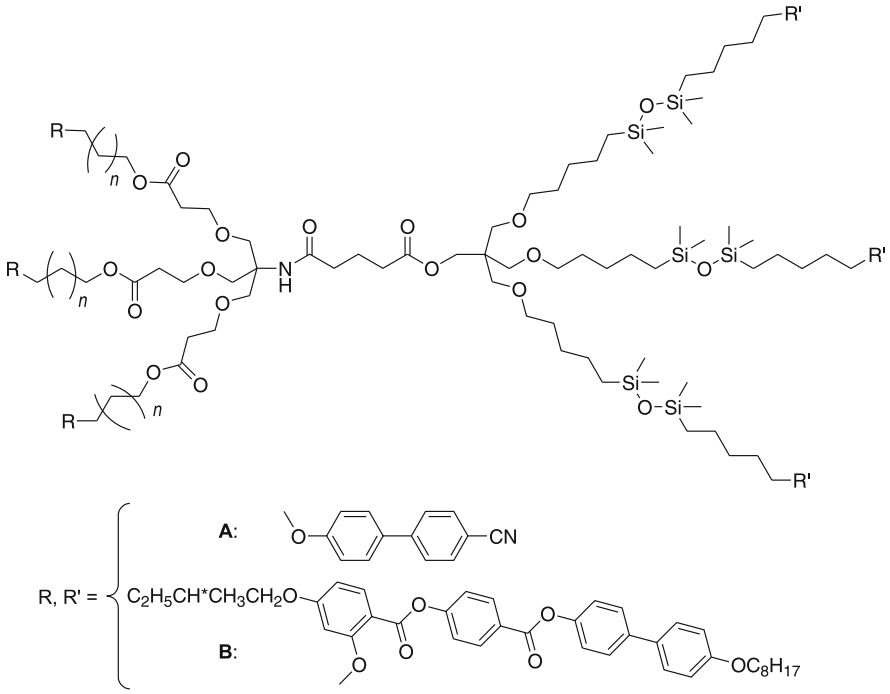

Fig. 76 Hexameric multipedes (Janus Liquid crystals)

or SmC*) depends on the overall topology of the molecule in respect to the inner core (in other words, which hemisphere carries which mesogen, Table 17).

In addition, these materials have very good thermal stabilities and nearly room temperature mesomorphic range and are serious candidates to compete with the famous commercial cyanobiphenyl compounds, and despite their high molecular weight, their physical properties are closer to those of low molecular mass materials than to polymers or dendrimers.

Table 18 Transition temperatures of the nematic supermesogens

G*n* (R)	I	II	III
G1 (A)	G 75 N 235 I	G 68 N 195 I	G 71 N 173 I (G 84 N 222 I) [a]
G2 (A)	G 106 N 183 I	G 108 N 197 I	G 102 N 187 I
G1 (B)	Cr 239 N > 360 I	Cr 200 N 310 I	Cr 150 N 305 I
G2 (B)	G 127 N 308 I	–	–

[a] Isomeric exo,exo-bicyclo[2.2.2]oct-7-ene-2,3,5,6-tetracarboxylic acid counterpart

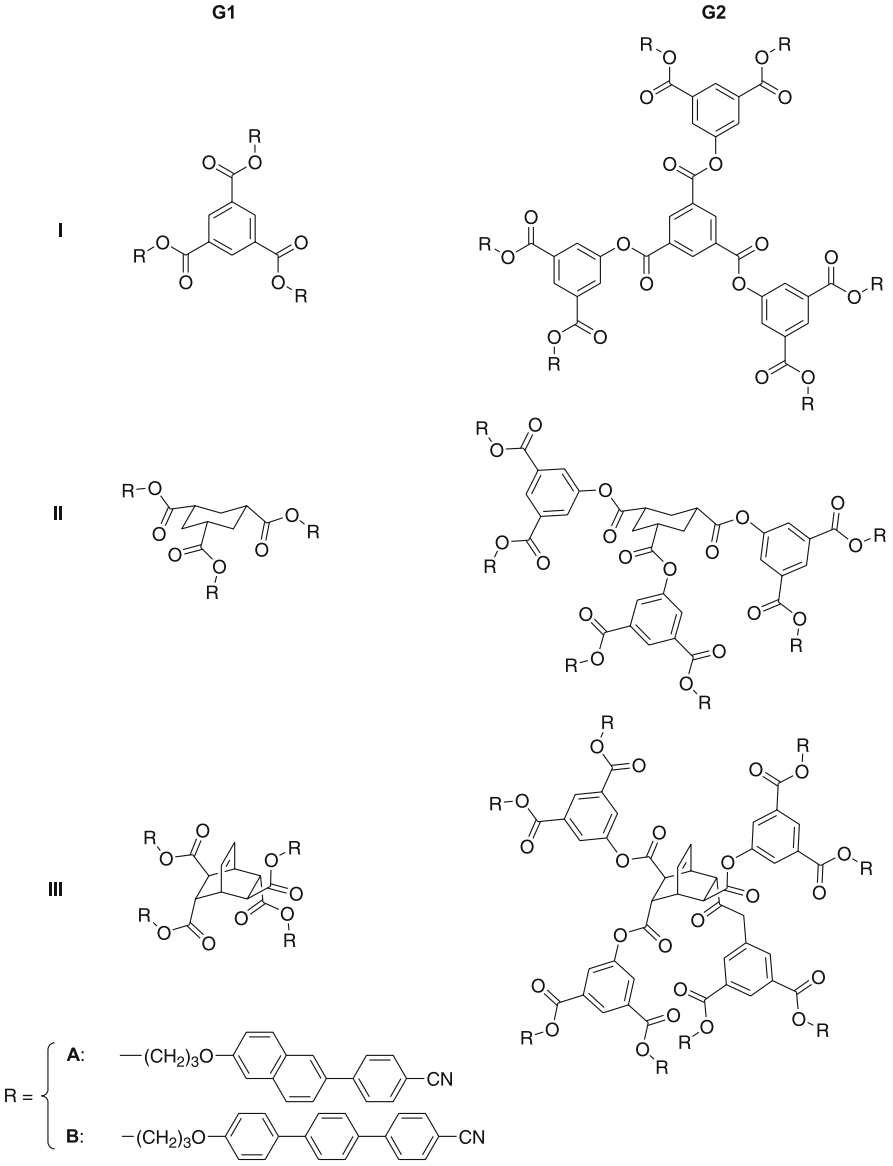

Fig. 77 Structure of the nematic glass-forming materials

Another nice piece of work was provided by Chen et al. [325, 326] on structurally related branched systems. In this work cyano-containing mesogenic pendants were grafted onto various polyvalent central cores.

These zeroth and first generation supermolecules were mesomorphic exhibiting almost exclusively a nematic phase (Table 18), which could be fur-

ther frozen into a glassy state. To assess the effects of the molecular structures on the thermal behavior, several structural parameters were systematically varied such as the shape and connectivity of the central cores namely 1,3,5-benzenetricarboxylic acids, *cis*,*cis*-1,3,5-cyclohexanetricarboxylic acids as well as bicyclo[2.2.2]oct-7-ene-(2,5)-*exo*-(3,6)-*endo*-tetracarboxylic acids, the mesogenic pendant and the spacer (Fig. 77).

Using the same strategy, photoresponsive glassy liquid crystals were also obtained using dithienylethene moieties [327].

9
Miscellaneous

9.1
Mesomorphic Dendrimers with Rigid Discotic Cores

Instead of having a flexible core, such as in the PAMAM and PPI LC dendrimers discussed in another section, the central node of the dendrimers can also be made of a rather rigid chemical unit. Fullerene-containing LC dendrimers are beautiful examples of such a morphology. Star-like discotic liquid crystals can also be considered as one of the first example of this category. The star-like heptamer of triphenylene has been shown to exhibit a hexagonal columnar mesophase between 69 and 122 °C (Fig. 78, R = R^1, R^2, R^3) [328]. Triphenylene has also been used as a central core from which oligomethyleneoxy-chains radiate symmetrically through amide bonds to be terminated by β-D-glucopyranosyl residues [329]. These unusual dendritic-like amphiphilic materials show two well-defined molecular regions, i.e. the central hydrophobic part and the peripheral hydrophilic part (Fig. 78, R = R^4, R^5, R^6, R^7). As a consequence, they exhibit amphotropic liquid crystalline properties, showing both thermotropic and lyotropic behavior. The nature of the molecular arrangements (hexagonal or rectangular) associated with the thermotropic columnar mesomorphism is shown to be strongly dependent on a delicate balance between the volume occupied by the central hydrophobic regions, corresponding to the triphenylene core and the side-chains, and the sizes of the hydrophilic sugar parts attached at the end of the chains. Note that Percec et al. reported hyperbranched liquid crystalline polyesters with discotic cyclotetraveratrylene mesogens as branching cores [330].

Peripheral substitution of phthalocyanine with one or four Fréchet-type dendrons (polyarylether without alkyl chains) surprisingly produces mesomorphic materials whose properties are dominated both by the columnar self-association of the Pc cores and by the glass-forming character of the dendritic wedges [331, 332]. The resulting glassy solids appear indefinitely stable towards crystallization and their structure is governed by the size, number and position of the dendritic wedges attached to the

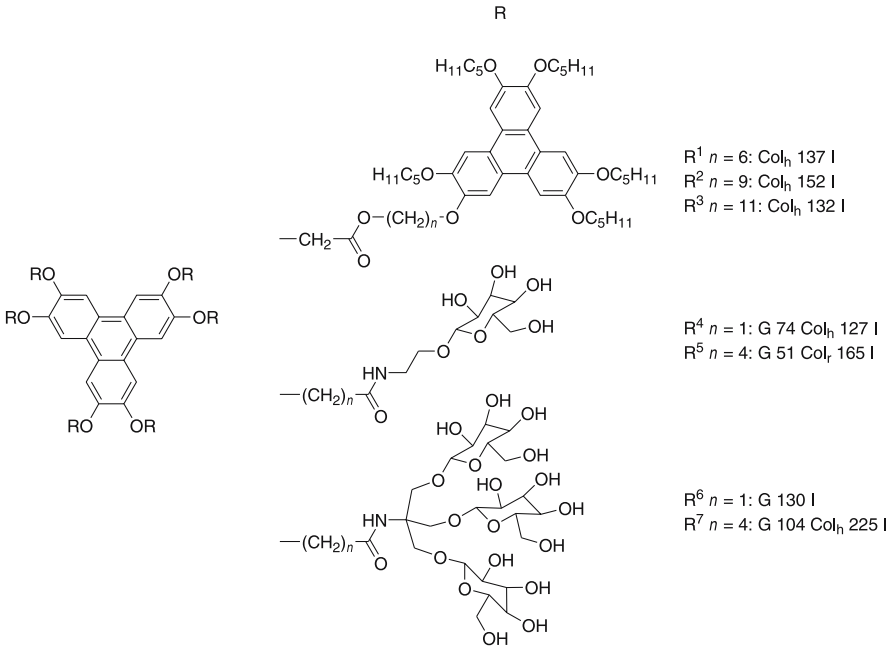

Fig. 78 Dendrimers with central triphenylene cores

Pc macrocycle. Some of them are mesomorphic and show a Col_h phase (Fig. 79: I-G1: G 115 Col_h 270 I; II-G1: G <– 20 Col_h > 320 I; II-G2: G 115 Col_h 250 I; II-G3: 94 Col_h 108 I) for which the structure of the columnar mesophase is frozen at room temperature (anisotropic glasses). The functionalization of these dendrons in the 3 and 5 position of the terminal rings by oligo(ethyleneoxy) chains $(OCH_2CH_2)_3OCH_3$, and their subsequent grafting onto the phthalocyanine of type I (Fig. 79) led to amphiphilic materials [333]. In concentrated ethanol solutions (~ 20–40% by mass), the compound with the functionalized G1 dendron behaves as a discotic amphiphile forming a columnar nematic lyotropic phase. In addition, it possesses a columnar mesophase stable from room temperature up to 260 °C. Systems of type III are not mesomorphic.

Another example of a rigid macrocycle used as the central core of a dendrimer is the porphyrin. First and second generation phenylene-based dendritic porphyrins with 8 and 16 long alkyl chains on their periphery have been studied (Fig. 80). Only the second generation exhibits mesomorphic behavior with the formation of a rectangular columnar mesophase upon heating (Cr 39 Col_r 110 I) [334]. A stable supramolecular 1 : 1 complex was formed between the second generation and C_{60}, which led to the enhancement of the mesophase stability of the formed (unidentified) columnar phase (Cr 99 Col 250 I).

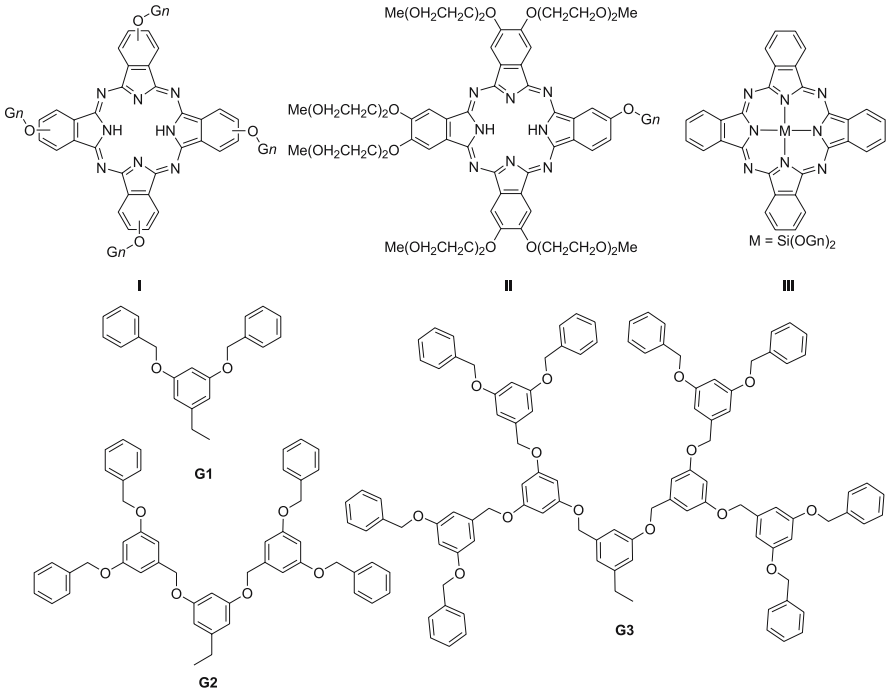

Fig. 79 Dendrimers with central phthalocyanine cores

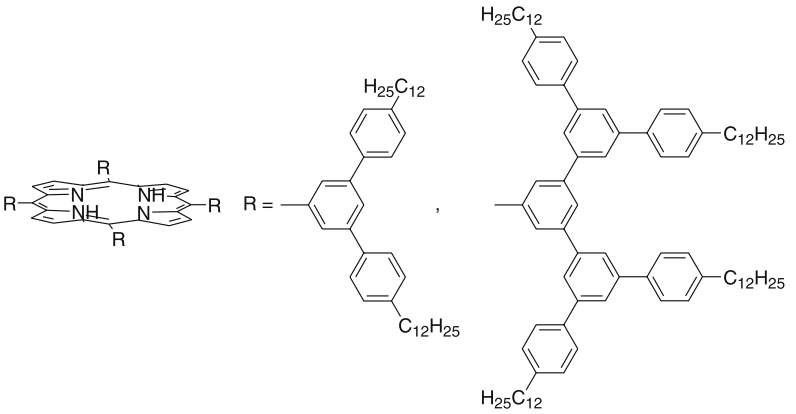

Fig. 80 Dendrimers with central porphyrin cores

9.2
Supramolecular Rod-Coil Block Codendrimers

In order to develop active materials for optics, supramolecular structures derived from rod-coil block copolymers appeared to be materials of par-

ticular interest [335]. Molecular dumbbells consisting of a conjugated rod and dendritic wedges have been synthesized and characterized, and their self-assembling behavior has been investigated (Fig. 81). For example, these dumbbell-shaped molecules are made of a conjugated rod segment consisting of three biphenyls connected through vinyl linkages, and of flexible amphiphilic dentritic wedges with different cross sections (Fig. 81) [336]. These molecular dumbbells self-assemble into discrete bundles of tuneable size that organize into three-dimensional superlattices. The molecules based on a dibranched dendritic wedge, organize into primitive monoclinic crystalline and body-centered tetragonal liquid crystalline (M_{tet}) structures, while the molecules based on tetra- and hexabranched dendritic wedges form only body-centered tetragonal liquid crystalline structures. The number of molecules per bundle decreases systematically when increasing the cross-section of the dendritic wedge (going down from 73 molecules for the dibranched wedge to 39 for the hexabranched wedge). Therefore, the size control of the bundles assembled from the rod building blocks is determined by the cross-section of the flexible segment attached to the rod ends. In addition, spectroscopic studies of these molecules demonstrate that the size of the optically active rod bundle has an influence on the photophysical properties of the conjugated rods (blue shift of the emission maximum when going from the dibranched to the hexabranched molecule).

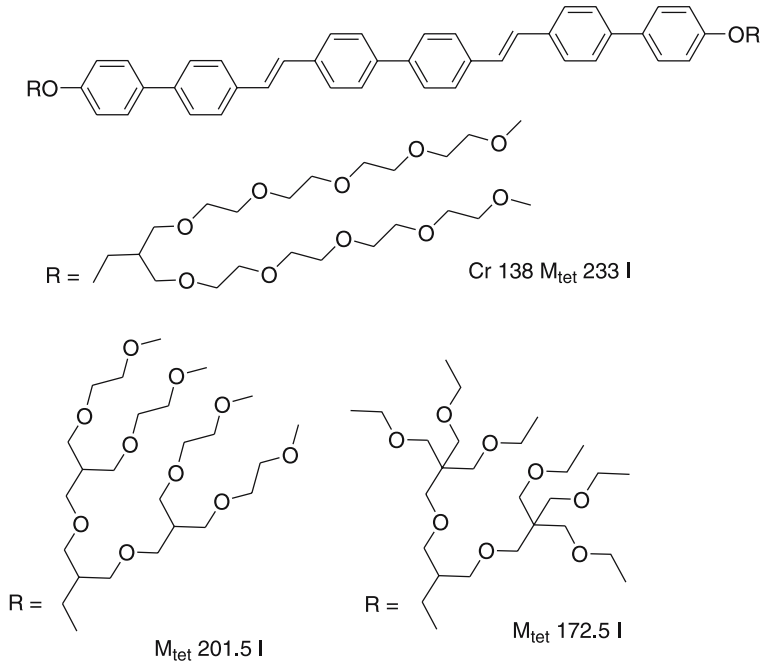

Fig. 81 Dumbbell-shaped molecules based on oligobiphenylene fragments

Another strategy to manipulate the aggregation structure assembled from a conjugated rod building block has been to connect hydrophilic, flexible dendritic branches to one side only, leading to a tree-shaped molecule. For example the latter consists of an octa-phenylene stem segment for the conjugation rod block and of oligo(ethylene oxide) dendrons for the flexible branches (Fig. 82) [337]. These molecular trees can also be considered as a new class of amphiphiles because they consist of a hydrophobic rod and a hydrophilic flexible head [338]. The molecular trees based on a small flexible head were found to self-assemble into a monolayer lamellar structure, whereas those with a larger head-group were found to self-assemble into bundles (containing seven molecules) that are organized according to a 3D primitive orthorhombic supercrystal. When both sides of the linear oligo-*p*-phenylene moiety are functionalized by amphiphilic dendritic wedges, formation of helical superstructures were observed in aqueous solutions [339].

New molecules based on a branched rod block and surrounding flexible ether-type coils represent a class of materials leading to similar self-organizations (Fig. 83, $n = 6$, 8). Such molecules have been shown, provided that the central rigid rod is long enough, to self-assemble into nanostructures (bundle type) that self-organize into a primitive monoclinic structure [340].

More recently, a novel combination of flexible and rigid conjugated parts has been tested, resulting in ABC wedge-coil triblock molecules made of a Y-shaped *p*-phenylene rigid wedge bearing aliphatic chains on one side and a flexible poly(ethylene oxide) (PEO) coil on the other side (Fig. 84A, $n = 12$, 17, 21, 34, 45, 77, 91, 114, 182) [341, 342]. These molecules self-assembled successively, as the length of the PEO chain is increased, into 3D micellar cubic phases with various symmetries (with $Im\bar{3}m$ for $n = 12$ and $Pm\bar{3}n$ for

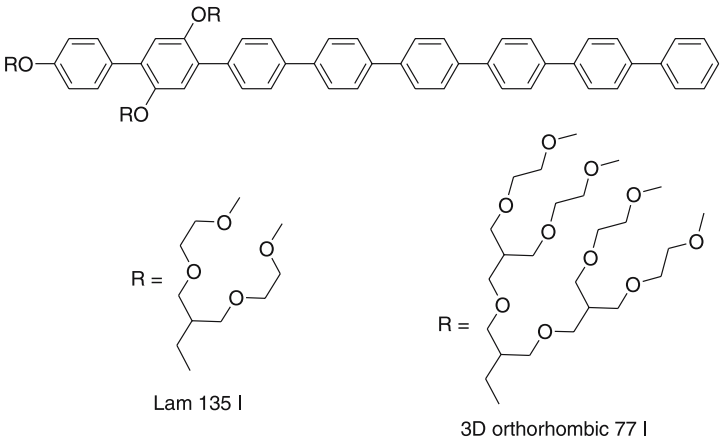

Fig. 82 Octa-*p*-phenylene molecular trees

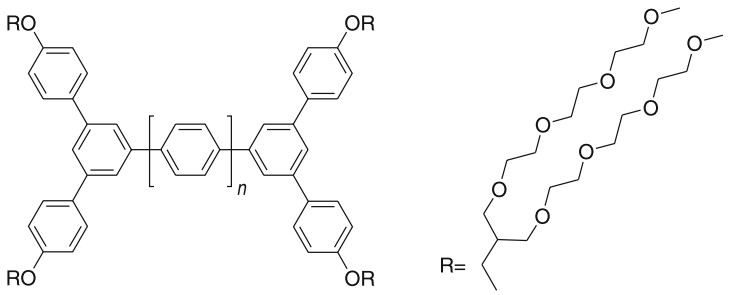

Fig. 83 Branched rod-block molecule with dendritic wedges

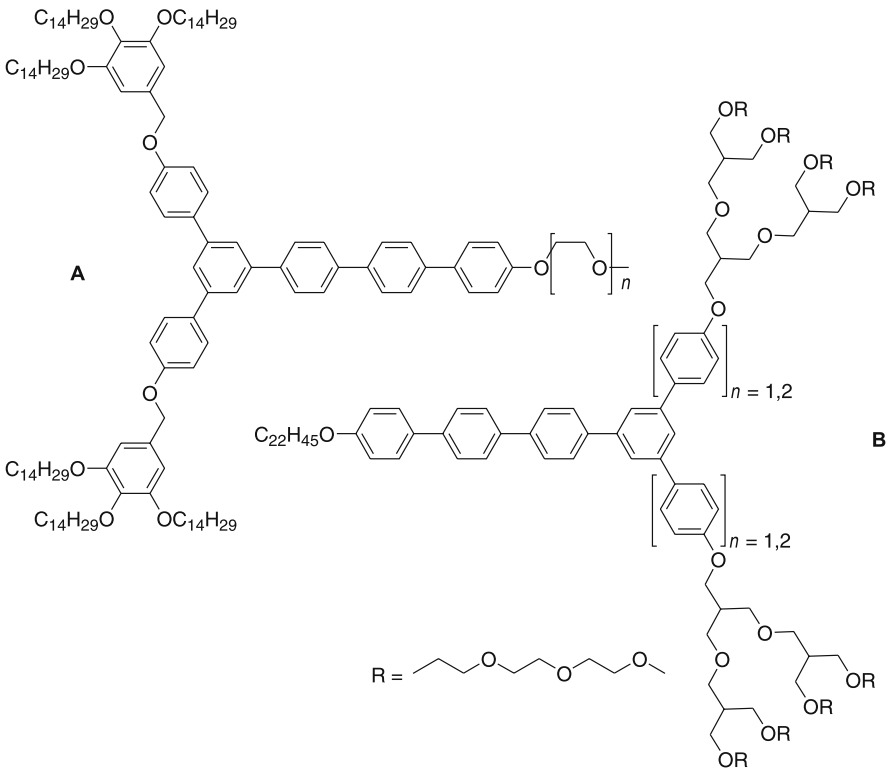

Fig. 84 Structure of the rigid wedge-flexible coil diblock molecules

$n = 17$), 2D hexagonal columnar ($n = 21$, 114, 182), 3D perforated lamellar ($n = 21$, 34), and smectic-like structures ($n = 45$, 77, 91). The melting temperatures remained almost the same (50–60 °C), whereas the clearing temperatures increased when increasing the PEO segment (from 80 to 145 °C). The primary force responsible for this structural change is believed to be

the combination of shape complementarity and microphase separation between the rigid and flexible segments. Among all the mesophases exhibited by such systems, let us point out the case of the unusual bilayered lamellar structure with in-plane ordered coil perforations (perforated lamellar mesophase).

This approach was pursued with the synthesis of "inverted" amphiphilic ABC triblock systems consisting of a hydrophilic dendritic block, a rigid aromatic part and a hydrophobic docosyl chain (Fig. 84B) [343]. X-ray scattering has demonstrated that the molecules with a rather rod-like aromatic unit self-organize into a 2D hexagonal columnar structure (B, $n = 1$: Col_h 36.4 I), while the molecules based on a more wedge-like aromatic unit self-organize into a 3D micellar cubic structure (B, $n = 2$: Cub-$Im\bar{3}m$ 46.1 I). The dimension (8.1 nm) of the hexagonal parameter implies that the rod-like rigid segments arrange axially with their preferred direction within a cross-sectional slice of the column, in which disordered docosyl chains pack in an interdigitated fashion. As for the cubic phase, it consists of a 3D body-centered arrangement of discrete polyhedral aggregates. Interestingly, dynamic light scattering and scanning electron microscopy studies of aqueous solution with the addition of $CHCl_3$ showed that these rigid-dendritic block molecules self-assemble into stable capsule-like micellar aggregates in the presence of a hydrophobic solvent.

10 Conclusions

The above examples show that liquid-crystalline phases can been produced with high molecular weight monodisperse dendrimers, dendrons and polypedes. Nematic, lamellar, columnar, cubic phases as well as less conventional mesophases are obtained depending upon the chemical nature of the terminal mesogenic groups, dendritic core and dendrimer generation. Such a tuning of the mesomorphic structure by an appropriate molecular design makes possible the development of new liquid-crystalline materials containing active molecular units with specific physical properties to be used in nanotechnology. The high sensitivity of such dendrimers to the surrounding environment (properties vs. molecular structure) could be, in principle, beneficial to some kinds of molecular sensors, i.e. to use such supermolecules as tools to test how properties in general may be altered or modulated through delicate external stimuli.

Acknowledgements B.D. and D.G. are grateful to Dr. Delphine Felder-Flesh (IPCMS) and Prof. Robert Deschenaux (Institute of Chemistry, Neuchâtel, Switzerland) for their kindness in reading the manuscript carefully, and offering us their critical and constructive remarks and comments. They are greatly acknowledged.

References

1. Tomalia DA, Fréchet JMJ (2002) Polym Sci A, Polym Chem 40:2719
2. Tomalia DA, Dupont Durst H (1993) Top Curr Chem 165:193
3. Ardoin N, Astruc D (1995) Bull Soc Chem Fr 132:875
4. Newkome GR, Moorefield CN, Vögtle F (eds) (1996) Dendritic Molecules: Concepts, Synthesis and Perspectives. Wiley, Weinheim
5. Ashton PR, Boyd SE, Brown CL, Nepogodiev SA, Meijer EW, Peerlings HWI, Stoddart JF (1997) Chem Eur J 3:974
6. Matthews OAN, Shipway N, Stoddart JF (1998) Prog Polym Sci 23:1
7. Newkome GR, Moorefield CN, Vögtle F (eds) (2001) Dendrimers and Dendrons: Concepts, Synthesis and Applications. Wiley, Weinheim
8. Voit BI (1995) Acta Polym 46:87
9. Fréchet JMJ, Tomalia DA (eds) (2001) Dendrimers and other Dendritic Polymers. Wiley Series in Polymer Sciences. Wiley, Weinheim
10. Special issues of C R Chim (2003) 6:709
11. Special issues of Prog Polym Sci (2005) 30:217
12. Grayson SM, Fréchet JM (2001) Chem Rev 101:3819
13. Hawker CJ (1999) Adv Polym Sci 147:113
14. Tomalia DA, Naylor AM, Goddard III WA (1990) Angew Chem Int Ed Engl 29:138
15. Tomalia DA (1994) Adv Mater 6:529
16. Feuerbacher N, Vögtle F (1998) Top Curr Chem 197:1
17. Issberner J, Moors R, Vögtle F (1994) Angew Chem Int Ed Engl 33:2413
18. Dykes GMJ (2001) Chem Technol Biotechnol 76:903
19. Boas U, Heegaard PMH (2004) Chem Soc Rev 33:43
20. Astruc D (1996) C R Acad Sci Paris Ser II 322:757
21. Uhrich K (1997) TRIP 5:388
22. Smith DK, Diederich F (1998) Chem Eur J 4:1353
23. Hecht S, Fréchet JMJ (2001) Angew Chem Int Ed 40:74
24. Cloninger MJ (2002) Curr Opinion Chem Bio 6:742
25. Chow HF, Mong TKK, Nongrum MF, Wan CW (1998) Tetrahedron 54:8543
26. Archut A, Vögtle F (1998) Chem Soc Rev 27:233
27. Fischer M, Vögtle F (1999) Angew Chem Int Ed 38:884
28. Inoue K (2000) Prog Polym Sci 25:453
29. Vögtle F, Gestermann S, Hesse R, Schwierz H, Windisch B (2000) Prog Polym Sci 25:987
30. Adronov A, Fréchet JMJ (2000) Chem Commun 1701
31. Beletskaya IP, Chuchurjukin AV (2000) Russ Chem Rev 69:639
32. Seebach D, Rheiner PB, Greiveldinger G, Butz T, Sellner H (1998) Top Curr Chem 197:125
33. Romagnoli B, Hayes W (2002) J Mater Chem 12:767
34. Constable EC (1997) Chem Commun 1073
35. Venturi M, Serroni S, Juris A, Campagna S, Balzani V (1998) Top Curr Chem 197:193
36. Gorman C (1998) Adv Mater 10:295
37. Newkome GR, He E, Moorefield CN (1999) Chem Rev 99:1689
38. Hearshaw MA, Moss JR (1999) Chem Commun 1
39. Stoddart FJ, Welton T (1999) Polyhedron 18:3575
40. Cuadrado I, Morán M, Casado CM, Alonso B, Losada J (1999) Coord Chem Rev 193–195:395
41. Majoral JP, Caminade AM (1998) Top Curr Chem 197:79

42. Majoral JP, Caminade AM (1999) Chem Rev 99:845
43. Frey H, Lach C, Lorenz K (1998) Adv Mater 10:279
44. Frey H, Schlenk C (2000) Top Curr Chem 210:69
45. Lang H, Lühmann B (2001) Adv Mater 13:1523
46. Collings PJ, Hird M (1997) Introduction to Liquid Crystals Chemistry and Physics. Taylor & Francis Ltd, London
47. Demus D, Goodby JW, Gray GW, Spiess HW, Vill V (eds) (1998) Handbook of Liquid Crystals. Wiley, Weinheim
48. Zeng F, Zimmerman SC (1997) Chem Rev 97:1681
49. Narayanan VV, Newkome GR (1998) Top Curr Chem 197:19
50. Constable EC, Housecroft CE (1998) Chimia 52:533
51. Emrick T, Fréchet JMJ (1999) Curr Opinion Coll Interface Sc 4:15
52. Smith DK, Diederich F (2000) Top Curr Chem 210:183
53. Goodby JW, Mehl GH, Saez IM, Tuffin RP, Mackenzie G, Auzély-Velty R, Benvegnu T, Plusquellec D (1998) Chem Commun 2057
54. Goodby JW (1999) Curr Opin Solid State Mater Sci 4:361
55. Ponomarenko SA, Boiko NI, Shibaev VP (2001) Polym Sci Ser A 43:1
56. Guillon D, Deschenaux R (2002) Curr Opinion Sol State Mater Sci 6:515
57. Saez IM, Goodby JW (2005) J Mater Chem 15:26
58. Hamley IW (2000) Introduction to Soft Matter: Polymers, Colloids, Amphiphiles and Liquid Crystals. Wiley, New York
59. Demus D (1989) Liq Cryst 5:75
60. Tschierske C (1996) Prog Polym Sci 21:775
61. Tschierske C (1998) J Mater Chem 8:1485
62. Tschierske C (2001) J Mater Chem 11:2647
63. Tschierske C (2002) Curr Opin Colloid Interface Sci 7:69
64. Tschierske C (2001) Annu Rep Prog Chem Sect C 97:191
65. Tschierske C (2002) Curr Opinion Coll Interface Sci 7:69
66. Cheng X, Prehm M, Das MK, Kain J, Baumeister U, Diele S, Dag L, Blume A, Tschierske C (2003) J Am Chem Soc 125:10977
67. Percec V, Kawasumi M (1992) Macromolecules 25:3843
68. Bauer S, Fischer H, Ringsdorf H (1993) Angew Chem Int Ed Engl 32:1589
69. Percec V, Chu P, Kawasumi M (1994) Macromolecules 27:4441
70. Hanh SW, Yun SYK, Jin JI, Han OH (1998) Macromolecules 31:6417
71. Sunder A, Quincy MF, Mülhaupt R, Frey H (1999) Angew Chem Int Ed 38:2928
72. Choi SH, Lee NH, Cha SW, Jin JI (2001) Macromolecules 34:2138
73. Park YS, Lee JW, Jin JI (2002) Bull Korean Chem Soc 23:1201
74. Flory PJ (1953) Principles of Polymer Chemistry. Cornell University Press, Ithaca, NY
75. Kim YH (1998) J Polym Sci A Polym Chem 36:1685
76. Frey H, Hölter D (1999) Acta Polym 50:67
77. Hult A, Johansson M, Malmström E (1999) Adv Polym Sci 143:1
78. Hamley IW (1998) The Physics of Block-Copolymers. Oxford University Press, Oxford
79. Percec V, Johansson G, Heck J, Ungar G, Batty SV (1993) J Chem Soc, Perkins Trans 1, 1411
80. Percec V, Heck JA, Tomazos D, Ungar G (1993) J Chem Soc, Perkin Trans 2, 2381
81. Percec V, Heck JA, Tomazos D, Falkenberg F, Blackwell H, Ungar G (1993) J Chem Soc, Perkin Trans 1, 2799
82. Percec V, Tomazos D, Heck JA, Blackwell H, Ungar G (1994) J Chem Soc, Perkin Trans 2, 31

83. Johansson G, Percec V, Ungar G, Abramic D (1994) J Chem Soc, Perkin Trans 1, 447
84. Ungar G, Batty SV, Percec V, Heck J, Johansson G (1994) Adv Mater Optics Electron 4:303
85. Chvalun SN, Blackwell J, Cho JD, Kwon YK, Percec V, Heck JA (1998) Polymer 39:4515
86. Kwon YK, Chvalun S, Schneider AI, Blackwell J, Percec V, Heck JA (1994) Macromolecules 27:6129
87. Percec V, Schlueter D, Ungar G, Cheng SZD, Zhang A (1998) Macromolecules 31:1745
88. Prokhorova SA, Sheiko SS, Möller M, Ahn CH, Percec V (1998) Macromol Rapid Commun 19:359
89. Percec V, Ahn CH, Cho WD, Jamieson AM, Kim J, Leman T, Schmidt M, Gerle M, Möller M, Prokhorova SA, Sheiko SS, Cheng ZD, Zhang A, Ungar G, Yeardley DJP (1998) J Am Chem Soc 120:8619
90. Percec V, Ahn CH, Ungar G, Yeardley DJP, Möller M, Shieko SS (1998) Nature 391:161
91. Chvalun SN, Blackwell J, Cho JD, Bykova IV, Percec V (1999) Adv Polym Sci 50:51
92. Yeardley DJP, Ungar G, Percec V, Holerca MN, Johansson G (2000) J Am Chem Soc 122:1684
93. Duan H, Hudson SD, Ungar G, Holerca MN, Percec V (2001) Chem Eur J 7:4134
94. Percec V, Holerca MN (2000) Biomacromolecules 1:6
95. Percec V, Bera TK (2002) Biomacromolecules 3:167
96. Malthête J, Collet A, Levelut AM (1989) Liq Cryst 5:123
97. Malthête J, Levelut AM (1991) Adv Mater 3:94
98. Malthête J (1996) New J Chem 20:925
99. Percec V, Johansson G, Ungar G, Zhou J (1996) J Am Chem Soc 118:9855
100. Johansson G, Percec V, Ungar G, Zhou JP (1996) Macromolecules 29:646
101. Jung HT, Kim SO, Hudson SD, Percec V (2002) Appl Phys Lett 80:395
102. Percec P, Holerca MN, Uchida S, Cho WD, Ungar G, Lee Y, Yeardley DJP (2002) Chem Eur J 8:1106
103. Naylor AM, Goddard WA, Kiefer GE, Tomalia DA (1989) J Am Chem Soc 111:2339
104. Balagurusamy VSK, Ungar G, Percec V, Johansson G (1997) J Am Chem Soc 119: 1539
105. Ungar G, Percec V, Holerca MN, Johansson GA, Heck JA (2000) Chem Eur J 6:1258
106. Hudson SD, Jung HT, Percec V, Cho WD, Johansson G, Ungar G, Balagurusamy VSK (1997) Science 278:449
107. Dukeson DR, Ungar G, Balagurusamy VSK, Percec V, Johansson GA, Glodde M (2003) J Am Chem Soc 125:15974
108. Vargas R, Mariani P, Gulik A, Luzzati V (1992) J Mol Biol 225:137
109. Luzzati V, Vargas R, Mariani P, Gulik A, Delacroix H (1993) J Mol Biol 229:540
110. Gulik A, Delacroix H, Kirschner G, Luzzati V (1995) J Phys France II 5:445
111. Luzzati V (1995) J Phys France II 5:1649
112. Percec V, Glodde M, Johansson G, Balagurusamy VSK, Heiney PA (2003) Angew Chem Int Ed 42:4338
113. Percec V, Cho WD, Mosier PE, Ungar G, Yeardley DLP (1998) J Am Chem Soc 120:11061
114. Percec V, Cho WD, Ungar G (2000) J Am Chem Soc 122:10273
115. Percec V, Cho WD, Ungar G, Yeardley DJP (2000) Angew Chem Int Ed 39:1597
116. Percec V, Cho WD, Möller M, Prokhorova SA, Ungar G, Yeardley DJP (2000) J Am Chem Soc 122:4249
117. Percec V, Cho WD, Ungar G, Yeardley DJP (2001) J Am Chem Soc 123:1302
118. Hudson SD, Jung HAT, Kewsuwan P, Percec V, Cho WD (1999) Liq Cryst 26:1493

119. Li Y, Lin ST, Goddard III WA (2004) J Am Chem Soc 126:1872
120. Ungar G, Liu Y, Zeng X, Percec V, Cho WD (2003) Science 299:1208
121. Zeng X, Ungar G, Liu Y, Percec V, Dulcey AE, Hobbs JK (2004) Nature 428:157
122. Ungar G, Zeng X (2005) Soft Matter 1:95
123. van der Vegt AK (2001) Order in space. VSSD, Edition on internet (http://www.vssd.nl/hlf)
124. Sadoc JF, Rivier N (eds) (1999) Foams and Emulsions. Kluwer, Dordrecht
125. Percec V, Cho WD, Ungar G, Yeardley DJP (2002) Chem Eur J 8:2011
126. Percec V, Mitchell CM, Cho WD, Uchida S, Glodde M, Ungar G, Zeng X, Liu Y, Balagurusamy VSK, Heiney PA (2004) J Am Chem Soc 126:6078
127. Jung HT, Kim SO, Ko YK, Yoon DK, Hudson SD, Percec V, Holerca MN, Cho WD, Moisier PE (2002) Macromolecules 35:3717
128. Yoon DK, Ko YK, Jung HT (2003) Liq Cryst 30:559
129. Yoon DK, Jung HT (2005) Mol Cryst Liq Cryst 412:417
130. Sidorenko A, Houphouet-Boigny C, Villavicencio O, Hashemzadeh M, McGrath DV, Tsukruk VV (2000) Macromolecules 16:10569
131. Pao WJ, Stetzer MR, Heiney PA, Cho WD, Percec V (2001) J Phys Chem B 105:2170
132. Frey H, Mülhaupt R, Lorenz K, Rapp U, Mayer-Posner FJ (1995) Polym Mater Sci Eng 73:127
133. Frey H, Lorenz K, Mülhaupt R, Rapp U, Mayer-Posner FJ (1996) Macromol Symp 102:19
134. Coen MC, Lorenz K, Kressler J, Frey H, Mülhaupt R (1996) Macromolecules 29:8069
135. Lorenz K, Hölter D, Frey H, Stühn B (1997) Polym Mater Sci Eng 77:168
136. Lorenz K, Hölter D, Stühn B, Mülhaupt R, Frey H (1996) Adv Mater 8:414
137. Trahasch B, Frey H, Lorenz K, Stühn B (1999) Colloid Polym Sci 277:1186
138. Lorenz K, Frey H, Stühn B, Mülhaupt R (1997) Macromolecules 30:6860
139. Stark B, Lach C, Frey H, Stuhn B (1999) Macromol Symp 146:33
140. Stark B, Stühn B, Frey H, Lach C, Lorenz K, Frick B (1998) Macromolecules 31:5415
141. Trahasch B, Stühn B, Frey H, Lorenz K (1999) Macromolecules 32:1962
142. Caminade AM, Turrin CO, Sutra P, Majoral JP (2003) Curr Opin Colloid Interface Sci 8:282
143. Terunuma D, Kato T, Nishio R, Matsuoka K, Kuzuhara H, Aoki Y, Nohira H (1998) Chem Lett 59
144. Terunuma D, Kato T, Nishio R, Aoki Y, Nohira H, Matsuoka K, Kuzuhara H (1999) Bull Chem Soc Jpn 72:2129
145. Terunuma D, Nishio R, Aoki Y, Nohira H, Matsuoka K, Kuzuhara H (1999) Chem Lett 565
146. Pelzl G, Diele S, Weissflog W (1999) Adv Mater 11:707
147. Dantlgraber G, Baumeister U, Diele S, Kresse H, Lühmann B, Lang H, Tschierske C (2002) J Am Chem Soc 124:14852
148. Ponomarenko SA, Rebrov EA, Bobrovski AY, Boiko NI, Muzafarov AM, Shibaev VP (1996) Liq Cryst 21:1
149. Platé NA, Shibaev VP (eds) (1987) Comb-Shaped Polymers and Liquid Crystals. Plenum, New York
150. Ryumtsev EI, Evlampieva NP, Lezov AV, Ponomarenko SA, Boiko NI, Shibaev VP (1998) Liq Cryst 25:475
151. Ponomarenko SA, Rebrov EA, Boiko NI, Muzafarov AM, Shibaev VP (1998) Polym Sci Ser A 40:763
152. Ponamorenko S, Boiko N, Rebrov E, Muzafarov A, Whitehouse I, Richardson R, Shibaev V (1999) Mol Cryst Liq Cryst 332:43

153. Richardson RM, Whitehouse IJ, Ponomarenko SA, Boiko NI, Shibaev VP (1999) Mol Cryst Liq Cryst 330:167
154. Lezov AV, Mel'nikov AB, Polushina GE, Ponomarenko SA, Boiko NI, Kossmehl E, Ryumtsev EI, Shibaev VP (1998) Doklady Akad Nauk 362:638
155. Lezov AV, Mel'nikov AB, Polushina GE, Antonov EA, Novitskaya ME, Boiko NI, Ponomarenko SA, Rebrov EA, Shibaev VP, Ryumtsev EI, Muzafarov AM (2001) Doklady Chem 381:313
156. Klenin VJ, Panina YuV, Yarotskii VI, Ponomarenko SA, Boiko NI, Shibaev VP (2001) Polym Sci Ser A 43:519
157. Wilson MR, Ilnystskyi JM, Stimson LM (2003) J Chem Phys 119:3509
158. Richardson RM, Ponomarenko SA, Boiko NI, Shibaev VP (1999) Liq Cryst 26:101
159. Ponomarenko SA, Agina EV, Boiko NI, Rebrov EA, Muzafarov AM, Richardson RM, Shibaev VP (2001) Mol Cryst Liq Cryst 364:93
160. Agina EV, Ponomarenko SA, Boiko NI, Rebrov EA, Muzafarov AM, Shibaev VP (2001) Polym Sci Ser A 43:1000
161. Kovshik AP, Ragimov DA, Kovshik SA, Boiko NI, Lezov AV, Ryumtsev EI (2003) Russ J Phys Chem 77:1041
162. Ponomarenko SA, Boiko NI, Shibaev VP, Magonov SN (2000) Langmuir 16:5487
163. Ponomarenko SA, Boiko NI, Zhu XM, Agina EV, Shibaev VP, Magonov SN (2001) Polym Sci Ser A 43:245
164. Genson KL, Holzmueller J, Leshchiner I, Agina E, Boiko N, Shibaev VP, Tsukruk VV (2005) Macromolecules 38:8028
165. Ponomarenko SA, Boiko NI, Shibaev VP, Richardson RM, Whitehouse IJ, Rebrov EA, Muzafarov AM (2000) Macromolecules 33:5549
166. Boiko N, Zhu X, Vinokur R, Rebrov E, Muzafarov A, Shibaev V (2000) Mol Cryst Liq Cryst 352:343
167. Boiko N, Zhu X, Vinokur R, Rebrov E, Muzafarov A, Shibaev V (2000) Ferroelectrics 243:59
168. Zhu XM, Vinokur RA, Ponomarenko SA, Rebrov EA, Muzafarov AM, Boiko NI, Shibaev VP (2000) Polym Sci Ser A 42:1263
169. Boiko NI, Lysachkov AI, Ponomarenko SA, Shibaev VP, Richardson RM (2005) Colloid Polym Sci 283:1155
170. Zhu XM, Boiko NI, Rebrov EA, Muzafarov AM, Kozlovsky MV, Richardson RM, Shibaev VP (2001) Liq Cryst 28:1259
171. Bobrovsky AY, Pakhomov AA, Zhu XM, Boiko NI, Shibaev VP (2001) Polym Sci Ser A 43:431
172. Bobrovski A, Ponomarenko S, Boiko N, Shibaev V, Rebrov E, Muzafarov A, Stumpe J (2002) Macromol Chem Phys 230:1539
173. Bobrovsky AY, Pakhomov AA, Zhu XM, Boiko NI, Shibaev VP, Stumpe J (2002) J Phys Chem B 106:540
174. Boiko N, Zhu X, Bobrovsky A, Shibaev V (2001) Chem Mater 13:1447
175. Mehl GH, Thornton AJ, Goodby JW (1999) Mol Cryst Liq Cryst 332:455
176. Mehl GH, Goodby JW (1999) Chem Commun 13
177. Kowalewska A, Lickiss PD, Lucas R, Stańczyk WA (2000) J Organomet Chem 597:111
178. Ponomarenko SA, Rebrov EA, Boiko NI, Vasilenko NG, Muzafarov AM, Freidzon YS, Shibaev V (1994) Polym Sci Ser A 36:896
179. Mehl GH, Goodby JW (1996) Chem Ber 129:521
180. Merkel K, Kocot A, Vij JK, Mehl GH, Meyer T (2004) J Chem Phys 121:5012
181. Kannan RY, Salacinski HJ, Butler PE, Seifalian AM (2005) Acc Chem Res 38:879
182. Mehl GH, Saez IM (1999) Appl Organomet Chem 13:261

183. De Gennes PG, Hervet H (1983) J Phys Lett 44:351
184. Mehl GH, Goodby JW (1997) Mol Cryst Liq Cryst 303:15
185. Kreuzer FH, Mauerer R, Spes P (1991) Makromol Chem-M Symp 30:215
186. Mehl GH, Goodby JW (1996) Angew Chem Int Ed Engl 35:2641
187. Saez IM, Styring P (1996) Adv Mater 8:1001
188. Sellinger A, Laine RM, Chu V, Viner C (1994) J Polym Sci Part A Polym Chem 32:3069
189. Laine RM, Zhang C, Sellinger A, Viculis L (1998) Appl Organometal Chem 12:715
190. Zhang C, Bunning TJ, Lainr RJ (2001) Chem Mater 13:3653
191. Elsäßer R, Mehl GH, Goodby JW, Photinos DJ (2000) Chem Commun 851
192. Saez IM, Goodby JW (1999) Liq Cryst 26:1101
193. Saez IM, Goodby JW, Richardson RM (2001) Chem Eur J 7:2758
194. Saez IM, Goodby JW (2001) J Mater Chem 11:2845
195. Elsäßer R, Mehl GH, Goodby JW, Veith M (2001) Angew Chem Int Ed 40:2688
196. Mehl GH, Elsäßer R, Goodby JW, Veith M (2001) Mol Cryst Liq Cryst 364:219
197. Elsäßer R, Goodby JW, Mehl GH, Rodriguez-Martin D, Richardson RM, Photinos DJ, Veith M (2003) Mol Cryst Liq Cryst 402:1
198. Tajber L, Kocot A, Vij JK, Merkel K, Zalewska-Rejdak J, Mehl GH, Elsässer R, Goodby JW, Veith M (2002) Macromolecules 35:8601
199. Barbera J, Donnio B, Gehringer L, Guillon D, Marcos M, Omenat A, Serrano JL (2005) J Mater Chem 15:4093
200. Baars MWPL, Söntjens SHM, Fischer HM, Peerlings HWI, Meijer EW (1998) Chem Eur J 4:2456
201. Stevelmans S, van Hest JCM, Jansen JFGA, van Boxtel DAFJ, de Brabander-van den Berg EMM, Meijer EW (1996) J Am Chem Soc 118:7398
202. Schenning APHJ, Elissen-Román C, Weener JW, Baars MWPL, van der Gaast SJ, Meijer EW (1998) J Am Chem Soc 120:8199
203. Baars MWPL, van Boxtel MCW, Bastiaansen CWM, Broer DJ, Söntjens SHM, Meijer EW (2000) Adv Mater 12:715
204. Suzuki K, Haba O, Nagahata R, Yonetake K, Ueda M (1998) High Perform Polym 10:231
205. Yonetake K, Suzuki K, Morishita T, Nagahata R, Ueda M (1998) High Perform Polym 10:373
206. Tsiourvas D, Felekis T, Sideratou, Paleos CM (2002) Macromolecules 35:6466
207. Seitz M, Plesnivy T, Schimossek K, Edelmann M, Ringsdorf H, Fischer H, Uyama H, Kobayashi S (1996) Macromolecules 29:6560
208. Cameron JH, Facher A, Lattermann G, Diele S (1997) Adv Mater 9:398
209. Usol'tseva N, Bykova V, Smirnova A, Grusdev M, Lattermann G, Facher A (2004) Mol Cryst Liq Cryst 409:29
210. Domracheva N, Mirea A, Schwoerer M, Torre-Lorente L, Lattermann G (2005) ChemPhysChem 6:110
211. Marcos M, Omenat A, Serrano JL (2003) C R Chimie 6:947
212. Barberá J, Marcos M, Serrano JL (1999) Chem Eur J 5:1834
213. Marcos M, Giménez R, Serrano JL, Donnio B, Heinrich B, Guillon D (2001) Chem Eur J 7:1006
214. Donnio B, Barberá J, Giménez R, Guillon D, Marcos M, Serrano JL (2002) Macromolecules 35:370
215. McKenna MD, Barberá J, Marcos M, Serrano JL (2005) J Am Chem Soc 127:619
216. Barberá J, Donnio B, Giménez R, Guillon D, Marcos M, Omenat A, Serrano JL (2001) J Mater Chem 11:2808

217. Pastor L, Barberá J, McKenna M, Marcos M, Martín-Rapún R, Serrano JL, Luckhurst GR, Mainal A (2004) Macromolecules 37:9386
218. Martín-Rapún R, Marcos M, Omenat A, Serrano JL, Luckhurst GR, Mainal A (2004) Chem Mater 16:4969
219. Severing K, Saalwächter K (2004) Phys Rev Lett 92:125501
220. Rueff JM, Barberá J, Donnio B, Guillon D, Marcos M, Serrano JL (2003) Macromolecules 36:8368
221. Van-Quynh A, Filip D, Cruz C, Sebastião PJ, Ribeiro AC, Rueff JM, Marcos M, Serrano JL (2005) Eur Phys J E 18:149
222. Rueff JM, Barberá J, Marcos M, Omenat A, Martín-Rapún R, Donnio B, Guillon D, Serrano JL (2006) Chem Mater 18:249
223. Precup-Blaga FS, Schenning APHJ, Meijer EW (2003) Macromolecules 36:565
224. Terzis AF, Vanakaras AG, Photinos DJ (1999) Mol Cryst Liq Cryst 330:517
225. Vanakaras AG, Photinos DJ (2001) J Mater Chem 11:2832
226. Terzis AF, Vanakaras AG, Photinos DJ (2000) Mol Cryst Liq Cryst 352:265
227. Vanakaras AG, Photinos DJ (2005) J Mater Chem 15:2002
228. Serrano JL, Marcos M, Martín R, González M, Barberá J (2003) Chem Mater 15:3866
229. Kardas D, Prehm M, Baumeister U, Pociecha D, Reddy RA, Mehl GH, Tschierske C (2005) J Mater Chem 15:1722
230. Tsiourvas D, Stathopoulou K, Sideratou Z, Paleos CM (2002) Macromolecules 35:1746
231. Diele S, Göring P (1998) In: Demus D, Goodby JW, Gray GW, Spiess HW, Vill V (eds) Handbook of Liquid Crystals. Wiley, Weinheim, vol 2B, chapter XIII, 887
232. Diele S (2002) Curr Opinion Coll Interface Sci 7:333
233. Kutsumizu S (2002) Curr Opinion Coll Interface Sci 7:537
234. Impéror-Clerc M (2005) Curr Opinion Coll Interface Sci 9:370
235. Cook AG, Baumeister U, Tschierske C (2005) J Mater Chem 15:1708
236. Felekis T, Tsiourvas D, Tziveleka L, Paleos CM (2005) Liq Cryst 32:39
237. Friberg SE, Podzimek M, Tomalia DA, Hedstrand DM (1988) Mol Cryst Liq Cryst 164:157
238. Ramzi A, Bauer BJ, Scherrenberg R, Froehling P, Joosten J, Amis EJ (1999) Macromolecules 32:4983
239. Ujie S, Yano Y, Mori A (2004) Mol Cryst Liq Cryst 411:483
240. Martín-Rapún R, Marcos M, Omenat A, Barberá J, Romero P, Serrano JL (2005) J Am Chem Soc 127:7397
241. Tsiourvas D, Felekis T, Sideratou Z, Paleos CM (2004) Liq Cryst 31:739
242. Weener JW, Meijer EW (2000) Adv Mater 12:741
243. Yonetake K, Masuko T, Morishita T, Suzuki K, Ueda M, Nagahata R (1999) Macromolecules 32:6578
244. Haba O, Okuyama K, Yonetake K (2001) Mol Cryst Liq Cryst 364:929
245. Haba O, Okuyama K, Osawa H, Yonetake K (2005) Liq Cryst 32:633
246. Cho BK, Jain A, Gruner SM, Wiesner U (2004) Science 305:1598
247. Cho BK, Jain A, Mahajan S, Ow H, Gruner SM, Wiesner U (2004) J Am Chem Soc 126:4070
248. Cho BK, Jain A, Nieberle J, Mahajan S, Wiesner U, Gruner SM, Türk S, Râder HJ (2004) Macromolecules 37:4227
249. Nithyanandhan J, Jayaraman N, Davis R, Das S (2004) Chem Eur J 10:689
250. Busson P, Ihre H, Hult A (1998) J Am Chem Soc 120:9070
251. Ihre H, Hult A, Fréchet JMJ, Gitsov I (1998) Macromolecules 31:4061
252. Malkoch M, Malmström E, Hult A (2002) Macromolecules 35:8307

253. Busson P, Örtegren J, Ihre H, Gedde UW, Hult A, Andersson G (2001) Macromolecules 34:1221
254. Örtegren J, Busson P, Ihre H, Gedde UW, Hult A, Eriksson A, Lindgren M, Andersson G (2001) Liq Cryst 28:861
255. Örtegren J, Tidlund J, Nykvist M, Busson P, Hult A, Sen S, Boyd RH, Gedde UW (2001) Polymer 42:10027
256. Busson P, Örtegren J, Ihre H, Gedde UW, Hult A, Andersson G, Eriksson A, Lindgren M (2002) Macromolecules 35:1663
257. Percec V (1997) From Molecular to Macromolecular Liquid Crystals. In: Collings PJ, Patel JS (eds) Handbook Of Liquid Crystal Research, chap 8. Oxford University Press, Oxford
258. Percec V, Chu P (1995) Polym Mater Sci Eng 73:125
259. Percec V, Chu P, Ungar G, Zhou J (1995) J Am Chem Soc 117:11441
260. Li JF, Crandall KA, Chu P, Percec V, Petschek RG, Rosenblatt C (1996) Macromolecules 29:7813
261. Jin AJ, Fisch MR, Mahajan MP, Crandall KA, Chu P, Huang CY, Percec V, Petschek RG, Rosenblatt C (1998) Eur Phys J 5:251
262. Liu Z, Zhu L, Shen Z, Zhou W, Cheng SZD, Percec V, Ungar G (2002) Macromolecules 35:9426
263. Liu Z, Zhu L, Zhou W, Cheng SZD, Percec V, Ungar G (2002) Chem Mater 14:2384
264. Gehringer L, Bourgogne C, Guillon D, Donnio B (2004) J Am Chem Soc 126:3856
265. Gehringer L, Guillon D, Donnio B (2003) Macromolecules 36:5593
266. Malthête J, Nguyen HT, Destrade C (1993) Liq Cryst 13:171
267. Nguyen HT, Destrade C, Malthête J (1997) Adv Mater 9:375
268. Fazio D, Mongin C, Donnio B, Galerne Y, Guillon D, Bruce DW (2001) J Mater Chem 11:2852
269. Smirnova AI, Fazio D, Iglesias EF, Hall CG, Guillon D, Donnio B, Bruce DW (2003) Mol Cryst Liq Cryst 396:227
270. Gehringer L, Bourgogne C, Guillon D, Donnio B (2005) J Mater Chem 15:1696
271. Moore JS (1997) Acc Chem Res 30:402
272. Pesak DJ, Moore JS (1997) Angew Chem Int Ed Engl 36:1636
273. Meier H, Lehmann M (1998) Angew Chem Int Ed Engl 37:643
274. Meier H, Lehmann M, Kolb U (2000) Chem Eur J 6:2462
275. Meier H, Lehmann M, Schnorpfeil C, Fetten M (2000) Mol Cryst Liq Cryst 352:85
276. Lehmann M, Schartel B, Hennecke M, Meier H (1999) Tetrahedron 55:13377
277. Lehmann M, Fischbach I, Spiess HW, Meier H (2004) J Am Chem Soc 126:772
278. Meier H, Holst HC, Oehlhof A (2003) Eur J Org Chem 4173
279. Lee CH, Yamamoto T (2001) Tetrahedron Lett 42:3993
280. Lee CH, Yamamoto T (2002) Bull Chem Soc Jpn 75:615
281. Binnemans K, Görller-Walrand C (2002) Chem Rev 102:2303
282. Donnio B, Guillon D, Deschenaux R, Bruce DW (2003) Metallomesogens. In: McCleverty JA, Meyer TJ (eds) Comprehensive Coordination Chemistry II. Elsevier, Oxford, vol 7, chap 7.9, 357
283. Donnio B (2002) Curr Opin Colloid Interface Sci 7:371
284. Serrette AG, Swager TM (1993) J Am Chem Soc 115:8879
285. Lai CK, Lu MY, Lin FJ (1997) Liq Cryst 23:313
286. Stebani U, Lattermann G, Wittenbger M, Wendorff JH (1996) Angew Chem Int Ed Engl 35:1858
287. Stebani U, Lattermann G (1995) Adv Mater 7:578

288. Barberá J, Marcos M, Omenat A, Serrano JL, Martínez JI, Alonso PJ (2000) Liq Cryst 27:255
289. Deschenaux R, Goodby JW (1995) In: Togni A, Hayashi T (eds) Ferrocenes: Homogeneous Catalysis, Organic Synthesis, Materials Sciences. Wiley, Weinheim, chap 9, 471
290. Deschenaux R, Serrano E, Levelut AM (1997) Chem Commun 1577
291. Chuard T, Béguin MT, Deschenaux R (2003) C R Chimie 6:959
292. Chuard T, Deschenaux R (2003) Chimia 57:597
293. Chuard T, Deschenaux R (2001) Chimia 55:139
294. Dardel B, Deschenaux R, Even M, Serrano E (1999) Macromolecules 32:5193
295. Chuard T, Dardel B, Deschenaux R, Even M (2000) Carbon 38:1573
296. Deschenaux R, Even M, Guillon D (1998) Chem Commun 537
297. Even M, Heinrich B, Guillon D, Guldi DM, Prato M, Deschenaux R (2001) Chem Eur J 7:2595
298. Guldi DM, Maggini M, Scorrano G, Prato M (1997) J Am Chem Soc 119:974
299. Chuard T, Deschenaux R (2002) J Mater Chem 12:1944
300. Guillon D, Nierengarten JF, Gallani JL, Eckert JF, Rio Y, Carreon MP, Dardel B, Deschenaux R (2003) Macromol Symp 192:63
301. Dardel B, Guillon D, Heinrich B, Deschenaux R (2001) J Mater Chem 11:2814
302. Yevlampieva NP, Dardel B, Lavrenko P, Deschenaux R (2003) Chem Phys Lett 382:32
303. Lavrenko P, Yevlampieva N, Dardel B, Deschenaux R (2004) Prog Colloid Polym Sci 127:61
304. Campidelli S, Eng C, Saez IM, Goodby JW, Deschenaux R (2003) Chem Commun 1520
305. Tirelli N, Cardullo F, Habicher T, Suter UW, Diederich F (2000) J Chem Soc, Perkin Trans 2, 193
306. Chuard T, Deschenaux R, Hirsch A, Schönberger H (1999) Chem Commun 2103
307. Felder-Flesch D, Rupnicki L, Bourgogne C, Donnio B, Guillon D (2006) J Mater Chem 16:304
308. Campidelli S, Lenoble J, Barberá J, Paolucci F, Marcaccio M, Paolucci D, Deschenaux R (2005) Macromolecules 38:7915
309. Campidelli S, Deschenaux R (2001) Helv Chim Acta 84:589
310. Campidelli S, Deschenaux R, Eckert JF, Guillon D, Nierengarten JF (2002) Chem Commun 656
311. Campidelli S, Vázquez E, Milic D, Prato M, Barberá J, Guldi DM, Marcaccio M, Paolucci D, Paolucci F, Deschenaux R (1994) J Mater Chem 14:1266
312. Saez IM, Goodby JW (2003) J Mater Chem 13:2727
313. Praefcke K, Psaras P, Eckert A (1993) Liq Cryst 13:551
314. Zab K, Joachimi D, Agert O, Neumann B, Tschierske C (1995) Liq Cryst 18:489
315. Andersch J, Diele S, Lose D, Tschierske C (1996) Liq Cryst 21:103
316. Van de Witte P, Lub J (1999) Liq Cryst 26:1039
317. Uedaira T, Koide N (2001) Mol Cryst Liq Cryst (2001) 365:23
318. Schulte JL, Laschat S, Vill V, Nishikawa E, Finkelmann H, Nimtz M (1998) Eur J Org Chem 2499
319. Pegenau A, Göring P, Tschierske C (1996) Chem Commun 2563
320. Pegenau A, Cheng XH, Tschierske C, Göring P, Diele S (1999) New J Chem 23:465
321. Pegenau A, Hegmann T, Tschierske C, Diele S (1999) Chem Eur J 5:1643
322. Cheng XH, Diele S, Tschierske C (2000) Angew Chem Int Ed 39:592
323. Saez IM, Goodby JW (2003) Chem Commun 1726
324. Saez IM, Goodby JW (2003) Chem Eur J 9:4869

325. Fan FY, Mastrangelo JC, Katsis D, Chen SH, Blanton TN (2000) Liq Cryst 27:1239
326. Fan FY, Culligan SW, Mastrangelo JC, Katsis D, Chen SH, Blanton TN (2001) Chem Mater 13:4584
327. Chen SH, Chen HMP, Geng Y, Jacobs SD, Marshall KL, Blanton TN (2003) Adv Mater 15:1061
328. Plesnivy T, Ringsdorf H, Schumacher P, Nütz U, Diele S (1995) Liq Cryst 18:185
329. Barberá J, Garcés AC, Jayaraman N, Omenat A, Serrano JL, Stoddart JF (2001) Adv Mater 13:175
330. Percec V, Cho CG, Pugh C, Tomazos D (1992) Macromolecules 25:1164
331. Brewis M, Clarkson GJ, Holder AM, McKeow NB (1998) Chem Commun 969
332. Brewis M, Clarkson GJ, Helliwell M, Holder AM, McKeown NB (2000) Chem Eur J 6:4630
333. Brewis M, Helliwell M, McKeown NB, Reynolds S, Shawcross A (2001) Tetrahedron Lett 42:813
334. Kimura M, Saito Y, Ohta K, Hanabusa K, Shirai H, Kobayashi N (2002) J Am Chem Soc 124:5274
335. Lee M, Cho BK, Zin WC (2001) Chem Rev 101:3869
336. Lee M, Jeong YS, Cho BK, Oh NK, Zin WC (2002) Chem Eur J 8:876
337. Yoo YS, Song JH, Oh NK, Zin WC, Park S, Chang T, Lee M (2004) J Am Chem Soc 126:6294
338. Holzmeuller J, Genson KL, Park Y, Yoo YS, Park MH, Lee M, Tsukruk V (2005) Langmuir 21:6392
339. Bae J, Choi JH, Yoo YS, Oh NK, Kim BS, Lee M (2005) J Am Chem Soc 127:9668
340. Yoo YS, Lee M (2005) J Mater Chem 15:419
341. Kim JK, Hong MK, Ahn JH, Lee M (2005) Angew Chem Int Ed 44:328
342. Bae J, Kim JK, Oh NK, Lee M (2005) Macromolecules 38:4226
343. Jang CJ, Ryu JH, Lee JD, Sohn D, Lee M (2004) Chem Mater 16:4226

Editor: K.-S. Lee